

Investigating reactive sputtered $\text{Ir}_x\text{Ni}_y\text{O}_z$ electrocatalysts for the oxygen evolution reaction

D Coertzen



orcid.org 0000-0001-7524-9255

Dissertation accepted in partial fulfilment of the
requirements for the degree *Master of Science in Chemistry*
at the North-West University

Supervisor:	Dr A Falch
Co-supervisor:	Prof RJ Kriek

Graduation May 2020

22832262

DECLARATION

I, De Wet Coertzen, declare that the dissertation entitled: “*Investigating reactive sputtered $\text{Ir}_x\text{Ni}_y\text{O}_z$ electrocatalysts for the oxygen evolution reaction*”, submitted in fulfilment of the degree of Master of Science in Chemistry, is my own work, except where acknowledged in text, and has not been submitted in whole or in part to any other tertiary institution.

Signed at North-West University (Potchefstroom Campus)



De Wet Coertzen

PREFACE

The research and results presented in this dissertation are in the field of electrochemistry, more specifically in the area of electrocatalysis. Literature related to alkaline water electrolysis (AWE) is reviewed and discussed, with emphasis on the oxygen evolution reaction (OER) as the limiting reaction in the efficient production of hydrogen as an alternative energy source. The development of electrocatalysts that exhibit exceptional and economically viable performance with regard to catalysing the OER, is of great importance for effective commercialised production of hydrogen by AWE. The electrocatalysts investigated in this study toward the OER in alkaline media, include various Ir and Ni containing oxide ($\text{Ir}_x\text{Ni}_y\text{O}_z$) combinations supported on Vulcan Carbon:Nafion (VC:Nafion) as electrocatalyst support. The research approach involved high-throughput and combinatorial (HTC) methods for the production and screening of various different $\text{Ir}_x\text{Ni}_y\text{O}_z$ combinations, followed by the employment of conventional rotating disk electrode (RDE) analysis and physical characterisation of the top five electrocatalysts (identified by HTC) showing promising activity towards the OER.

The dissertation is written in British English. All articles were written in the English required by the journals. This dissertation is submitted in article format, as allowed by the North-West University (NWU) and stated in the General Academic Rules 2017 (4.3.3, 4.4.2, 4.10.4, 4.10.5, 4.10.8) and in the Faculty of Natural and Agricultural Sciences Quality Manual 2018 (6.12.4.D.1 and 6.12.4.D.2) for master studies. This entails that an article(s) forms part of the dissertation as it was submitted and accepted for publication, substituting the conventional “Experimental” and “Results and Discussion” chapters. It is also stated that co-authors of article(s) grant permission of the research product to be used (Appendix A). The dissertation must be submitted as a unit, as required by the General Academic Rules 2017 (4.10.5), and should be supplemented with a problem statement, an introduction and synoptic conclusion. Hence, this dissertation consists of the following chapters: Background with aim and objectives (Chapter 1), Literature study (Chapter 2), Article 1 (Chapter 3), Article 2 (Chapter 4), and Evaluation and conclusion (Chapter 5). In this regard some repetition of ideas/text/figures will occur in some of the chapters and in the included article(s).

RATIONALE OF SUBMITTING THE DISSERTATION IN ARTICLE FORMAT

The dissertation was submitted in article format to ensure the quality of the dissertation and the article(s). Submitting the article(s) to peer reviewed journals subjects the candidate and the article(s) to constructive criticism from experts in the respective fields, hence ensuring quality and relevance of the research. The Faculty of Natural and Agricultural Sciences at the NWU Potchefstroom campus adopted this model so as to train students in article writing as well as to encourage publication of the research results (Faculty of Natural and Agricultural Sciences Quality Manual 2018, 6.12.4.D.1).

“The Faculty of Natural and Agricultural Sciences adopted the article model for the submission of the research component of postgraduate studies in terms of the general rules of the North-West University, which make provision for this model. Advantages are that this encourages publication of the research results in scientific journals and also that students are trained in article writing in the course of their postgraduate studies.”

The requirements of Master's training (as stated by the Faculty of Natural and Agricultural Sciences Quality Manual 2018, 6.12.4.D.2):

“The basic quality and scientific requirements for Master's and Doctoral students, who prefer the article format, are the same as for the traditional model concerning completion of a dissertation, mini-dissertation or a thesis.

The General Rules of the University contain the following requirements for dissertations and mini-dissertations in article format:

Where a candidate is allowed to submit the research product in the form of a research article or articles, such research product must be presented for examination purposes as an integrated unit, supplemented with a problem statement, an introduction and a synoptic conclusion as prescribed by faculty rules and the manuscript submission guidelines, or the url link to the manuscript guidelines, of the journal or journals concerned.

Where any research article or internationally examined patent to which the candidate for a master's degree and other authors or inventors have contributed is submitted as the research product of a master's degree programme, the candidate must obtain a written statement from each co-author and co-inventor in which it is stated that such co-author or co-inventor grants permission for the research product to be used for the stated purpose, and in which it is further indicated what each co-author's or co-inventor's academic contribution to the research product concerned was.

Where co-authors or co-inventors were involved in the development of the research product, the candidate must mention this fact in the preface, and must include the statement of each co-author or co-inventor immediately following the preface to the research product.”

The student prepared two articles, one of which was published in the journal *Electrocatalysis* (Springer, impact factor: 2.311). This journal was chosen as the focus of the article (Chapter 3) aligned with the scope of *Electrocatalysis* which provides a unique international forum solely dedicated to the exchange of novel ideas in electrocatalysis for academic, government, and industrial researchers. The author guidelines that were followed in preparation of the article (Chapter 3) are available at the following link:

<https://www.springer.com/journal/12678/submission-guidelines>

The prerequisites of the NWU have therefore been complied with.

CONTRIBUTIONS TO ARTICLES

The conceptualisation of this work, substantiated by ideas and recommendations, was suggested by Dr. A. Falch (supervisor) and Prof. R.J. Kriek (co-supervisor). The acquisition of data, decisions/interpretation and compilation of articles was done by myself, D. Coertzen, with participation and assistance by Dr. A. Falch and Prof. R.J. Kriek. I was assisted by Dr. I. Shuro and Dr. A. Jordaan with SEM and EDX characterisation conducted at the North-West University, Potchefstroom Campus. Dr. C.W. Dunnill and Dr D.R. Jones assisted in XPS analysis conducted at the University of Swansea. Dr. P.B.J. Levecque from the HySA Catalysis centre of competence, contributed financially, allowing successful execution of this study.

ACKNOWLEDGEMENTS

I want to acknowledge and thank the following people without whom my study would not have been possible:

Dr. A. Falch

Prof. R.J. Kriek

Dr. P.B.J. Levecque

Dr. A. Jordaan

Dr. C.W. Dunnill

Dr. D.R. Jones

Mrs. A. Benade



I would also like to thank my parents, Soekie and De Wet Coertzen, my brother Stefan and my love Jeandri for their love and support. Thank you for always being there for me.

"Appreciate your parents, you never know what sacrifices they went through for you".

Thank you for your sacrifices to get me where I am today.

ABSTRACT

Alkaline water electrolysis (AWE) is a promising, simple and environmentally friendly technology, when coupled with renewable energy sources (e.g. wind and solar), to produce high purity hydrogen gas for clean energy conversion and storage. In spite of the significant advances and progress made in AWE, modern electrolysis cells are performing at somewhat limited operating current densities with high energy consumption. Contributing to this unsatisfactory performance is the slow oxygen evolution reaction (OER) kinetics on the anode which requires the use of efficient electrocatalysts to lower initial electrical energy input. From the numerous papers being published in the field of electrocatalysis for the OER, it is evident that the development of an efficient electrocatalyst to serve as the anode for the OER, is a necessity to realise optimal industrial performance. Among the various electrocatalysts that have been developed and studied (Co, Mn, Fe and Ni, along with their oxides etc.), Ni and Ni-based oxides have received much attention, exhibiting superior performance in terms of activity and stability of the studied non-noble metals for the OER in alkaline conditions. However, improvement in performance is still required to compete with the performance of the best electrocatalysts in acidic media, Ir and IrO₂. Electrocatalyst research is multifaceted and depends on many factors contributing to the observed activity. In this study, focus was placed on two main aspects, namely the supporting structure of the electrocatalyst and the elemental composition of the electrocatalyst. The development of support structures for electrocatalysts (i.e. graphite, Vulcan carbon (VC), graphene etc.), has received a great deal of attention over the last decade. Carbon support structures are known to increase the surface area, stability and activity of electrocatalysts in most cases, and can be used to overcome the delamination of thin films from electrode substrates. Two types of electrode substrates were used in this study, which include an Au/SiO₂ wafer and glassy carbon (GC) disk inserts. In an attempt to (i) obtain surface structures and areas on Au/SiO₂ wafer electrode pads, for combinatorial high-throughput sputtering and screening, that are comparable to GC, (ii) eliminate delamination of the electrocatalyst, and (iii) increase activity and stability, the first part of the study focused on the preparation technique of VC:Nafion support. Four different VC:Nafion inks were prepared and used as carbon support on GC electrode inserts to analyse their effect on the activity of sputtered Ni thin films towards the OER in alkaline media. Scanning Electron Microscopy (SEM) and energy-dispersive X-ray spectroscopy (EDX) were employed for physical characterisation of the VC:Nafion supported GC before and after electrochemical characterisation. Linear sweep voltammetry (LSV) and chronopotentiometry (CP) were employed for electrochemical characterisation to compare the catalytic activity and stability of these sputtered Ni thin films on the various VC supports. Results exhibit improved performance achieved by the sputtered Ni on VC:Nafion (1:0.67) support for the OER in alkaline media (in comparison to unsupported Ni), indicating improved Ni utilisation as well as improved short-term

stability of the Ni thin films. These results validate the use of VC:Nafion as support for sputtered electrocatalysts. Various reactive sputtered $\text{Ir}_x\text{Ni}_y\text{O}_z$ electrocatalyst combinations were subjected to high-throughput electrochemical characterisation, with the aim of identifying an attractive alternative OER electrocatalyst, showing satisfactory activity and stability in alkaline conditions. The concept of investigating a spread of $\text{Ir}_x\text{Ni}_y\text{O}_z$ electrocatalyst combinations was based on (i) the huge body of literature supporting the activity of Ir/IrO₂ in acid media, (ii) the evidence of the activity and stability of Ni and NiO in alkaline media, and (iii) ultimately exploiting the possibility of an optimally modulated mix of these elements resulting from desired synergistic effects. Rotating disk electrode (RDE) techniques, which included LSV and CP were used with the VC:Nafion supported GC as electrode substrate for in-depth electrochemical analysis along with SEM, EDX and X-ray photoelectron spectroscopy (XPS) as physical characterisation techniques of the best $\text{Ir}_x\text{Ni}_y\text{O}_z$ electrocatalyst combinations. Overpotential, Tafel slopes and exchange current along with results from physical characterisation were employed as key performance indicators. Overall the $\text{Ir}_x\text{Ni}_y\text{O}_z$ electrocatalyst combinations containing higher amounts of Ir ($\text{Ir}_{92}\text{Ni}_8\text{O}_x$, $\text{Ir}_{68}\text{Ni}_{32}\text{O}_x$ and $\text{Ir}_{62}\text{Ni}_{38}\text{O}_x$) performed the best of the tested mixed metal electrocatalysts with overpotentials after stability testing of 389, 390 and 530 mV, respectively with Ni performing the best out of all testes electrocatalysts with 278 mV. However, evident from this study was the fact that the combination of Ir with Ni did not result in a mixed metal electrocatalyst that could outperform pure Ni. Nonetheless, it is also clear that a synergy does indeed exist for the $\text{Ir}_x\text{Ni}_y\text{O}_z$ combination, however, in this study it was not optimal (maybe due to various factors) to satisfy the compromise between electrocatalyst performance and cost.

Key terms: *Reactive sputtering, high-throughput screening, electrocatalysts, carbon support, alkaline water electrolysis, oxygen evolution reaction, hydrogen production, activity, stability*

OPSOMMING

Alkaliëse water-elektrolise (AWE) is 'n belowende, eenvoudige en omgewingsvriendelike tegnologie as dit saam met hernubare energiebronne gebruik word om waterstofgas met 'n hoë suiwerheid te produseer vir die opwekking van elektriese energie. Ten spyte van die beduidende vooruitgang en vordering wat in AWE gemaak is, presteer moderne elektroliseselle teen 'n ietwat beperkte bedryfstroomdigtheid met 'n hoë energieverbruik. Die bydrae tot hierdie onbevredigende prestasie is die kinetika van die stadige suurstofontwikkelings-reaksie (OER) op die anode, wat die gebruik van doeltreffende elektrokatalisators benodig om die aanvanklike elektriese energie-inset te verlaag. Uit die talle artikels wat op die gebied van elektrokatalise vir die OER gepubliseer is, blyk dit dat die ontwikkeling van 'n doeltreffende elektrokatalisator om as die anode vir die OER te dien, 'n noodsaaklikheid is om optimale industriële prestasie te behaal. Onder die verskillende elektrokatalisators wat ontwikkel en bestudeer is (Co, Mn, Fe en Ni, tesame met hul oksiede, ens.), Ni- en Ni-basis-oksiede het baie aandag geniet, met uitstekende prestasies ten opsigte van die aktiwiteit en stabiliteit van die bestudeerde nie-edelmetale vir die OER in alkaliëse toestande. Verbetering in prestasie is egter steeds nodig om mee te ding met die prestasie van die beste elektrokatalisators vir suurmedia, Ir en IrO₂. Elektrokatalisatornavorsing is veelsydig en hang af van baie faktore wat bydra tot die waargenome aktiwiteit. In hierdie studie is daar gefokus op twee hoofaspekte, naamlik die ondersteuningstruktuur van die elektrokatalisator en die elementêre samestelling van die elektrokatalisator. Die ontwikkeling van ondersteuningstrukture vir elektrokatalisators (dws grafiet, Vulcan-koolstof (VC), grafeen, ens.) het die afgelope dekade baie aandag geniet. Dit is bekend dat koolstofondersteuningstrukture die oppervlakte, stabiliteit en aktiwiteit van elektrokatalisators in die meeste gevalle verhoog, en dit kan gebruik word om die delaminering van dun films van elektrodesubstrate te oorkom. Twee soorte elektrodesubstrate is in hierdie studie gebruik, wat 'n Au/SiO₂-wafel en glasagtige koolstof (GC) skyfinsetsels insluit. In 'n poging om (i) oppervlakstrukture en -areas op Au/SiO₂-elektrode-kussings te verkry, vir kombinatoriese hoëdeurvloeiervstuiwing en -sifting, wat vergelykbaar is met GC, (ii) die delaminering van die elektrokatalisator te verhoed, en (iii) aktiwiteit en stabiliteit te verhoog, het die eerste deel van die studie gefokus op die voorbereidingstegniek van VC:Nafion-ondersteuning. Vier verskillende VC:Nafion-inke is voorberei en gebruik as koolstofondersteuning op GC-elektrode-insetsels om hul effek op die aktiwiteit van verstuipte Ni-dunfilms tydens die OER in alkaliëse media te ontleed. Skandeerelektronmikroskopie (SEM) en energiegedispergeerde X-straal-spektroskopie (EDX) is gebruik vir die fisiese karakterisering van GC-gesteunde VC:Nafion voor en na elektrochemiese karakterisering. Lineêre aftas-voltammetrie (LSV) en chronopotensiometrie (CP) is gebruik vir elektrochemiese karakterisering om die katalitiese aktiwiteit en stabiliteit van hierdie verstuipte Ni-dunfilms op die verskillende VC-draers te vergelyk. Resultate toon verbeterde prestasies behaal deur die verstuipte Ni op VC: Nafion

ondersteuning (1:0,67) vir die OER in alkaliese media (in vergelyking met onondersteunde Ni), wat dui op verbeterde Ni-gebruik asook verbeterde korttermynstabiliteit van die Ni-dunfilms. Hierdie resultate bevestig die gebruik van VC:Nafion as ondersteuning vir verstuipte elektrokatalisators. Verskeie reaktief-verstuipte $\text{Ir}_x\text{Ni}_y\text{O}_z$ elektrokatalisator-kombinasies is onderwerp aan elektrochemiese karakterisering met 'n hoë deurvloei, met die doel om 'n aantreklike alternatiewe OER-elektrokatalisator te identifiseer, met bevredigende aktiwiteit en stabiliteit in alkaliese toestande. Die konsep van die ondersoek na 'n verspreiding van $\text{Ir}_x\text{Ni}_y\text{O}_z$ elektrokatalisator-kombinasies is gebaseer op (i) die groot volume literatuur wat die aktiwiteit van Ir/IrO_2 in suur media ondersteun, (ii) die getuigenis van die aktiwiteit en stabiliteit van Ni en NiO in alkaliese media, en (iii) uiteindelik die moontlike benutting van 'n optimaal gemoduleerde mengsel van hierdie elemente as die gevolg van gewenste sinergistiese effekte. Roterendeskyf-elektrodetegnieke (RDE), wat LSV en CP ingesluit het, is saam met die VC:Nafion-ondersteunde GC as elektrodesubstraat gebruik vir deeglike elektrochemiese analise saam met SEM, EDX en X-straal-foto-elektron-spektroskopie (XPS) as fisiese karakteriseringstegnieke vir die beste $\text{Ir}_x\text{Ni}_y\text{O}_z$ -elektrokatalisator-kombinasies. Oorpotensiaal, Tafel-hellings en uitruilstrome sowel as resultate van fisiese karakterisering is as sleutelprestasie-aanwysers gebruik. In die algemeen het die $\text{Ir}_x\text{Ni}_y\text{O}_z$ -elektrokatalisator-kombinasies wat hoër hoeveelhede Ir bevat ($\text{Ir}_{92}\text{Ni}_8\text{O}_x$, $\text{Ir}_{68}\text{Ni}_{32}\text{O}_x$ en $\text{Ir}_{62}\text{Ni}_{38}\text{O}_x$) die beste van die getoetsde gemengde-metaal-elektrokatalisatore gevaar met oorpotensiaal na stabiliteits toetse van 389, 390 en 530 mV onderskeidelik met Ni wat die beste gevaar het van al die getoetsde elektrokataliste met 278 mV. Maar duidelik uit hierdie studie is die feit dat die kombinasie van Ir met Ni nie by uitstek daartoe lei dat 'n gemengde-metaal-elektrokatalisator suiwer Ni kon oortref nie. Desondanks is dit ook duidelik dat daar inderdaad 'n sinergie bestaan vir die $\text{Ir}_x\text{Ni}_y\text{O}_z$ -kombinasie; maar in hierdie studie was dit egter nie optimaal nie (miskien as gevolg van verskillende faktore) om die kompromis tussen elektrokatalisator-prestasie en koste te bevredig.

Sleuteltermes: *reaktiewe verstuiwing, hoë-deurset-sifting, elektrokatalisators, koolstofondersteuning, alkaliese water-elektrolise, suurstofontwikkelingsreaksie, waterstofproduksie, aktiwiteit, stabiliteit*

TABLE OF CONTENTS

DECLARATION	I
PREFACE	II
RATIONALE OF SUBMITTING THE DISSERTATION IN ARTICLE FORMAT	III
CONTRIBUTIONS TO ARTICLES	IV
ACKNOWLEDGEMENTS	V
ABSTRACT	VI
OPSOMMING	VIII
CHAPTER 1: BACKGROUND, AIM AND OBJECTIVES	1
1.1 Background and Problem Statement	1
1.2 Methods of Investigation.....	4
1.3 Aim and Objectives	5
1.4 References	6
CHAPTER 2: LITERATURE STUDY	8
2.1 Energy Consumption and the Environment	8
2.2 Renewable Energy Sources.....	10
2.3 Alkaline Water Electrolysis	13
2.4 References	21
CHAPTER 3: VULCAN CARBON AS SUPPORT FOR SPUTTERED OXYGEN EVOLUTION ELECTROCATALYSTS	27
CHAPTER OVERVIEW	27
3.1 Introduction	27
3.2 Experimental.....	29
3.2.1 Preparation and physical characterisation of VC:Nafion support.....	29
3.2.2 Electrochemical characterisation	30

3.3	Results and Discussion	31
3.4	Conclusion.....	39
3.5	References	40
CHAPTER 4: REACTIVE SPUTTERED IR_xNI_yO_z ELECTROCATALYSTS FOR THE OXYGEN EVOLUTION REACTION IN ALKALINE MEDIA		44
CHAPTER OVERVIEW.....		44
4.1	Introduction	44
4.2	Experimental.....	47
4.2.1	Preperation of Ir _x Ni _y O _z electrocatalyst compositions	47
4.2.2	Electrochemical characterisation	48
4.2.3	Physical characterization	49
4.3	Results and Discussion	49
4.4	Conclusion.....	59
4.5	References	61
CHAPTER 5: EVALUATION AND CONCLUSION		69
5.1	Reiteration of the Problem Statement, Aim and Objectives	69
5.2	Dissertation Overview	71
5.3	Recommendations and area for improvement	73
5.3.1	Alternative supports.....	73
5.3.2	Alternative support binder.....	73
5.3.3	Role of Fe.....	74
5.3.4	Loading of VC:Nafion ink.....	74
5.3.5	General areas for improvement	75
5.4	References	76

ANNEXURES A: PERMISSION GRANTED BY CO-AUTHORS.....	79
ANNEXURES B: CONSENT BY JOURNAL(S)	80

LIST OF TABLES

Table 3-1:	SEM images of the different VC:Nafion inks deposited on GC insert electrodes at different drying rotation rates.	32
Table 4-1:	Electrocatalyst metal compositions confirmed with EDX (atomic %) and overpotential values of the top five electrocatalyst combinations from high-throughput screening	51
Table 4-2:	Overpotential of all electrocatalysts before and after CP measurements.....	54
Table 4-3:	Tafel slopes of all electrocatalysts before and after CP measurements.....	58
Table 4-4:	Exchange current densities of all electrocatalysts before and after CP measurements	59

LIST OF FIGURES

Figure 1-1:	An illustration of an electrolysis cell, with slow kinetics for the anodic reaction which needs to be catalysed. The need exists to develop an improved electrocatalyst with good activity and cost effectiveness for the anode to increase overall efficiency.	2
Figure 2-1:	Schematic presentation of global electricity demand (redrawn from World Energy Resources) [1]	9
Figure 2-2:	Comparison of CO ₂ emissions from fuel combustion in 1973 and 2012 (redrawn from World Energy Resources) [1]	9
Figure 2-3:	The age of energy gases; redrawn from Hefner [8]	11
Figure 2-4:	A Sustainable energy scenario redrawn from Kreuter et al. [17].....	12
Figure 2-5:	Brief historical timeline of OER catalyst development and the foreseen shift in research focus to future OER electrocatalysts (redrawn from Lee et al.) [28]......	15
Figure 3-1:	Top view of the custom manufactured cell with (1) the temperature controlled electrolyte compartment (compartment 1 fits inside compartment 3), (2) the water inlet, (3) the temperature controlled water compartment, (4) the water outlet, (5) the enclosure fasteners, and (6-9) ports for the electrodes and gas purge.	30
Figure 3-2:	LSV measurements of the different VC:Nafion supports prepared at 0 rpm drying rotation rate, compared to clean GC and polycrystalline Ni (current density was calculated by dividing the current by the geometric area of a GC electrode (0.196 cm ²))	34
Figure 3-3:	LSV results for the different VC:Nafion supports (prepared with different drying rotation rates containing a 40 nm Ni thin film). Precise overpotential values at the benchmarking value of 10 mA.cm ⁻² , are included in the legend.	35
Figure 3-4:	LSV of Ni with and without support (insert: i) delamination of Ni in the absence of support [scale = 1 mm], insert ii) no delamination of Ni on sample B [scale = 500 µm]).....	37

Figure 3-5:	CP data for Ni with and without support	37
Figure 3-6:	Illustration of the high-throughput wafer pattern with an inset of the actual working electrodes containing VC:Nafion support	39
Figure 4-1:	a) Illustration of the Au/SiO ₂ (working pad geometric area 0.09 cm ²) wafer pattern with an inset of the actual working electrodes containing VC:Nafion support, and b) an image of VC:Nafion supported GC (5 mm diameter) used for RDE measurements	48
Figure 4-2:	Overpotential results from high-throughput screening of 64 different electrocatalysts on a VC:Nafion supported Au/SiO ₂ wafer at 10 mA.cm ⁻² _{geo}	50
Figure 4-3:	Micrographs of the metal/metal oxide films deposited on VC:Nafion GC electrodes. A scale of 3 μm applies to all three micrographs.	52
Figure 4-4:	Linear sweep voltammetry of Ir, IrO ₂ , Ni, NiO and selected mixed metal oxide samples a) before, and b) after CP	52
Figure 4-5:	EDX and XPS (atomic % Ir) values of the mixed metal oxides before and after CP.....	55
Figure 4-6:	a) Tafel plots at low and high overpotential regions of all the tested metal/metal oxides before CP, b) the relationship between the atomic % Ir with the Tafel slope value before CP, c) Tafel plots of tested metal/metal oxides which reached benchmarking current density at low and high overpotential regions after CP and d) the relationship between the atomic % Ir with the Tafel slope value after CP.....	57

CHAPTER 1: BACKGROUND, AIM AND OBJECTIVES

This chapter is intended to give a general background together with the aims and objectives of this study

Please note that as this dissertation is in article format, the literature referred to in the following sections of Chapter 1 is in addition to the literature used in the introduction of the article(s) listed in Chapters 3 and 4, and in that regard overlap may occur.

1.1 Background and Problem Statement

Sustainable energy production is key to satisfy increasing global energy consumption [1, 2]. Fossil fuels are the primary energy source used to supply the current demand, however, limited reserves and the large contribution to pollution (global warming, air quality, acid rain) render a need to explore alternative energy sources that are sustainable and environmentally accommodating [1, 2]. Renewable energy sources such as solar energy and wind power in conjunction with the appropriate energy technologies, can provide inexhaustible energy with limited to no pollution. However, a fundamental problem related to some renewable energy sources/technologies is the inability to supply the immediate demand that is required or supplying in excess when there is no demand. Consequently, the efficient production and storage of energy is of great concern [1, 3].

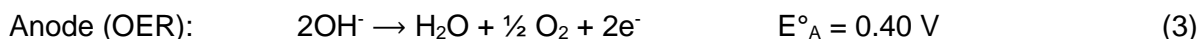
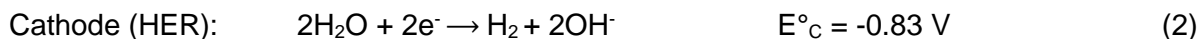
Fuel cell technology offers a sustainable and pollution free means of producing energy by utilising the energy carrier characteristics of hydrogen [1-3]. In a fuel cell, hydrogen and oxygen react to form water and produce energy [4] (reaction 1):



The process of producing water and energy (reaction 1) requires a hydrogen feed. Currently, hydrogen is mainly produced by steam reforming of natural gas, coal gasification and partial oxidation of hydrocarbons [1]. These methods, however, contribute to the global carbon footprint. An increasingly compelling technology which can produce clean hydrogen, while simultaneously addressing the carbon footprint issue, is water electrolysis, i.e. “renewable” hydrogen vs “fossil” hydrogen. Three types of electrolysis technologies are available, i.e. alkaline, proton-exchange membrane (PEM) and solid oxide electrolysis. These technologies can be dated back to the 1800s, where Nicholson and Carlisle discovered the electrolytical decomposition ability of water into hydrogen and oxygen [5, 6]. Solid oxide electrolysis units were developed in 1972 with the first alkaline water electrolysis (AWE) systems available in 1978 [5, 6]. The development of PEM for electrolyzers and fuel cells are a more recent development (~1989) [6]. Alkaline electrolysis of water, however, (hydrogen evolution (reaction 2) on the cathode, (HER) and oxygen evolution

(OER, reaction 3) on the anode) is the favoured technology as it does not require harsh working environments and is already commercially operational [1].

The reactions and standard electrode potentials (E° vs SHE) at 25°C and 1 atm in an alkaline electrolyte are [7]:



One of the common drawbacks of this technology in terms of economic viability and efficient performance, is the catalyst being employed. The OER in comparison with the HER exhibits “sluggish” kinetics and is the main barrier that limits the overall efficiency of AWE (Figure 1-1) [8, 9]. Investigating alternative electrocatalysts for the anodic OER is essential in addressing (i) the poor kinetic performance, and (ii) the efficient operation of the electrolysis process as a whole.

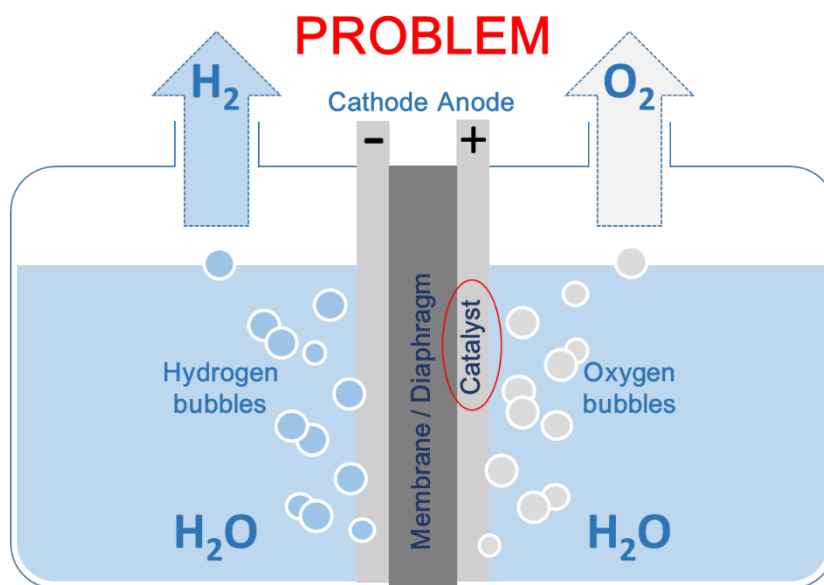


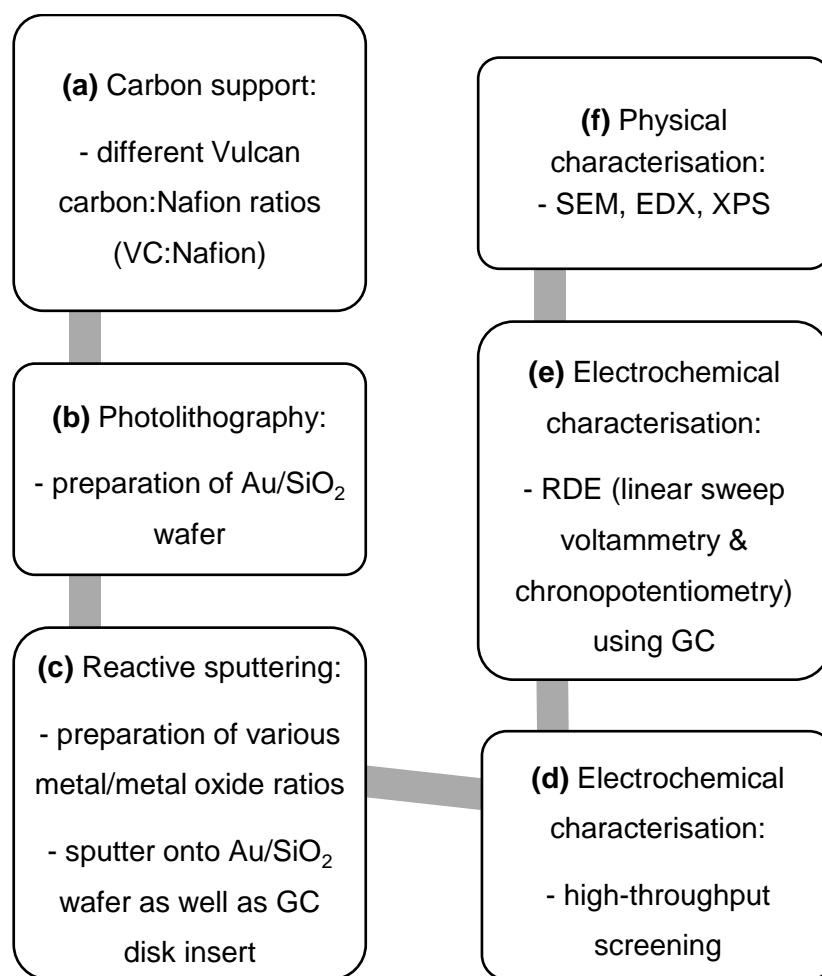
Figure 1-1: An illustration of an electrolysis cell, with slow kinetics for the anodic reaction which needs to be catalysed. The need exists to develop an improved electrocatalyst with good activity and cost effectiveness for the anode to increase overall efficiency.

From literature it has been observed that the OER prefers to occur on an oxide surface [4, 9]. This is supported with the optimal oxygen evolution materials being oxides, RuO_2 and IrO_2 in acidic media [1, 8, 10-12]. These materials, however, are not cost effective when weighed against their poor long-term stability, which is the main drive to search for alternative materials to act as the anode [8, 9, 13]. Many materials, mainly metal based, have been studied in the search for

electrocatalysts that exhibit good activity for the OER. These metals include Fe, Co, Ni, Cd, Pd, Pt and Zn with some of these studied metals exhibiting promising activity, however, with high overpotential, thus making their viability for the use as an electrocatalyst obsolete [4, 11, 12, 14, 15]. Studies conducted on Ni and Ni alloys, however, have shown promising activities and corrosion resistance in alkaline solutions [1, 9, 16]. With the relatively low cost of nickel and the above-mentioned characteristics it possesses, it has become an electrocatalyst material that receives a lot of attention in regard to catalysing the OER in alkaline media [4, 8, 11]. However, Ni and Ni-based electrocatalysts still possess overpotentials that are higher than that of their counterparts in acidic media, Ir and IrO₂. Thus, more research and development are needed to produce electrocatalysts with improved performance and acceptable stability in alkaline media.

The proposed electrocatalyst for this study towards the OER in alkaline media is reactive sputtered Ir_xNi_yO_z electrocatalyst combinations. As mentioned, Ir and IrO₂ are good electrocatalysts for OER in acidic media with Ni-based electrocatalysts showing good activity and stability in alkaline media. Based on these properties, Ir in combination with Ni as an oxide, could render a new electrocatalyst with promising stability and durability, whilst maintaining good activity in an alkaline environment. In addition to the composition that influences the performance of the electrocatalyst, the preparation of the oxides as well as the morphology of the active surface are also important factors to consider [4]. The support for the electrocatalyst plays a role in the overall activity and stability [17]. An increase in surface area of the active material leads to an increase in activity, where stability can be improved by eliminating delamination of the electrocatalyst from the electrode substrate. Vulcan carbon on glassy carbon (VC/GC) will be used as a support for electrocatalysts due to its unique electrical (high electrical conductivity) and structural characteristics (chemical stability in acidic as well as alkaline media) in alkaline solutions rendering it the ability to improve activity and stability [17].

1.2 Methods of Investigation



- a) Different VC:Nafion ratios are evaluated as a support on glassy carbon (GC) disk electrodes in an attempt to increase the active surface area of the electrocatalyst for improved activity, as well as to improve stability (prevent delamination of the electrocatalyst from the electrode substrates, i.e Au/SiO₂ wafer and GC).
- b) Photolithography is used to develop a Au circuit consisting of 64 working electrode pads on a SiO₂ wafer substrate.
- c) Reactive sputtering is employed to deposit Ir, Ni, IrO₂, NiO and 64 different Ir_xNi_yO_z electrocatalyst combinations onto (i) a Au/SiO₂ wafer and (ii) GC disk electrodes.
- d) Electrochemical characterisation performed initially on the electrocatalysts includes high-throughput screening (HTC) of 64 different metal/metal oxide ratios in alkaline media to identify the best electrocatalysts based on overpotential.

- e) Electrochemical characterisation performed on the best performing electrocatalysts according to HTC using GC includes linear sweep voltammetry (LSV) and chronopotentiometry (CP) in a conventional three electrode cell with the use of an alkaline electrolyte to identify the overall best performing metal/metal oxide electrocatalyst.
- f) Physical characterisation performed on the electrocatalysts include SEM, EDX and XPS to evaluate morphology and determine bulk as well as surface metal compositions.

1.3 Aim and Objectives

The aim of this study is to investigate and compare various reactive sputtered $\text{Ir}_x\text{Ni}_y\text{O}_z$ electrocatalyst combinations, with the focus on identifying a possible active and stable $\text{Ir}_x\text{Ni}_y\text{O}_z$ combination to serve as anode electrocatalyst towards the OER in alkaline media.

Objectives:

1. Evaluate available literature on the use of VC as support for electrocatalysts, i.e. preparation techniques and applications.
2. Investigate different VC:Nafion ratios and identify the VC:Nafion ratio which exhibits the best even coverage of GC substrates, highest activity as well as good stability and durability towards the OER.
3. Scrutinise literature on the progress made for electrocatalyst characterisation and evaluation, applicable to the OER in alkaline water electrolysis.
4. Employ reactive oxide sputtering to prepare 64 different $\text{Ir}_x\text{Ni}_y\text{O}_z$ electrocatalyst combinations, using a VC:Nafion supported Au/SiO₂ wafer.
5. Subject the 64 different $\text{Ir}_x\text{Ni}_y\text{O}_z$ electrocatalyst combinations to high-throughput screening by employing a specialised electrochemical cell connected to a 64 channel potentiostat and identify the best (top five) $\text{Ir}_x\text{Ni}_y\text{O}_z$ electrocatalyst combinations for OER.
6. Critically characterise the top five $\text{Ir}_x\text{Ni}_y\text{O}_z$ electrocatalyst combinations, together with their single metal counterparts on GC as substrate, by electrochemical evaluation (RDE) and physical analysis (SEM, EDX, and XPS).
7. Compare and validate where possible, the obtained results with available literature results.
8. Publish results and findings.

1.4 References

1. F.M. Sapountzi, J.M.Gracia, C.J. Weststrate, H.O.A. Fredriksson, J.W. Niemantsverdriet, Electrocatalysts for the generation of hydrogen, oxygen and synthesis gas. *Progress in Energy and Combustion Science*, 2016. 58: p. 1-35.
2. S. Gimenez, J. Bisquert, Photoelectrochemical Solar Fuel Production, ed. J. Bisquert, S. Gimenez. 2016: Springer.
3. C.J. Winter, Hydrogen energy - Abundant, efficient, clean: A debate over the energy-system-of-change. 2009. (34) p. 1-52.
4. R.L. Doyle, M.E.G.Lyons, Chapter 2: The oxygen Evolution Reaction: Mechanistic Concepts and Catalyst Design. 2016: Springer: p.41-104.
5. W. Kreuter, H. Hofmann, Electrolysis: The important energy transformer in a world of sustainable energy. *International Journal of Hydrogen Energy*, 1998. 23(8): p. 661-666.
6. E. Zoulias, E.Varkaraki, N. Lymberopoulos, C.N. Christodoulou, G.N. Karagiorgis, A Review on Water Electrolysis. 2004.
7. Y. Cheng, S.P. Jiang, Advances in electrocatalysts for oxygen evolution reaction of water electrolysis-from metal oxides to carbon nanotubes. *Progress in Natural Science: Materials International*, 2015. 25(6): p. 545-553.
8. M.E.G. Lyons, M.P.Brandon, The Oxygen Evolution Reaction on Passive Oxide Covered Transition Metal Electrodes in Aqueous Alkaline Solution Part-1 Nickel. *International Journal of Electrochemical Science*, 2008. 3: p. 1386-1424.
9. M. Wang, Z. Wang, X. Gong, Z. Guo, The intensification technologies to water electrolysis for hydrogen production A review. *Renewable and Sustainable Energy Reviews*, 2014. 29: p. 573-588.
10. Y. Chen, K. Rui, J. Zhu, S.X. Dou, W. Sun, Recent progress of nickel-based oxide/(oxy)hydroxide electrocatalysts for oxygen evolution reaction. *Chemistry – A European Journal*, 2018. 25(3): p. 703-713.
11. M.Z. Iqbal, R.J. Kriek, Silver/Nickel Oxide (Ag/NiO) Nanocomposites Produced Via a Citrate Sol-Gel Route as Electrocatalyst for the Oxygen Evolution Reaction (OER) in Alkaline Medium. *Electrocatalysis*, 2018. 9(3): p. 279-286.

12. V. Maruthapandian, T. Pandiarajan, V. Saraswathy, S. Muralidharan, Oxygen evolution catalytic behaviour of Ni doped Mn₃O₄ in alkaline medium. RSC Advances, 2016. 6(54): p. 48995-49002.
13. J. Lee, B. Jeong, J.D. Ocon, Oxygen electrocatalysis in chemical energy conversion and storage technologies. Current Applied Physics, 2013. 13(2): p. 309-321.
14. S.Y. Tee, W.S. Teo, L.D. Koh, S. Liu, C. P. Teng, M.Y. Han, Recent Progress in Energy-Driven Water Splitting. Advanced Science, 2017. 4(5): p. 1600337 (1-24)
15. L. Trotochaud, J.K. Ranney, K.N. Williams, S.W. Boettcher, Solution-Cast Metal Oxide Thin Film Electrocatalysts for Oxygen Evolution. Journal of the American Chemical Society, 2012. 134(41): p. 17253-17261.
16. G. Li, L. Anderson, Y. Chen, M. Pan, P.Y.A. Chuang, New insights into evaluating catalyst activity and stability for oxygen evolution reactions in alkaline media. Sustainable Energy & Fuels, 2018. 2(1): p. 237-251.
17. A.L. Dicks, The role of carbon in fuel cells. Journal of Power Sources, 2006. 156(2): p. 128-141.

CHAPTER 2: LITERATURE STUDY

This chapter is intended to give a more in-depth perspective of the research topic at hand.

Please note that as this dissertation is in article format, the literature referred to in the following sections of Chapter 2 is in addition to the literature used in the introduction of the published article(s) listed in Chapters 3 and 4, and in that regard overlap may occur.

“Energy cannot be created or destroyed, it can only be converted from one form to another (as per the first law of thermodynamics). It is this conversion of energy that allows man to progress, however, it is also this very same conversion that causes the environment (and ultimately man) to suffer. Energy is everything, and everything is energy. Man, and the universe in itself is energy, as per Einstein’s equation of $E = mc^2$. The very existence of man and the universe is energy.”
Prof. R.J. Kriek, North-West University

2.1 Energy Consumption and the Environment

Energy usage and supply have significant economic and environmental impacts [1, 2]. The ongoing growth and development of the human race, together with the growing world population and increase in living standards, contribute to the primary concern of the 21st century of sustainable energy supply along with regulated environmental impact. Inevitably this results in a demand for abundant and renewable supply of water, food and energy which is crucial for the sustainability of humanity and the environment. Globally, our energy use totals 370 exajoules (EJ, 10^{18}) per annum; in terms of oil it estimates to around 170 million barrels of oil per day [2, 3]. As a result of the ever-growing global population, global energy consumption also increases rapidly and is predicted to peak at 30 TW (terra watts, per annum) by 2050 [4]. Energy, especially electrical energy, can be seen as the lifeblood of development [2]. Electrical energy production has increased from 12 607 TWh (terra watt hours) per annum in 1993 to 22 202 TWh in 2011 and is estimated to increase to 23 000 TWh by 2020 [1]. Figure 2-1 illustrates the global electricity demand in 2013, with the three main sectors which account for approximately 83% of total electricity consumption being motor vehicles (40-45%), lighting (19%) and household appliances and consumer electronics (21%) [1]. Global energy production can roughly be divided into six main primary sources: 44% petroleum, 26% natural gas, 25% coal, 2.5% hydroelectric power, 2.4% nuclear power and 0.2% non-hydro renewable energy, which accounts for 95% of our energy drawn from fossil fuels [2]. Coal remains the most wide-spread used fossil fuel for energy production around the world despite having very poor environmental credentials, especially CO₂ emissions (Figure 2-2), particulates and other pollutants [1]. Carbon Capture Utilisation and Storage (CCS/CCUS) is a large-scale technology that is being developed to decrease the CO₂

emissions impact from fossil fuels, but due to high cost and low efficiency, the future of this technology is uncertain [1]. Coal reserves have decreased from 1 031 610 Mt (mega ton) to 891 530 Mt while coal production has increased from 4 474 Mt to 7 520 Mt from 1993 to 2011 [1]. Despite the drawbacks which coal possesses, it still remains a primary energy source due to the low cost of mining, the stability and reliability of energy production and the research conducted on increasing efficiency and environmental performance [1].

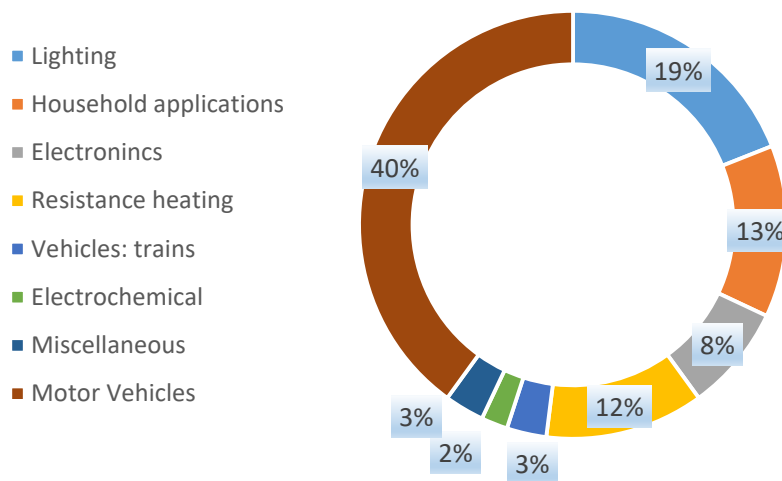


Figure 2-1: Schematic presentation of global electricity demand (redrawn from World Energy Resources) [1]

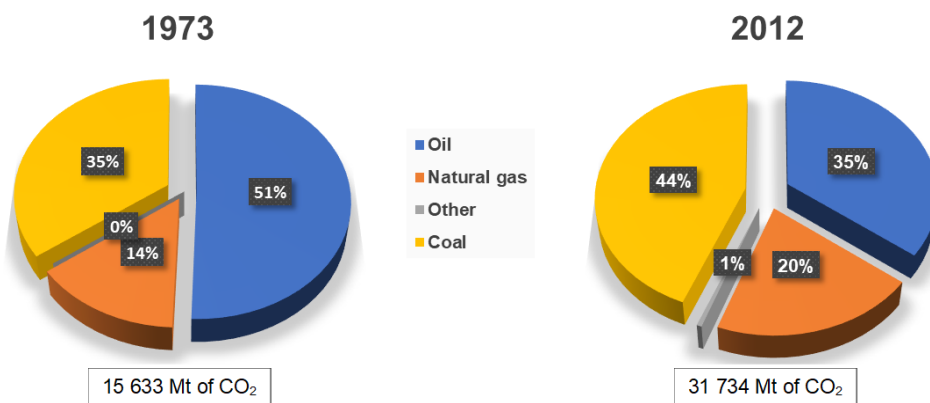


Figure 2-2: Comparison of CO₂ emissions from fuel combustion in 1973 and 2012 (redrawn from World Energy Resources) [1]

Oil is seen as the best energy resource because of its wide range of possible applications, with the main use found in the transport and petrochemical sector [1]. The global oil reserve is approximately 60% larger than it was 20 years ago while production has increased by 25% [1]. Oil reserves and production in the top 5 countries (Venezuela, Saudi Arabia, Canada, Iran and Iraq) and the rest of the world have increased from 140 676 Mt to 223 545 Mt and 3 179 Mt to 3 973 Mt, respectively, between 1993 and 2011 [1]. Natural gas is the “cleanest” fossil-based energy source [1]. Global reserves have increased by 36% over the past 20 years while natural gas production has increased by 61%. Its benefits include relatively clean, flexible and efficient energy production while the drawbacks include the increase of off-shore and remote gas fields, high upfront investment and costly transport and distribution systems [1]. The nuclear industry was developed and initiated in 1954, with uranium as the main source of fuel for nuclear reactors [1]. With high efficiency and no CO₂ emissions, this energy producing system seems to provide an alternative to fossil fuels, but waste disposal and system operation is highly concerning due to the high radioactive nature of uranium [1].

There have been significant changes in the energy industry over the past two decades. Even though certain fossil fuels were thought to be plentiful and able to last for decades in a survey conducted in 2013, it might not be the case [1]. In addition to diminishing reserves, the large contribution to pollution (global warming, air quality, acid rain, carbon foot print, etc.) and strict legislation enforcing environment protection, render a need to explore alternative energy sources that are not dependent on fossil fuels, able to meet increasing energy demands, as well as have a tolerable environmental impact [4-6].

2.2 Renewable Energy Sources

Among renewable energy sources, hydrogen is considered an alternative to fossil fuels [7]. Figure 2-3 illustrates global energy trends based on actual data (1850-2000) and predictions (2000-2150) of different solids, liquids and gases as energy sources. Hefner suggests that the dependability on solids (coal and nuclear, etc.) and liquids (oil and natural gas liquids etc.) for energy production will decrease, whereas the dependability on gases, hydrogen in particular, will become our primary source of energy [8]. It is predicted that by the year 2030 our primary sources of energy will be provided by gases of which hydrogen in particular will be the main energy source [8].

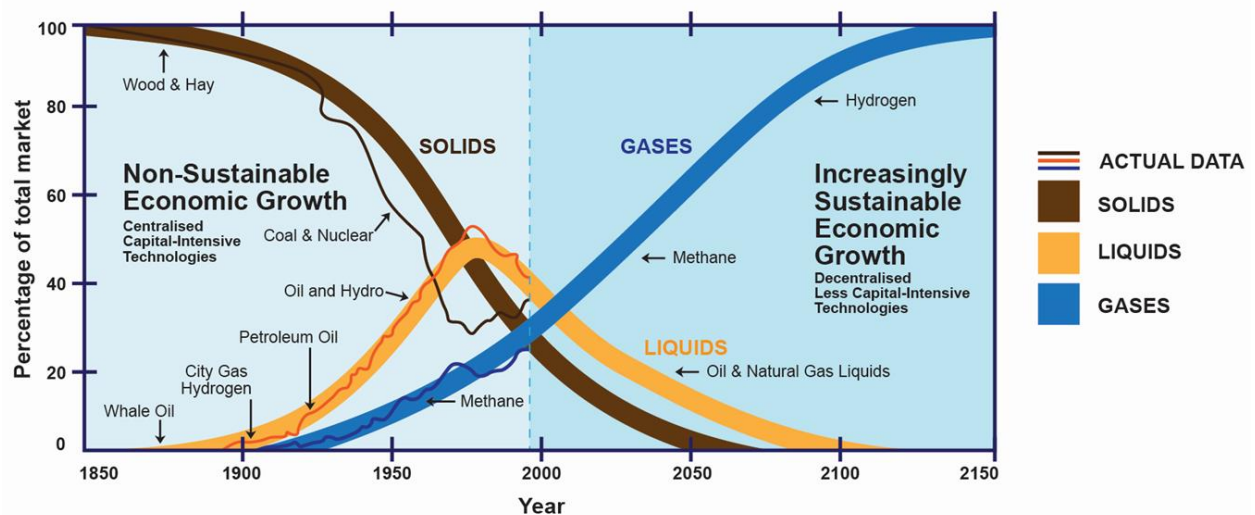


Figure 2-3: The age of energy gases; redrawn from Hefner [8]

Hydrogen is an element consisting of only one proton and one electron [9]. It is the most abundant element in the universe and is a very energy-dense fuel by mass [10]. Hydrogen is present in almost every compound on earth. It is also found in the hydrocarbons that make up the fuels that are currently used as the primary energy producers (gasoline, natural gas, methanol and propane) [9]. Hydrogen is a non-carbon containing energy carrier [10], thus no harmful by-products such as CO, CO₂, CH₄, SO_x, NO_x, heavy metals, etc. is formed during energy production [9], compared to CO₂ emissions produced by combustion of primary energy producing fuels. Hydrogen has no radiotoxicities or radioactivity, making the long-term storage possible when mass produced [10]. In its molecular form (H₂) it is considered to be the ultimate energy source as it can be transported and utilised where needed [9]. As hydrogen is not found in its free form in nature, namely H₂, it requires chemical processing to separate it from other chemical elements [7]. Hydrogen can be extracted from various sources with the majority of hydrogen produced from fossil fuel conversion, that is 48% from natural gas, 30% from the oil industry, 18% from coal gasification and the minority from electrolysis (3,9%) and from other processes (0.1%) [11]. The production of hydrogen is, however, more economically favourable when produced from non-renewable sources, but production from renewable sources is more environmentally accommodating [7].

One of the most promising clean alternative energy producing technologies to date is fuel cell technology, which directly converts chemical energy into electrical energy with no harmful emissions [12]. In 1801 the British chemist, Humphry Davy (1778-1829), discovered the metals sodium, potassium and the alkali metals by splitting common compounds utilising electrolysis via a voltaic pile (first discovered by Alessandro Volta in 1800 [13]) [12]. With his discovery, he later laid the scientific foundation for fuel cells, which was then designed by Christian Frederick Schönbein (1799-1868) in 1838 [12, 14]. The Welsh chemical-physicist, William Robert Grove

(1811-1896), proved that electricity is produced by the electrochemical reaction between oxygen (O_2) and hydrogen (H_2) in the first gas voltaic cell [14, 15]. Thus, for a fuel cell to produce energy in the form of electricity, it has to be fed by oxygen and hydrogen.

Electrolysis is a relatively simple means of producing high purity H_2 and O_2 [16]. A detrimental factor governing the efficient production of H_2 from electrolysis in terms of cost and environmental impact is the electrical source necessary to drive the electrolytic reactions. The most powerful sources of sustainable and environmentally friendly energy, all with individual advantages and disadvantages, include sunlight, hydropower, wind and biomass (Figure 2-4) [5, 17].

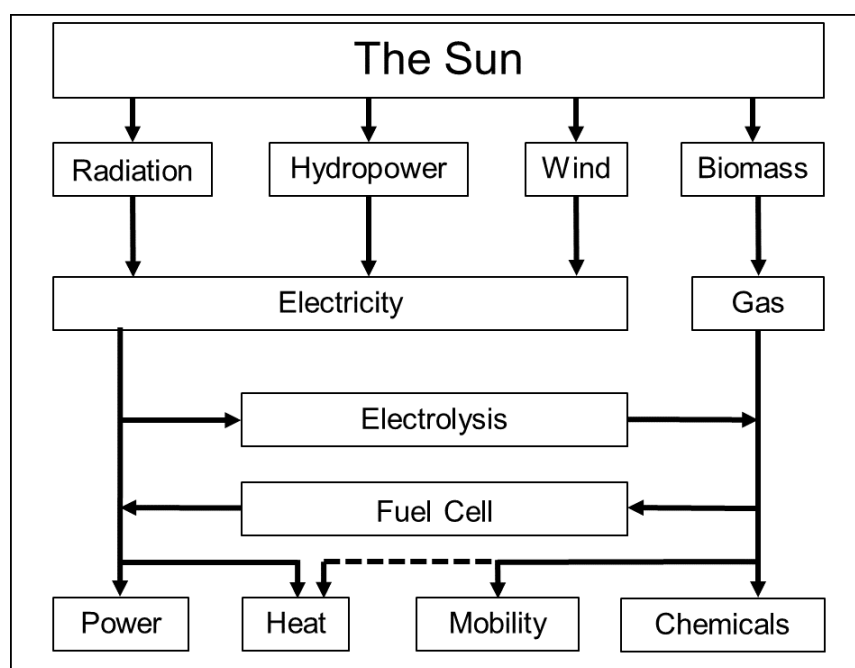


Figure 2-4: A Sustainable energy scenario redrawn from Kreuter et al. [17]

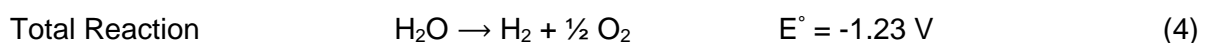
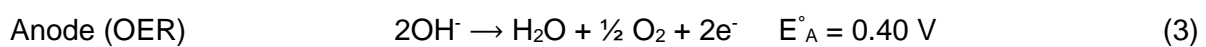
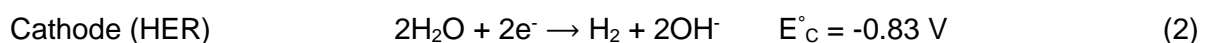
The amount of solar radiation is greater than human needs [18] and can be converted into useable energy by means of photovoltaic cells or solar thermal systems [7]. A disadvantage of solar energy is that sunlight varies with the time of day, season, and daily weather, and at present the conversion efficiency of solar energy to electrical energy is not yet sufficient [6]. The generation of energy utilising wind to drive wind turbines can also be considered a competitive renewable and environmentally friendly energy producer. The usage of wind to generate energy produces zero emissions, it is a relatively simple technology and has almost zero cost for primary fuel generation [19]. The natural variability of the wind is one of the biggest problems facing wind energy alongside aesthetic and ecological objections [19]. Hydroelectric energy is one of the oldest energy production technologies first used in the 19th century [19]. It has one of the lowest

operating costs when compared to other technologies and longer power plant lifetime [19]. It can produce electricity within a few seconds when there is an increase in demand [19]. When weighed against the small fraction of hydro potential that can be utilised in a sustainable fashion, CO₂ and CH₄ emissions from decaying vegetation and the destruction of archaeological and natural ecosystems, this source of energy is still not a viable alternative to fossil fuels [19]. However, irrespective of renewable sources driving electrolysis, the hydrogen that is produced via electrolysis can be stored for later use by fuel cells, overcoming some of the disadvantages of renewable sources driving the electrolytic reactions.

2.3 Alkaline Water Electrolysis

Water electrolysis is one of the most promising, convenient and simplest means of producing hydrogen gas [11-14, 20]. Alkaline water electrolysis (AWE) and proton exchange membrane (PEM) electrolysis are two of the most studied water electrolysis technologies [4, 7]. However, the harsh acidic electrolyte environment requiring the employment of expensive noble metal catalysts, complex operation because of high temperature, the requirement of water purification, and the laboratory scale application, in other words scaling this technology (PEM) to commercial standards for high production rates, renders the large-scale application of this technology unfavourable [4, 7].

AWE has been used since the 1920's for large scale industrial hydrogen production and is sometimes referred to as a mature technology [7]. This technology does not require the harsh working conditions that PEM water electrolysis requires [4]. Using an alkaline media allows for (i) cheaper materials to be used as the electrocatalysts and (ii) circumvents severe corrosion [21, 22]. Applying a current to an alkaline water electrolyser (AWe) produces clean hydrogen by the splitting of water (H₂O) into hydrogen and oxygen (reaction 2,3), as was discovered by Carlisle and Nicholson in the early 1800 [17]. The main reactions taking place inside the AWe are the hydrogen evolution reaction (HER, reaction 2) on the cathode (-) and the oxygen evolution reaction (OER, reaction 3) on the anode (+). The standard electrode potentials (E° vs SHE) given in reactions 2-4 are at 25°C and 1 atm in a 1 M alkaline electrolyte [23]:



Hydrogen evolution (reaction 2) on the cathode proceeds with relatively low overpotential close to its equilibrium potential [24]. Oxygen evolution at the anode, however, suffers from poor kinetics, i.e. low current densities and high overpotentials, making the OER the limiting reaction when compared to the HER. This poor catalytic performance contributes to the total inefficient operation of the AWe [24-26]. Therefore, even though AWE is a mature technology, immense effort is poured into the investigation and development of anode electrocatalysts which exhibit exceptional performance in terms of high current densities, with minimum overpotential, whilst also showing sufficient stability [4, 7].

Various materials to catalyse the electrolysis of water have been discovered since Carlisle and Nicholson conducted their first experiments (Figure 2-5). For an electrocatalyst to be seen as a good catalyst, it must satisfy two basic requirements: i) it must be highly active for the respective reaction, in this case the OER, i.e. it must be able to produce large quantities of oxygen at a minimum overpotential, and ii) the electrocatalyst must be stable/robust enough to maintain efficient oxygen production at commercial working conditions [27]. Electrocatalysts that are used commercially generally meet these requirements, but continued research suggests that improvements are still beneficial to improve on overall efficiency and to adhere to added environmental issues [27]. To evaluate the activity of studied electrocatalysts, the relationship between the current and potential (the driving force) is of primary concern [24]. The Tafel relationship (slope or plot) and the exchange current are the two parameters that are used in this regard [27]. The following Tafel relationship describes the catalytic performance for the oxygen evolution reaction:

$$\eta = b \log (I/I_0) \quad (5)$$

where η is the overpotential, I the observed current, I_0 the exchange current and b the Tafel slope [27]. The Tafel plot is an indication of the increase of potential required for an increase in current 1 order of magnitude and is given in mV/decade (mV.dec^{-1}), in other words an indication of how efficient the electrocatalyst can respond to an applied potential to produce current [27]. It can also provide information on quantitative and mechanistic characterisation of an electrocatalytic process [24]. Along with the Tafel slope, the exchange current, more used and described in terms of geometric area as the exchange current density (j_0 (A.cm^{-2})), is an indication of how vigorously the forward and backward reaction occur [27]. These two parameters together give an indication

on the electronic, geometric (surface area) or combined effects of an electrocatalyst after modification is made for improved catalyst performance [27].

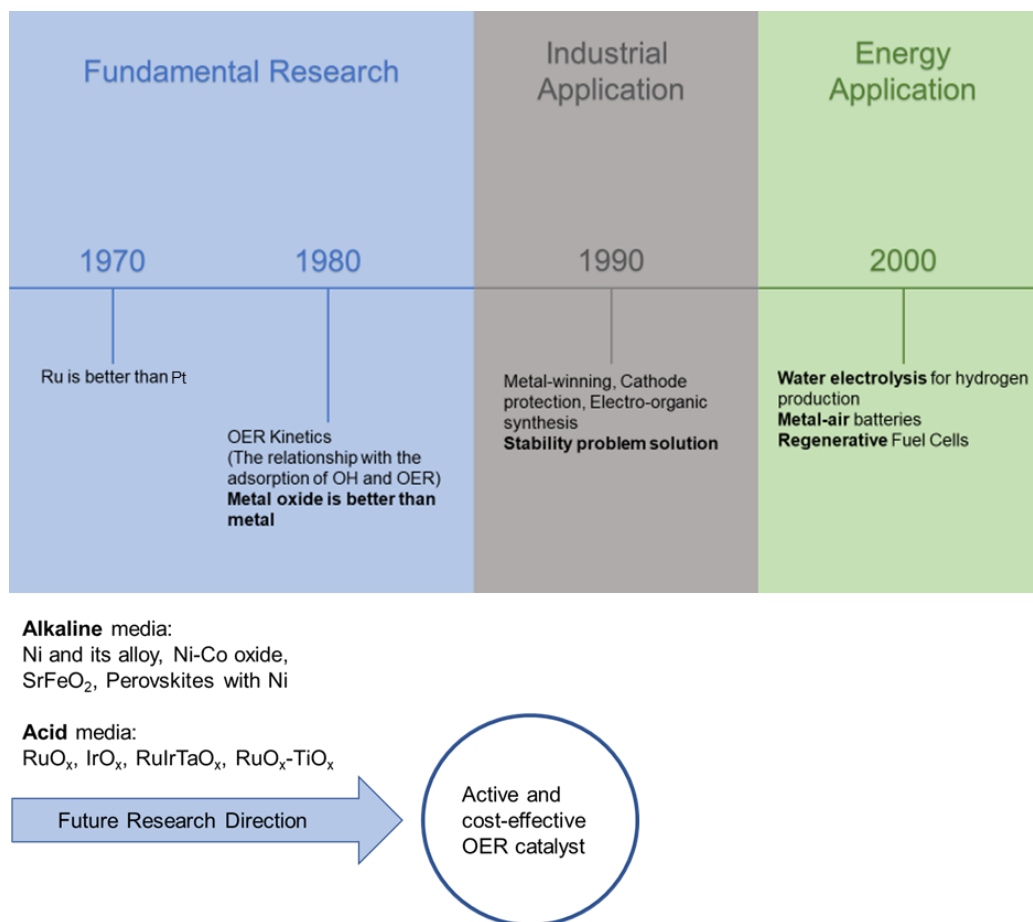


Figure 2-5: Brief historical timeline of OER catalyst development and the foreseen shift in research focus to future OER electrocatalysts (redrawn from Lee et al.) [28].

Much attention is devoted to research on developing electrocatalysts that contain lower amounts of noble metals while still possessing good activity (low overpotentials) and good durability (corrosion resistance in alkaline media) [4, 29-31]. Fine tuning electrocatalysts by combining characteristics of different catalyst components could lead to the development of improved electrocatalysts for the OER in alkaline water electrolysis systems [26, 31].

Under OER conditions, in both alkaline and acidic media, the most active and stable materials are suggested to be metal oxides [24, 25, 28, 32]. In terms of noble metals, it is well known that the most active metal oxides for the OER are RuO₂ and IrO₂, owing to their low overpotential at practical power densities [24, 25, 28, 32]. RuO₂ is usually prepared through thermal decomposition of metal salts onto Ti substrates, and more specifically for OER, produced as sintered-type with Teflon binder, sputtered film or single crystal electrodes [28]. RuO₂ has a disadvantage in alkaline media because of the loss of activity due to the attack by the alkaline

electrolyte [28]. This dissolution has been found to occur even if the electrocatalytic activity is good, and any increase in activity leads to a decrease in stability [4, 28, 30, 33]. Studies on the stability comparison of Ru metal and RuO₂ found that RuO₂/Ti was more corrosion resistant but suffered from a short lifetime due to the unstable RuO₄ formation which leads to dissolution [28]. RuO₂ nanoparticles have also been studied. These nanoparticles can be produced by chemical vapour deposition, electrochemical deposition and polyol methods [34]. Higher activity of RuO₂ nanoparticles compared to Ru on carbon support was reported, but also suffered from instability due to oxide formation on the surface and corrosion of both the nanoparticle and carbon support surfaces above OER potentials [34]. Dissolution of Ru nanoparticles has also been reported with the clear disappearance of nanoparticles from the electrode [33]. Mixing RuO₂ with Ni was found to increase the activity towards the OER, dependent on the Ni content, with severe corrosion still apparent under PEM conditions [31].

IrO₂ exhibits the lowest overpotential for the OER in acidic media [28]. IrO₂ electrodes can be prepared through thermal decomposition, the sputtering of thin films or electrolytic growth from Ir precursors [28]. Even with the most promising activity in acid media, this electrocatalyst undergoes corrosion [28]. Producing IrO₂ nanoparticles increases stability, but like RuO₂ nanoparticles undergo destabilisation due to oxide formation and support corrosion in acid [28]. If IrO₂ and RuO₂ are compared, IrO₂ exhibits the best combination of activity and stability in acidic as well as alkaline media [4]. Both these materials, however, are expensive and not naturally abundant, and therefore make their widespread commercial utilisation unfavourable [24, 35]. Studies have shown that combining RuO₂ and IrO₂ with other metals (transition metals Ni, Co, Mn) improves the stability and corrosion resistance [28, 36]. Transition metals are typically unstable in acidic media but exhibit long term corrosion resistance in alkaline media while being relatively inexpensive [4, 24, 28]. It was found that for alkaline media, the activities of noble as well as non-noble metal oxides are as follows: RuO_x > RhO_x > NiO_x ~ IrO_x > PtO_x ~ PdO_x at fixed overpotential [4, 24, 28]. Studies on oxidising a series of metals (MnO₂, Co₃O₄, NiO, CuO and Fe_xO_y) on nitrogen-doped carbon nanotubes indicated that NiO was the most active electrocatalyst for the OER with Fe_xO_y the least active as well as least efficient [4, 37]. Perez-Alonzo *et al.* studied the effect of combining the activity and stability of Ni with a second element, which showed improvement in electrode performance [4, 38, 39]. They prepared different Ni-Fe electrodes on various substrates (nickel foam, stainless steel mesh, nickel mesh and nickel sheets) and found that the incorporated Fe₂O₃ layer increased the OER activity [4, 39]. Similar studies indicated that the incorporation of Co and Fe could reduce overpotential losses [4, 40]. Studies done by Zhang *et al.* and Wang *et al.* on co-deposited Co and Ni on a nickel plate as hydroxides and a Ni(OH)₂ electrode modified by Co respectively, found that the Co content influenced the OER activity without changing the reaction mechanism [4, 41, 42]. Chi *et al.* also

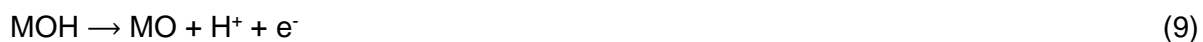
indicated that alloying Co with Ni improved electrocatalytic properties compared to pure Ni for oxygen evolution [4, 43]. Sadiek et al. [44] compared the activity and stability of binary nickel oxide and cobalt oxide nanoparticles on glassy carbon and gold electrodes and found that the binary oxides performed better than the individual oxide-modified electrodes [4, 44]. Tan et al. investigated Zn and Cu spinel type oxides which showed better performance than a metal Ni electrode, with ZnCo_2O_4 and $\text{Cu}_{0.9}\text{Co}_{2.1}\text{O}_4$ outperforming NiCo_2O_4 as well [4, 45]. Even with the studies conducted with different electrocatalyst and with different preparation techniques along with supporting structures, McGrory et al. still suggests that the activity of transition metal oxides is inferior to IrO_2 [4, 46, 47]. However, with evaluation of OER electrocatalyst with benchmarking protocols in terms of catalytic activity, stability, electrocatalytic active surface area, etc., it was found that the overpotential range of 0.35 – 0.43 V at a current density of $10 \text{ mA}\cdot\text{cm}^{-2}$ using NiO_x , CoO_x , NiFeO_x , NiLaO_x , NiCuO_x , NiCeO_x , CoFeO_x and CoP , compared to the overpotential of IrO_2 of 0.32 V, could be compensated for by the lower cost of Ni-based materials [4, 46, 47].

In terms of non-noble metals, Ni is identified as the most practical OER electrode in alkaline water electrolyzers due to its low cost, good corrosion resistance and relative activity for OER, however, it undergoes deactivation with time [4, 25, 28, 29, 37]. On its own, it has a slightly higher overpotential when compared to RuO_2 and IrO_2 in acidic media, but studies have shown that even with state-of-the-art RuO_2 -based catalysts, mixing with Ni can increase OER activity, bearing in mind that different supports, structures and preparation techniques are used [24, 25]. More specifically, combining Ni with IrO_2 as core-shell nanoparticles prepared thermally has shown to improve Ir utilisation and activity towards the OER in PEM electrolyzers [31]. In an effort to understand why this enhanced catalytic activity of Ni modified RuO_2 and IrO_2 occurs, a proposed hydrogen acceptor model, where stabilisation of the MOOH (M = metal) intermediated occurs due to an associative reaction pathway through localised hydrogen bonding for full proton transfer [24]. The added Ni activates O bridge positions, which are normally inactive, such that these bridging O accepts a strong hydrogen bond or can even absorb the hydrogen from the MOH and MOOH intermediates [24]. In terms of OH^- bond strength, Subbaraman et al. [48] showed that the overpotential at a fixed current density of $5 \text{ mA}\cdot\text{cm}^{-2}$ increased in the order $\text{Ni} < \text{Co} < \text{Fe} < \text{Mn}$, indicating that activity is inversely proportional to OH^- bond strength [24]. Nickel exhibits the lowest OH^- bond strength of the studied metals which makes for a promising catalyst. NiO as OER electrocatalyst in alkaline media, however, shows some controversy. Some studies suggest that NiO is a good electrocatalyst [24-26, 46, 47] whereas others suggest otherwise [31, 49]. Studies suggest that a decrease in activity of NiO may be due to the oxidation state of the Ni, specifically $\text{Ni}^{2+,3+,4+}$, the nature of the structure in terms of crystallinity and the possibility of the formation of $\gamma\text{-NiOOH}$ and $\beta\text{-NiOOH}$ (controversy also exists about which form of NiOOH is more favourable for the OER, as some literature suggests the γ -state is active for the OER and others suggest the

β -state as more active.) [44, 49-51]. Furthermore, Jovic et al. [49] suggest that the formation of NiO_2 leads to a substantial reduction in electrical conductivity of the thin film which in turn leads to a reduction in electrocatalytic activity [49].

In an effort to produce an improved electrocatalyst for the OER, analysis and optimisation of surface and bulk structures of the electrocatalysts, electrocatalyst compositions, the preparation method of these electrocatalysts as well as the experimental history of the electrodes are key factors to consider [7, 24, 25]. Different electrode materials have been studied to rationalise electrocatalytic activity in terms of physicochemical properties to determine if one single microscopic parameter controls the entire catalytic process [4, 25]. This microscopic parameter could be any number of catalyst or catalyst-electrolyte interaction properties, of which the interaction between the reaction intermediate and the catalytic surface is key [4, 24]. If the interaction between the intermediate and catalytic surface is too weak, the reactant does not get activated by the catalyst whereas if the interaction is too strong, the catalytic surface can get clogged by intermediates or products which cannot dissociate from the surface which decreases the electrocatalyst activity [4, 24]. This principle is known as the Sabatier principle and states that the best catalyst binds the intermediate neither too weakly nor too strongly [24].

From years of research done on the kinetic and mechanistic components of oxygen evolution, studies are complicated by the fact that it is the metal oxide and not so much the metal that is the catalytic species in the OER (Figure 2-5) [24, 25]. Specifically, for the OER at metal and metal oxide surfaces, suggested intermediates include MOH, MO and MOOH (M = metal) (reactions 8, 9, 10, 11):



This associative mechanistic model was proposed by Norskov et al. [52] and Rossmeisl et al. [53] by utilising quantum chemical calculations based on Density Functional Theory (DFT) [24]. From a thermochemical point of view, the overall rate of the OER is dependent on the energy of the reaction steps involving the bound intermediates and since the energy is dependent on the nature of the catalyst, i.e. surface structure, catalyst support etc., it is important to develop catalysts that use the least amount of energy to be commercially viable [5, 24, 25].

Different surface conditions have been studied in terms of activity and stability, where one metal surface with all bridge and coordinated unsaturated sites occupied by oxygen and one surface occupied by hydroxyl groups [24]. The oxygen covered surface was found to exhibit the highest activity as well as the best stability at the potentials required for the OER to proceed [24]. Thus, the OER can be seen as the formation and decomposition or dissociation of metal surface oxides [24]. The bonding strength of the OH⁻ group to the metal determines the effectiveness of the catalyst, that is the stronger the OH⁻ bond, the weaker the catalyst [24]. Thus, it is suggested that the rate of oxygen evolution is determined by the degree of difficulty in removing the OH⁻ intermediates from the catalyst surface and is thus the rate determining step [24]. It should be noted that this study did not focus on the mechanism of the reaction, thus only a few independent studies were examined. The discussion on the mechanism of the OER as a whole requires its own study. It should also be noted that absolute comparison of mechanisms and the performance of electrocatalysts with literature is to a degree ambiguous due to differences in experimental testing conditions, for example, no equilibrium corrections done for different temperatures and electrolyte concentrations, unclear internal resistance (iR) compensations, and different approaches for normalising data [54-56].

Accompanying the efficiency of an electrocatalyst is the catalyst support. The catalyst support can increase the performance of the electrocatalyst as well as help with material/metal recovery [4, 57]. The support should possess a large surface area as to increase the available active sites of the electrocatalyst, have good electronic conductivity and optimal porosity to allow for example, the dissociation of oxygen bubbles which affects the availability of active sites [4, 57]. Carbon as supporting structure has been studied and shown to improve catalytic properties in comparison to unsupported catalysts [57-59]. Different forms of carbon supporting structure exist and are used, for example, graphene, carbon black and carbon nanotubes [57]. Graphene is a form of carbon that consists of a two-dimensional structure comprising of layers of carbon atoms arranged in six-membered rings, with an increase in layers producible [60]. Carbon black is basically any carbon-containing material that is heated in an inert, oxygen-free environment [57]. It is an amorphous form of carbon with near-spherical particles of graphite with a para-crystalline structure, with the particle size and structure dependent on the source material this type of carbon is synthesised from [57, 61]. Carbon nanotubes are layers of graphite/graphene rolled in a cylindrical manner with single- and multi-walled nanotubes that are often closed off at both ends [57]. Of these forms of carbon each possesses its own unique characteristics and electronic properties with some exhibiting superconductivity, unusual magnetic susceptibility and some show metallic or semi-conductor behaviour [57]. A common, high surface area carbon black that is used for fuel-cell and electrolysis application is Vulcan carbon (VC). It is prepared in the same manner as carbon black and is used as a carbon supporting structure. Qiu et al. investigated the

effect of depositing Ni-Fe hydroxide nanoparticles on VC as support and showed that overpotentials of 280 mV at 10 mA.cm⁻² in 1 M KOH could be achieved [58, 62]. Other studies have shown that using VC as electrocatalyst support increases activity as well as durability in alkaline media [28, 57-59]. A problem that also occurs in electrocatalyst studies is the delamination of the electrocatalyst from GC electrodes and so decreases the durability of the studied electrocatalyst. This problem can be overcome by the utilisation of VC as electrocatalyst support on GC. Thus, the investigation into using VC as electrocatalyst support is fundamental in the aim to research and develop an improved electrocatalyst for the OER in AWE. The characteristics, effects and use of VC are discussed in Chapter 3.

To conclude, AWE is a promising technology that can provide sustainable energy for the growing world population and economy, especially in the transportation sector, with a low to possible zero environmental impact in terms of emissions. This technology however still requires the research and development of highly active, stable, durable and cheap(er) electrocatalyst for the OER to make AWE a viable replacement for current fossil fuel-based energy suppliers. Thus, this study aims to investigate Ir_xNi_yO_z electrocatalyst combinations as an alternative electrocatalyst(s) that provides good activity and stability for oxygen evolution in an alkaline media. The selection of Ir and Ni as the main components in the electrocatalyst is based on (i) the ample literature and evidence that indicates Ir/IrO₂ to exhibit excellent activity performance in acid media, and (ii) the corrosion resistance and activity of Ni(O) in alkaline media. Combining the best properties of these two metals in oxide form (Ir-activity and Ni-stability and activity), alongside the use of Vulcan carbon as supporting structure, may result in an improved Ir_xNi_yO_z electrocatalyst combination for the OER in alkaline media (Chapter 4). The successful completion of this study can add value to the ongoing research and development in alternative electrocatalysts for AWE for the OER.

2.4 References

1. World Energy Council 2013 Survey, World Energy Resources. 2013.
2. J. Chow, R.J. Kopp, P.R. Portney, Energy Resources and Global Development, in Science Mag. 2003. p. 1528-1531.
3. A.K Hussein, Applications of nanotechnology in renewable energies—A comprehensive overview and understanding. Renewable and Sustainable Energy Reviews, 2015. 42: p. 460-476.
4. F.M. Sapountzi, J.M. Gracia, C.J. Weststrate, H.O.A. Fredriksson, J.W. Niemantsverdriet, Electrocatalysts for the generation of hydrogen, oxygen and synthesis gas. Progress in Energy and Combustion Science, 2016. 58: p. 1-35.
5. S. Gimenez, J. Bisquert, Photoelectrochemical Solar Fuel Production, ed. J. Bisquert, S. Gimenez. 2016: Springer.
6. M.S. Dresselhaus, I.L. Thomas, Alternative energy technologies. Nature, 2001. 414: p. 332-337.
7. D.D.A. de Fátima Palhares, L.G.M. Vieira, J.J.R. Damasceno, Hydrogen production by a low-cost electrolyzer developed through the combination of alkaline water electrolysis and solar energy use. International Journal of Hydrogen Energy, 2018. 43(9): p. 4265-4275.
8. R.A. Hefner III, The age of energy gases. International Journal of Hydrogen Energy, 2002. 27(1): p. 1-9.
9. M. Momirlan, T.N. Veziroglu, The properties of hydrogen as fuel tomorrow in sustainable energy system for a cleaner planet. International Journal of Hydrogen Energy, 2005. 30(7): p. 795-802.
10. C.J. Winter, Hydrogen energy - Abundant, efficient, clean: A debate over the energy-system-of-change. 2009. (34) p. 1-52.
11. F. Suleman, I. Dincer, M. Agelin-Chaab, Environmental impact assessment and comparison of some hydrogen production options. International Journal of Hydrogen Energy, 2015. 40(21): p. 6976-6987.
12. U. Lucia, Overview on fuel cells. Renewable and Sustainable Energy Reviews, 2014. 30: p. 164-169.

14. R. Meldola, Christian Friedrich Schönbein, 1799–1868. Ein Blatt zur Geschichte des 19. Jahrhunderts. *Nature*. 1900, 62: p.97-99
15. W.R. Grove, On the Gas Voltaic Battery. Experiments Made with a View of Ascertaining the Rationale of Its Action and Its Application to Eudiometry. *Philosophical Transactions*, 1843. 133: p. 91-112.
16. A. Ursua, L.M. Gandia, P. Sanchis, Hydrogen Production from Water Electrolysis: Current Status and Future Trends. *Proceedings of the IEEE*, 2012. 100(2): p. 410-426.
17. W. Kreuter, H. Hofmann, Electrolysis: The important energy transformer in a world of sustainable energy. *International Journal of Hydrogen Energy*, 1998. 23(8): p. 661-666.
18. M. Fereidooni, A. Mostafaeipour, V. Kalantar, H. Goudarzi, A comprehensive evaluation of hydrogen production from photovoltaic power station. *Renewable and Sustainable Energy Reviews*, 2018. 82: p. 415-423.
19. N. Armaroli, V. Balzani, The Future of Energy Supply: Challenges and Opportunities. *Angewandte Chemie International Edition*, 2007. 46(1-2): p. 52-66.
20. A. Manabe, M.Kashiwase, T. Hashimoto, T. Hayashida, A. Kato, K. Hirao, I. Shimomura, I. Nagashima, Basic study of alkaline water electrolysis. *Electrochimica Acta*, 2013. 100: p. 249-256.
21. V. Maruthapandian, T. Pandiarajan, V. Saraswathy, S. Muralidharan, Oxygen evolution catalytic behaviour of Ni doped Mn₃O₄ in alkaline medium. *RSC Advances*, 2016. 6(54): p. 48995-49002.
22. M. Schalenbach, O. Kasian, K.J.J. Mayrhofer, An alkaline water electrolyzer with nickel electrodes enables efficient high current density operation. *International Journal of Hydrogen Energy*, 2018. 43(27): p. 11932-11938.
23. M. Wang, Z. Wang, X. Gong, Z. Guo, The intensification technologies to water electrolysis for hydrogen production A review. *Renewable and Sustainable Energy Reviews*, 2014. 29: p. 573-588.
24. R.L. Doyle, M.E.G.Lyons, Chapter 2: The oxygen Evolution Reaction: Mechanistic Concepts and Catalyst Design. 2016: Springer. p. 41-104.

25. M.E.G. Lyons, M.P.Brandon, The Oxygen Evolution Reaction on Passive Oxide Covered Transition Metal Electrodes in Aqueous Alkaline Solution Part-1 Nickel. *International Journal of Electrochemical Science*, 2008. 3: p. 1386-1424.
26. M.Z. Iqbal, R.J. Kriek, Silver/Nickel Oxide (Ag/NiO) Nanocomposites Produced Via a Citrate Sol-Gel Route as Electrocatalyst for the Oxygen Evolution Reaction (OER) in Alkaline Medium. *Electrocatalysis*, 2018. 9(3): p. 279-286.
27. M.G. Walter, E.L. Warren, J.R. McKone, S.W. Boettcher, Q. Mi, E.A. Santori, N.S Lewis, Solar Water Splitting Cells. *Chemical Reviews*, 2010. 110(11): p. 6446-6473.
28. J. Lee, B. Jeong, J.D. Ocon, Oxygen electrocatalysis in chemical energy conversion and storage technologies. *Current Applied Physics*, 2013. 13(2): p. 309-321.
29. G. Li, L. Anderson, Y. Chen, M. Pan, P.Y.A. Chuang, New insights into evaluating catalyst activity and stability for oxygen evolution reactions in alkaline media. *Sustainable Energy & Fuels*, 2018. 2(1): p. 237-251.
30. Y. Chen, K. Rui, J. Zhu, S.X. Dou, W. Sun, Recent progress of nickel-based oxide/(oxy)hydroxide electrocatalysts for oxygen evolution reaction. *Chemistry – A European Journal*, 2018. 25(3): p. 703-713.
31. T. Reier, Z. Pawolek, S. Cherevko, M. Burns, T. Jones, D. Teschner, S. Selve, A. Bergmann, H.N. Nong, R. Schogl, K.J.J. Mayrhofer, P. Strasser, Molecular Insight in Structure and Activity of Highly Efficient, Low-Ir Ir–Ni Oxide Catalysts for Electrochemical Water Splitting (OER). *Journal of the American Chemical Society*, 2015. 137(40): p. 13031-13040.
32. Y. Lee, J.Suntivich, K.J. May, E.E. Perry, Y. Shao-Horn, Synthesis and Activites of Rutile IrO₂ and RuO₂ Nanoparticles for Oxygen Evolution in Acid and Alkaline Solutions. *The Journal of Physical Chemistry* 2012. 3: p. 399-404.
33. S. Cherevko, S. Geiger, O. Kasian, N. Kulyk, J.P. Grote, A. Savan, B.R. Shrestha, S. Merzlikin, B. Beitbach, A.Ludwig, K.J.J Mayrhofer, Oxygen and hydrogen evolution reactions on Ru, RuO₂, Ir, and IrO₂ thin film electrodes in acidic and alkaline electrolytes: A comparative study on activity and stability. *Catalysis Today*, 2016. 262: p. 170-180.
34. Y. Lee, J.Suntivich, K.J. May, E.E. Perry, Y. Shao-Horn, Synthesis and Activites of Rutile IrO₂ and RuO₂ Nanoparticles for Oxygen Evolution in Acid and Alkaline Solutions. *The Journal of Physical Chemistry* 2012. 3: p. 399-404.

35. B.M. Hunter, H.B. Gray, A.M. Müller, Earth-Abundant Heterogeneous Water Oxidation Catalysts. *Chemical Reviews*, 2016. 116(22): p. 14120-14136.
36. M.H. Miles, Y.H. Huang, S. Srinivasan, The Oxygen Electrode Reaction in Alkaline Solutions on Oxide Electrodes Prepared by the Thermal Decomposition Method. *Journal of Electrochemistry Society*, 1978. 125(12): p. 1931 - 1934.
37. N.I. Andersen, A. Serov, P. Atanassov, Metal oxides/CNT nano-composite catalysts for oxygen reduction/oxygen evolution in alkaline media. *Applied Catalysis B: Environmental*, 2015. 163: p. 623-627.
38. S. Seetharaman, R. Balaji, K. Ramya, K.S. Dhatharhreyan, M. Velan, Electrochemical behaviour of nickel-based electrodes for oxygen evolution reaction in alkaline water electrolysis. *Ionics*, 2014. 20(5): p. 713-720.
39. F.J. Pérez-Alonso, C. Adan, S. Rojas, M.A. Pena, J.L.G. Fierro, Ni/Fe electrodes prepared by electrodeposition method over different substrates for oxygen evolution reaction in alkaline medium. *International Journal of Hydrogen Energy*, 2014. 39(10): p. 5204-5212.
40. X. Li, F.C. Walsh, D. Pletcher, Nickel based electrocatalysts for oxygen evolution in high current density, alkaline water electrolyzers. *Physical Chemistry Chemical Physics*, 2011. 13(3): p. 1162-1167.
41. Y. Zhang, X. Cao, H. Yuan, W. Zhang, Z. Zhou, Oxygen evolution reaction on Ni hydroxide film electrode containing various content of Co. *International Journal of Hydrogen Energy*, 1999. 24(6): p. 529-536.
42. X. Wang, H. Lou, H. Yang, P.J. Sebastian, S.A. Gomboa, Oxygen catalytic evolution reaction on nickel hydroxide electrode modified by electroless cobalt coating. *International Journal of Hydrogen Energy*, 2004. 29(9): p. 967-972.
43. C. Chi, X. Yang, Y. Gong, N. Wang, Deposition of Ni–Co by cyclic voltammetry method and its electrocatalytic properties for oxygen evolution reaction. *International Journal of Hydrogen Energy*, 2005. 30(1): p. 29-34.
44. I.M. Sadiq, A.M. Mohammad, M.E. El-Shakre, M.S. El-Deab, B.E. El-Anadouli, Enhanced electrolytic generation of oxygen gas at binary nickel oxide–cobalt oxide nanoparticle-modified electrodes. *Journal of Solid-State Electrochemistry*, 2013. 17(3): p. 871-879.

45. Y. Tan, C. Wu, H. Lin, J. Li, B. Chi, J. Pu, Li Jian, Insight the effect of surface Co cations on the electrocatalytic oxygen evolution properties of cobaltite spinels. *Electrochimica Acta*, 2014. 121: p. 183-187.
46. C.C.L. McCrory, S.Jung, J.C. Peters, T.F. Jaramillo, Benchmarking Heterogeneous Electrocatalysts for the Oxygen Evolution Reaction. *Journal of the American Society*, 2013. 135: p. 16977-16987.
47. C.C.L. McCrory, S.Jung, I.M. Ferrer, S.M. Chatman, J.C. Peters, T.F. Jaramillo, Benchmarking Hydrogen Evolving Reaction and Oxygen Evolving Reaction Electrocatalysts for Solar Water Splitting Devices. *Journal of the American Chemical Society*, 2015. 137: p. 4347 - 4357.
48. R. Subbaraman, D. Tripkovic, K.C Chang, D. Strmcnik, A.P. Paulikas, P. Hirunsit, M. Chan, J. Greeley, V. Stamenkovic, N.M. Markovic, Trends in activity for the water electrolyser reactions on 3d M(Ni,Co,Fe,Mn) hydr(oxy)oxide catalysts. *Nature Materials*, 2012. 11(6): p. 550-557.
49. B.M. Jovic, V.D.Jovic, U.C. Lacnjevac, L.J. Gajic-Krstajic, N.V. Krstajic, Electrodeposited Ni-Sn coatings as electrocatalysts for hydrogen and oxygen evolution in alkaline solutions. *Zaštita materijala*, 2016. 57(1): p. 136-147.
50. A.J. Tkalych, K. Yu, E.A. Carter, Structural and Electronic Features of β -Ni(OH)₂ and β -NiOOH from First Principles. *The Journal of Physical Chemistry C*, 2015. 119(43): p. 24315-24322.
51. M. Merrill, M. Worsley, A. Wittstock, J. Biener, M. Stadermann, Determination of the "NiOOH" charge and discharge mechanisms at ideal activity. *Journal of Electroanalytical Chemistry*, 2014. 717-718: p. 177-188.
52. J. Greeley, I.E.L. Stephens, A.S. Bondarenko, T.P. Johansson, H.A. Hansen, T.F. Jaramillo, J. Rossmeisl, I. Chorkendorff, J.K. Nørskov, Alloys of platinum and early transition metals as oxygen reduction electrocatalysts. *Nature Chemistry*, 2009. 1(7): p. 552-556.
53. J. Rossmeisl, Z.W.Qu, H. Zhu, G.J. Kroes, J.K. Nørskov, Electrolysis of water on oxide surfaces. *Journal of Electroanalytical Chemistry*, 2007. 607(1): p. 83-89.
54. K. Zeng, D. Zhang, Recent progress in alkaline water electrolysis for hydrogen production and applications. *Progress in Energy and Combustion Science*, 2010. 36(3): p. 307-326.

55. A.N. Colli, H.H. Girault, A. Battistel, Non-Precious Electrodes for Practical Alkaline Water Electrolysis. *Materials*, 2019. 12(8): p. 1336.
56. D. Pletcher, X. Li, Prospects for alkaline zero gap water electrolyzers for hydrogen production. *International Journal of Hydrogen Energy*, 2011. 36(23): p. 15089-15104.
57. A.L. Dicks, The role of carbon in fuel cells. *Journal of Power Sources*, 2006. 156(2): p. 128-141.
58. M. Görlin, J.F de Araujo, H. Schmies, D. Bernsmeier, S. Dresp, M. Gliech, Z. Jusys, P. Chernev, R. Kraehnert, H. Dau, P. Strasser, Tracking Catalyst Redox States and Reaction Dynamics in Ni–Fe Oxyhydroxide Oxygen Evolution Reaction Electrocatalysts: The Role of Catalyst Support and Electrolyte pH. *Journal of the American Chemical Society*, 2017. 139(5): p. 2070-2082.
59. E. Auer, A. Freund, J. Pietsch, T. Tacke, Carbons as supports for industrial precious metal catalysts. *Applied Catalysis A: General*, 1998. 173(2): p. 259-271.
60. C.N.R. Rao, K.S. Subrahmanyam, A. Govindaraj, Graphene: The New Two-Dimensional Nanomaterial. *Angewandte Chemie International Edition*, 2009. 48(42): p. 7752-7777.
61. J. Bayer, S. Ergun, An X-ray study of carbon blacks produced from coals. *Carbon*, 1967. 5(2): p. 107-111.
62. Y. Qiu, L. Xin, W. Li, Electrocatalytic Oxygen Evolution over Supported Small Amorphous Ni–Fe Nanoparticles in Alkaline Electrolyte. *Langmuir*, 2014. 30(26): p. 7893-7901.

CHAPTER 3: VULCAN CARBON AS SUPPORT FOR SPUTTERED OXYGEN EVOLUTION ELECTROCATALYSTS

CHAPTER OVERVIEW

The development of support structures for electrocatalysts has received a great deal of attention over the last decade, with carbon structures (i.e. nanostructures, Vulcan carbon (VC), etc.) having been studied extensively. Carbon support structures increase the surface area, stability and activity of electrocatalysts in most cases, and can be used to overcome the delamination of thin films. In an attempt to (i) obtain surface structures and areas on SiO₂ wafer pads, for combinatorial high-throughput sputtering and screening, that are comparable to glassy carbon (GC), (ii) eliminate delamination of the electrocatalyst, and (iii) increase activity and stability, this study focused on VC:Nafion support preparation techniques. Four VC inks with different VC:Nafion ratios were prepared and used as carbon support on GC electrode inserts to analyse their effect on the activity of sputtered Ni thin films (40 nm) towards the oxygen evolution reaction (OER) in alkaline media. Linear sweep voltammetry (LSV) and chronopotentiometry (CP) were employed to compare the catalytic activity and stability of these sputtered Ni thin films on the various VC supports. Results suggest that similar activity compared to IrO₂ and RuO₂ could be achieved by sputtered Ni on VC:Nafion (1:0.67) support, indicating improved Ni utilisation as well as improved short-term stability of the Ni thin films. These results validate the use of VC:Nafion support as substrate for sputtered electrocatalysts.

Publication reference: Coertzen, D., Kriek, R.J., Levecque, P.B.J. et al. *Electrocatalysis* (2019) 10: 604. <https://doi.org/10.1007/s12678-019-00549-y>

3.1 Introduction

The development of support structures for electrocatalysts, as a means of increasing activity, stability and/or durability during electrocatalyst testing and evaluation [1, 2], has received a great deal of interest and attention over the last decade, with carbon support structures in particular having been studied to a great extent [1, 3-11]. Carbon support structures have found widespread application due to its enhancement of the catalytic properties of electrocatalysts, i.e. good dispersion of metallic particles, the stabilisation of these particles in both acidic and especially basic environments, and improved catalytic activity [1, 5, 11, 12]. The main carbon supporting structures include nanostructures, graphite, composite materials, fullerenes, carbon fibre, carbon black and VC [1, 5, 8, 13].

The use of carbon support structures has furthermore increased the economic lifecycle of precious metal electrocatalysts in that it allows for ease of electrocatalyst removal and recycling [1, 5]. The most widely used form of carbon support is activated carbon, graphite, carbon black and VC [5], with VC (XC 72R) possessing high electrical conductivity, acceptable chemical stability in highly acidic and basic media, as well as low cost [1, 3]. The morphology of carbon has a large influence on metal activity in that it increases surface area as well as disperses the active metal on the electrode due to its porous structure and particle size [1, 3]. When employing VC as a catalyst support, it is generally mixed with perfluorosulfonic acid (Nafion) to (i) ensure good dispersion of the VC, thereby optimising the area of catalytic activity [10, 14], and (ii) create a durable bond between the carbon support and the substrate/electrode [10, 15]. The Nafion ionomer surface microstructure consists of hydrophobic and hydrophilic structures with the primary role of facilitating proton (H^+) transport to and from catalytic sites [8]. The performance of the electrocatalyst is therefore dependent on an optimum Nafion content, which is directly connected to the effectivity of the VC to be loaded onto the GC [10, 14]. As there does not exist one specific VC:Nafion ratio that is generally used when investigating an electrocatalyst for use in a specific application or reaction of interest, it is important to invest time in identifying an optimum VC:Nafion ratio applicable to a specific application/reaction of interest.

In this paper the reaction of interest is the OER in alkaline media. The OER receives substantial interest due to the kinetic limitations it imposes on efficient water electrolysis as a means of producing a clean and renewable energy storage medium, in the form of hydrogen. Investigating alternative electrocatalysts for the OER is the preferred route in overcoming these kinetic limitations towards realising alkaline water electrolysis as an effective large-scale hydrogen production technology. A fast and effective means of investigating alternative electrocatalysts is through high-throughput screening. It is a method to rapidly produce a large library of electrocatalysts and associated data, compared to the conventional single sample synthesis and testing procedures [16, 17].

Investigation of the VC:Nafion as support would seem to be a futile exercise as this has been well-scrutinised, specifically with regard to nanoparticle catalyst synthesis. However, to sputter thin films on top of a VC:Nafion support is a novel approach, which results in the active material not mixing into the bulk of the VC:Nafion support, but being present at the surface with all the active materials being in contact with the reaction of interest. This study is multifaceted, with the main goal being to identify a specific VC:Nafion preparation procedure that is beneficial for studying electrocatalysts that are prepared as sputtered thin films on (i) SiO_2 wafers containing Au as electric circuit, i.e. Au/ SiO_2 acting as the high-throughput testing substrate, and (ii) GC electrode inserts acting as the substrate for more accurate single electrode controlled testing.

This is important as it is imperative to (i) minimise physical/structural differences when comparing data that result from utilising different substrates (in this case Au/SiO₂ and GC), and (ii) prevent delamination of the thin film from the substrate during testing, with the ultimate goal being to improve electrocatalyst performance in terms of current output and stability.

As Ni has been found to be the most practical OER electrocatalyst/electrode for alkaline water electrolysis, it will serve as the electrocatalyst of choice for identifying an effective VC:Nafion ratio that can be implemented in both high-throughput screening and conventional electrochemical testing.

3.2 Experimental

3.2.1 Preparation and physical characterisation of VC:Nafion support

VC:Nafion support was deposited onto GC as electrode substrate for RDE measurements. The technique used for preparing the GC electrode insert surface was discussed in detail in previously reported work [18]. VC (XC-72R) was dried at 40°C and used to create the carbon ink that was deposited onto the GC surface. 5 wt% Nafion (Sigma Aldrich) was diluted to 1 wt% by adding isopropanol (Merck). VC:Nafion mass ratios of 1:0.5, 1:0.67, 1:1 and 1:1.5 were subsequently prepared. The carbon ink was then sonicated for 2h to ensure proper mixing of VC and Nafion to produce the VC:Nafion support. 10 µl of VC:Nafion support was loaded onto the GC and dried utilising different rotation rates (0 rpm, 500 rpm, 700 rpm) so as to investigate the effect thereof on the drying characteristics of the VC supports [19]. For the rotation rate of 0 rpm the GC, containing the VC:Nafion ink, was covered with a glass beaker to encourage even drying. Physical characterisation of the dried supports included scanning electron microscopy (SEM FEI Quanta 250 FEG (Bruno, Czech Republic) with integrated software) for visual evaluation of the different VC inks, sputtering, calibration and electrochemical characterisation

A custom-designed physical vapour deposition (PVD) system (PVD Products, USA) was employed for the sputtering of Ni thin films on clean, smooth GC and VC:Nafion supported GCs as well as on an Au/SiO₂ wafer [20, 21]. The Au/SiO₂ wafer was prepared as described earlier [26]. The Au circuit, excluding the working and contact pads, was covered with epoxy resin to isolate the circuit from the support and the electrolyte. VC:Nafion support was loaded onto the Au/SiO₂ substrate by employing a patterned plastic (stencil) with pressure sensitive adhesive on one side, that matches the working pads of the circuit pattern. The sputtering rate of Ni was calibrated at a base pressure of 10 mTorr and an Ar flow rate of 0.025 L/min. The following

calibration relation, $y = 0.1144x - 0.0022$ (y = sputtering rate (nm/min) and x = power (W)), was obtained and employed to determine the thickness (40 nm) and amount (6.8 μg) of sputtered Ni.

3.2.2 Electrochemical characterisation

Electrochemical characterisation employing the sputtered GC as the working electrode, a Hg/HgO reference electrode (0.1 M KOH, ALS, distributed by BAS Inc.), a Pt spiral counter electrode, and 0.1 M KOH (CC Immelmann) as electrolyte, were conducted in a plastic (high density KOH resistant polypropylene) three electrode cell configuration (Figure 3-1) [9]. High-throughput screening was conducted in a coated glass cell (alkaline resistant). Calibration of the reference electrode was done in 0.1 M KOH using a polycrystalline Pt working electrode under H_2 saturation, employing a scan rate of 5 mV.s^{-1} and a potential range of -0.1 V to -0.9 V vs Hg/HgO [9, 22]. The potential at which hydrogen evolution changes to hydrogen oxidation was measured to be -0.866 V. This value was used to convert all potentials relative to the Reversible Hydrogen Electrode ($E(\text{RHE}) = E(\text{Hg/HgO}) + 0.866 \text{ V}$) and correlated very well with a reported value of -0.855 V [9]. All subsequent reported potentials are in reference to the RHE.

Internal resistance (iR) was determined (21.65 Ω) for a 0.1 M KOH solution with a polycrystalline Pt working electrode and Hg/HgO reference electrode under O_2 purging, and the associated iR -drop was compensated for in-situ by using the EC-lab software (version 11.01).



Figure 3-1: Top view of the custom manufactured cell with (1) the temperature controlled electrolyte compartment (compartment 1 fits inside compartment 3), (2) the water inlet, (3) the temperature controlled water compartment, (4) the water outlet, (5) the enclosure fasteners, and (6-9) ports for the electrodes and gas purge.

LSV measurements were performed with a scan rate of 5 mV.s^{-1} and a potential range of 0 V – 0.9 V vs Hg/HgO at 1600 rpm [22-26] under O_2 saturation [23, 27]. O_2 saturation ensures that the equilibrium potential is not influenced by the O_2 produced during the OER. Rotation is used to facilitate removal of O_2 from the electrocatalytic surface, that may be formed during the reaction, and intermediate (OH^-) transport to the electrocatalytic surface [22, 24, 26]. CP measurements

were also performed under O₂ saturation, with an applied current of 2 mA (comparative to 10 mA.cm⁻²) for 6 hours.

A benchmarking value of 10 mA.cm⁻² for the activity and durability testing of the Ni thin film on clean VC:Nafion supported GC was employed [11, 24, 25, 28-32]. This value was reported as the norm in literature and is also employed specifically for thin film analysis for alkaline water electrolysis [11, 22, 24-26, 28-32].


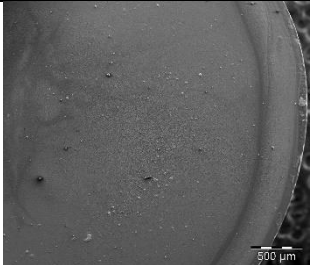

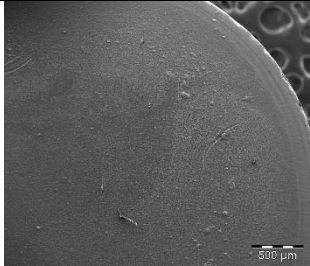


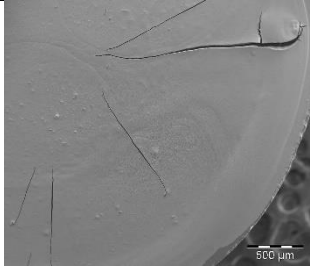
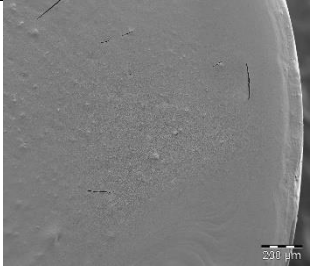

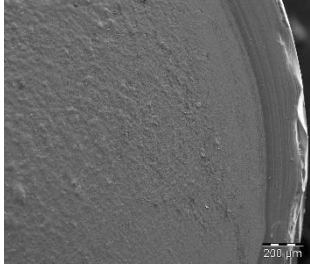

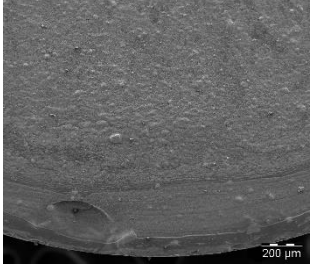
3.3 Results and Discussion

The goal of using a carbon support is twofold: (i) to increase the electrode surface roughness, i.e. to increase the contact area between the electrocatalyst and the species of interest for adsorption, electron transfer, intermediate formation, and desorption of the intermediates/products from the electrocatalyst surface [2, 33], and (ii) to increase the durability/lifetime of the electrocatalyst in that delamination from the electrode substrate is reduced/eliminated [1, 3]. For a carbon support to be classified as being well prepared, it should exhibit the following characteristics: be conductive, show good coverage of the electrode surface, show no cracking of the surface, have no peripheral “coffee ring”, and be stable in the selected electrolyte medium [1, 3, 10].

SEM images of the four VC:Nafion supports on GC, at two different magnifications, are depicted in Table 3-1. Sample A shows varying VC:Nafion coverage with varying drying rotation rates. Clear clumping of the support on the surface and the formation of a coffee ring for all the rotations are noticeable. Sample B shows similar coverage to sample A, also with different degrees of irregular clumping of the support and the formation of noticeable coffee rings for all the rotation rates. Clear signs of cracking are also visible at a drying rotation of 500 rpm. Sample C shows initial smooth coverage with no clear clumping of the support and no visible coffee ring, however, severe cracking of the surface occurred. Sample D shows the most homogeneous coverage, with no signs of a cracked surface, no irregular clumping of the support, and a coffee ring only being visible in the absence of rotation. In general, the formation of a coffee ring is attributed to the drying of a liquid droplet containing suspended particles on a solid planar surface (at the pinned contact line at the edge of the drop) as a result of capillary flow [19, 34]. As evaporation proceeds liquid loss at the edge of the droplet is greater than in the centre, which causes an outward flow of liquid from the centre of the droplet to the edge. This liquid flow carries suspended particles along with it, causing agglomeration to occur and results in a non-uniform layer of substrate on the GC surface [19, 34]. In an attempt to overcome this phenomenon, a spin coating methodology was implemented with the expectation of producing more uniform covered surfaces [19]. In

contrast to the natural flow of ink from the centre of the electrode to the edge in the absence of rotation, rotation of the electrode results in (i) faster distribution of the ink to the edge of the GC substrate through centrifugal force, and (ii) an increased rate of evaporation of the isopropanol. However, as can be seen from SEM data, drying the surfaces at different rotation rates does not seem to have a consistent effect on the uniformity of the surface [19].

Table 3-1: SEM images of the different VC:Nafion inks deposited on GC insert electrodes at different drying rotation rates.

Sample (VC:Nafion)	Rotation rate		
	0 rpm	500 rpm	700 rpm
A (1:1.5)			
B (1:0.67)			
C (1:0.5)			
D (1:1)			

It was also noted that using water in the production of the ink worsened the effect of the coffee ring and associated agglomeration. This is due to the fact that water has a higher surface tension and dries much slower than isopropanol, which resulted in water being excluded as an ingredient for ink production.

A preferred support cannot, however, be selected based purely on the physical characterisation (SEM) thereof, as the effect of conductivity, activity and stability of the support (with and without electrocatalyst), on the OER, has to be investigated electrochemically. In addition, it is not clear from the SEM data, whether utilising different drying rotation rates are necessary for improving the drying of a VC:Nafion support.

A requirement for electrocatalyst development, especially in the case of new alternative metal/metal oxide combinations for the OER, is that the support assists in improving the activity and stability of the electrocatalyst that it supports, however, the observed activity should not be a direct result of the support participating in the reaction. Thus, the activity that is observed should be a result of the electrocatalyst(s) under investigation and not the support. The contrary is also true, i.e. that the support should not inhibit the activity of the active component (in this case the thin film electrocatalyst). Hence, the different VC:Nafion supports were evaluated, in the absence of any deposited electrocatalytic material, for their indirect activity enhancement towards the OER (Figure 3-2), if any, and how significant this activity is compared to that of a known electro-active metal (such as Ni) for the OER [2, 13, 33, 35, 36]. A standard polycrystalline Ni disk electrode was used for activity comparison as Ni is known to be active for the OER [2, 13, 33, 35, 36]. A clean GC, which serves as the substrate for these supports, was also included in the evaluation.

All of the VC:Nafion supports resulted in a, though small, higher activity towards the OER than the clean GC, which can be attributed to the functionalised groups present in Nafion (Figure 3-2) [8, 14]. However, overall, the different VC:Nafion supports and clean GC did not exhibit significantly higher current outputs in comparison with the active polycrystalline Ni. This observation of negligible low currents is attributed to the fact that Nafion is not a suitable ionomer binder to be used when in direct contact with an alkaline environment [37], as it results in lower estimates of activity [37]. To this regard any observed current is a direct result of the electrocatalysts employed and not the support.

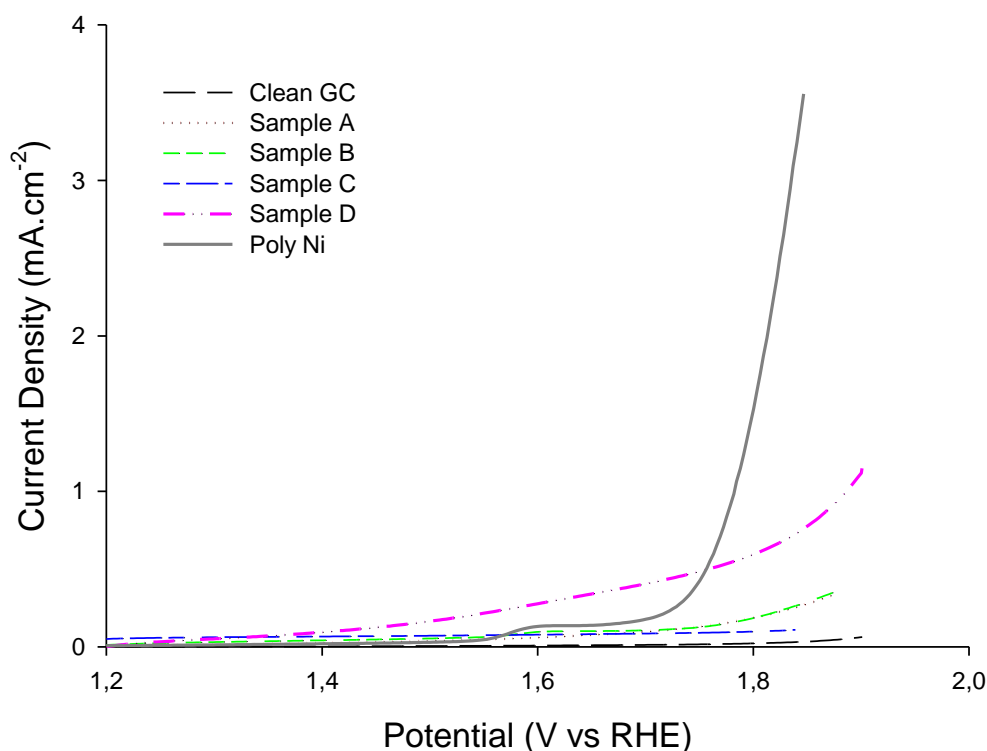


Figure 3-2: LSV measurements of the different VC:Nafion supports prepared at 0 rpm drying rotation rate, compared to clean GC and polycrystalline Ni (current density was calculated by dividing the current by the geometric area of a GC electrode (0.196 cm²))

To study the effect of the different VC:Nafion supports on the activity and stability of the electrocatalysts, 40 nm thin films of Ni were sputtered onto the GCs containing a 10 μ L loading of each of the four different VC:Nafion supports. Due to the cracking of the surface of sample C, it was excluded for further evaluation. A small difference in overpotential at the benchmarking current of 10 mA.cm⁻² could be observed for the different samples at the corresponding rotation rates (Figure 3-3). It is clear that the employment of different rotation rates, as a means to dry the VC:Nafion support(s) evenly, has very little effect on significantly improving the activity of the Ni electrocatalyst. In general, sample B at a drying rotation of 0 rpm, exhibited the lowest overpotential (0.401 ± 0.003 V) at the benchmarking current of 10 mA.cm⁻². Taking both the electrochemical behaviour and the visual evaluation (Table 3-1) into consideration, sample B was selected for further investigation as (i) this sample exhibited the lowest overpotential towards the OER, (ii) employing a 0 rpm to dry the support resulted in fast and parallel substrate preparation as no rotation equipment was required, and (iii) a minimal “coffee ring” was present, with acceptable coverage of the GC substrate.

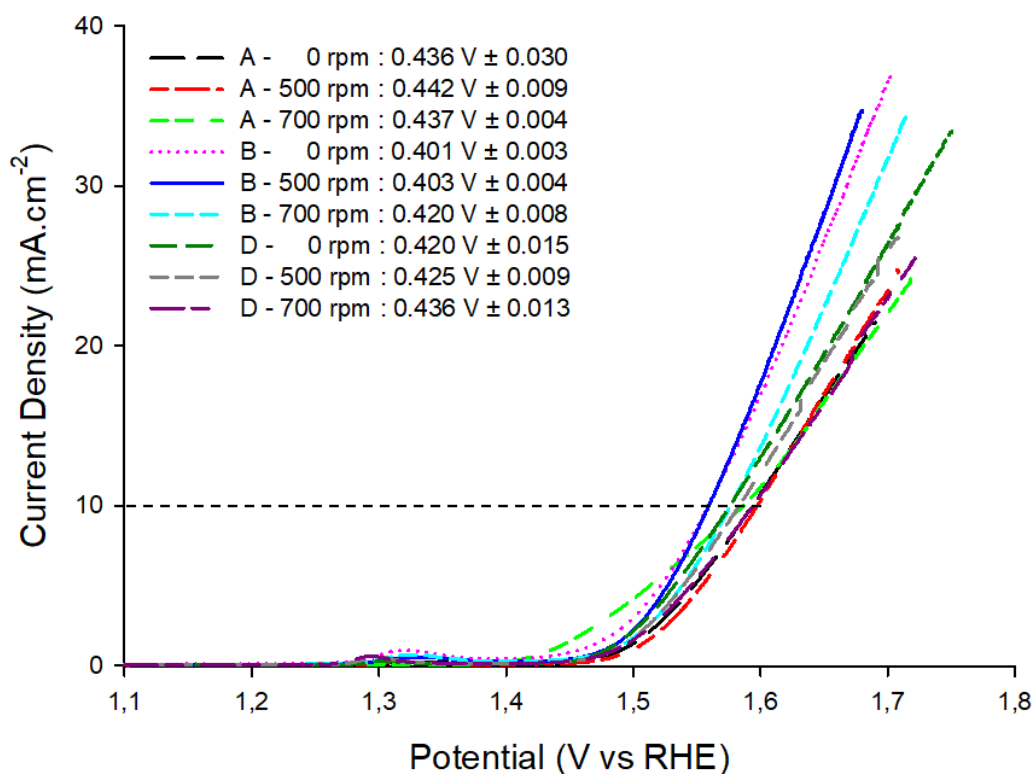


Figure 3-3: LSV results for the different VC:Nafion supports (prepared with different drying rotation rates containing a 40 nm Ni thin film). Precise overpotential values at the benchmarking value of 10 mA.cm⁻², are included in the legend.

Sample B was then compared to a GC containing a 40 nm Ni thin film only (no support), as a means of determining whether the VC:Nafion support (sample B) improves the activity of the Ni towards catalysing the OER (Figure 3-4). From Figure 3-4 it is clear that, at the benchmarking current of 10 mA.cm⁻², the support improves the overpotential from 0.447 ± 0.020 V (GC without support) to 0.401 ± 0.003 V (GC with sample B as support), before the commencement of long-term testing. The overpotential of the Ni deposited on sample B correlates well with one of the best noble metal-containing OER electrocatalysts, i.e. RuO₂, which exhibits an overpotential of 0.38 V - 0.40 V, but not as low as the overpotential for IrO₂, which varies between 0.32 V - 0.38 V [38-40]. This observation validates that Nafion as the selected binder in the support, which is preferred for acid electrolytes [37], does not inhibit the activity of the Ni thin films sputtered onto the VC:Nafion support in alkaline media. If Nafion is to be used as a binder in direct contact with an alkaline medium, it is suggested that the Nafion is neutralised and hydroxide-doped so as to not affect the performance of the electrocatalysts. The use of an alkaline-based ionomer binder would be a better option. Nonetheless, novel to this study is the fact that the active metal component is not mixed with the ink, but sputtered as a thin film directly onto the VC:Nafion support, which results in the thin film covering the support and thereby limiting direct contact (if

any) of the support with the alkaline electrolyte. As Nafion is non-conductive, the specific VC:Nafion ratio (1:0.67) of sample B, containing more conductive material (VC) than non-conductive material (Nafion), ensures effective electron transfer between the conductive electrocatalyst layer and the support.

As a main aim of this study is to prevent delamination of the thin film electrocatalyst from the electrode substrate, CP was used to evaluate the stability of the Ni (with and without support (sample B) over a period of 6 hours (Figure 3-5). After a 6-hour CP measurement, an increase in current activity and improvement in overpotential was observed for the Ni without support. This may be due to the Ni being activated by the formation of an oxide on the surface of the Ni [2, 23, 31, 33], which is known to enhance the activity towards the OER [2, 23, 33]. However, upon physical evaluation of the electrode surfaces (Ni, with and without support), the Ni sample that contained no support was fragile and delaminated from the GC substrate (inset in Figure 3-4(i)). On the contrary, no delamination of the Ni sputtered onto sample B, was visible, and the surface of the electrode was intact and quite robust, i.e. physically scratching the surface after testing did not remove the support-electrocatalyst layer (insert Figure 3-4(ii)). The results obtained therefore exhibit that employing a VC:Nafion support, improves the structural stability of the electrocatalyst performance without compromising the electrochemical performance of Ni, i.e. no delamination with similar electrochemical activity compared to sputtered Ni without a support.

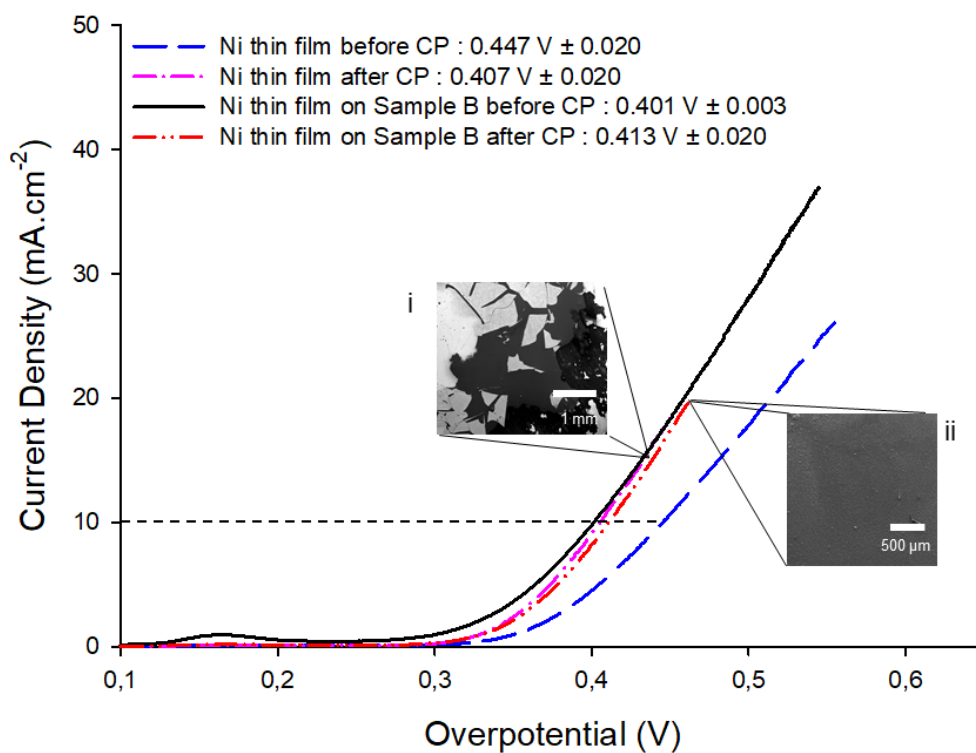


Figure 3-4: LSV of Ni with and without support (insert: i) delamination of Ni in the absence of support [scale = 1 mm], insert ii) no delamination of Ni on sample B [scale = 500 μm])

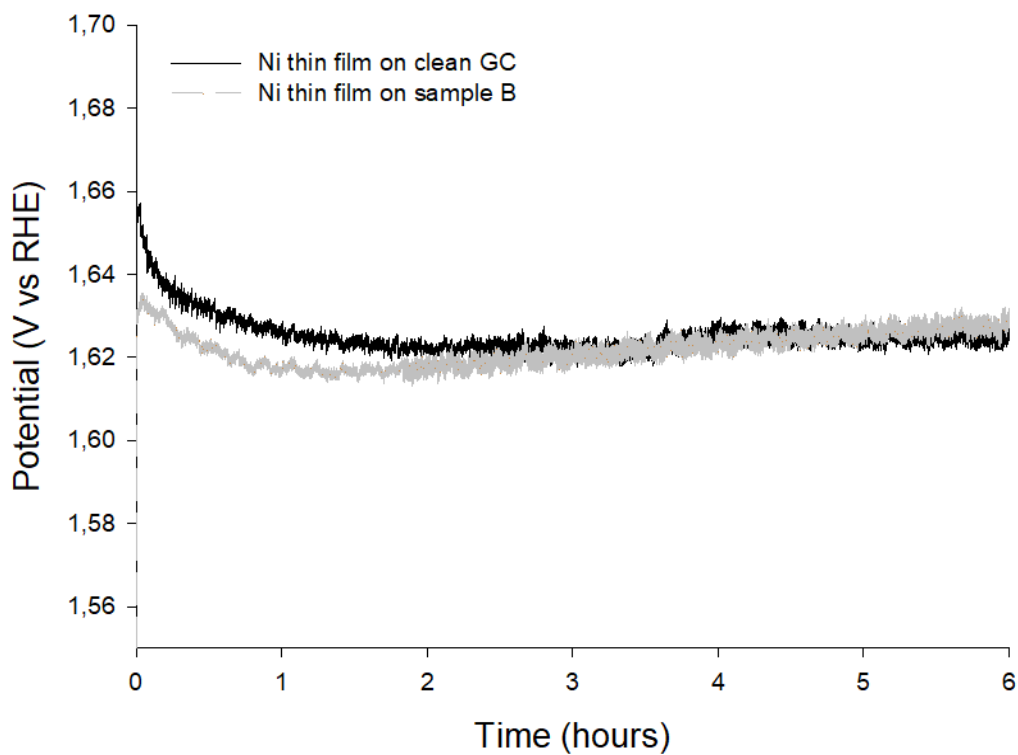


Figure 3-5: CP data for Ni with and without support

Delamination is not only problematic during single electrode testing using GC as substrate [41], it has also been observed to be a problem during high-throughput testing when using Au/SiO₂ as the substrate [41]. Hence, sample B was evaluated as a support for a Ni thin film on an Au/SiO₂ wafer towards catalysing the OER reaction in alkaline media and compared to the results obtained when GC was used as the substrate. Ni thin films were sputtered at different positions (working electrode pads) onto the VC:Nafion supported Au/SiO₂ (sample B, Figure 3-6) and evaluated electrochemically towards the OER. Acceptable current activity and overpotential were observed with no signs of delamination during or after testing. Hence, sample B proved to be effective in that no delamination occurred. However, the results obtained for Au/SiO₂ ($0.526\text{ V} \pm 0.06$) and the GC ($0.401\text{ V} \pm 0.003\text{ V}$), showed to be not directly comparable, although being within range. This is mainly attributed to the substrates, circuits and cell resistances for the two electrochemical setups being totally different. Irrespective of these differences, the support allows for accurate high-throughput screening with no signs of delamination, making the high-throughput identification of alternative Ni-based electrocatalysts for OER feasible. It also allows for more accurate kinetic characterisation on GC electrode inserts without the interference of mechanical deterioration of the thin film electrocatalyst. As high-throughput screening is used for fast and effective characterisation (current output and overpotential) of electrocatalysts, long term stability was not evaluated on the SiO₂ wafer.

Scrutinising the literature has revealed only one study, conducted by Geurin *et al.* [42], where a carbon support was used in high-throughput screening. This study utilised a carbon support for high-throughput screening in an acidic medium with ink-impregnated Pt/C (varying Pt/C ratios) for fuel cell electrocatalysts. It was employed to demonstrate the speed and effectiveness of high-throughput screening technology for CO electro-oxidation, oxygen reduction and methanol oxidation [42]. Hence, the use of VC:Nafion as support for non-impregnated thin film electrocatalysts sputtered on both an Au/SiO₂ and GC substrate, towards investigating the OER in alkaline medium, is a first.

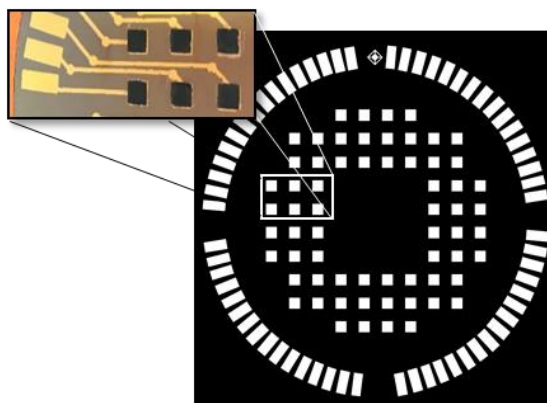


Figure 3-6: Illustration of the high-throughput wafer pattern with an inset of the actual working electrodes containing VC:Nafion support

3.4 Conclusion

A new approach for the loading of VC:Nafion supports onto GC and Au/SiO₂ substrates, as a means of preventing delamination of sputtered electrocatalysts during/after electrochemical testing, is presented and discussed. Different ratios of VC:Nafion support inks were prepared and subjected to physical and electrochemical characterisation. Physical characterisation by SEM analysis indicated that (i) a support with too high a carbon content cracks when dried, and (ii) employment of rotation, as a means to facilitate even drying, does not have an effect on producing an evenly dried support surface. Upon electrochemical characterisation, using a GC as substrate, a VC:Nafion support with a 1:0.67 ratio exhibited the best overpotential for the OER without any signs of delamination. This support was then loaded onto an Au/SiO₂ substrate that served as a support for high-throughput screening of sputtered Ni thin films as electrocatalyst for the OER in alkaline media. Comparison between the Au/SiO₂ and GC as substrate (both containing VC:Nafion support) revealed results that were not directly comparable, although still within range of what is expected for all OER electrocatalysts. This work has shown that the major problem of delamination of sputtered electrocatalysts, during high-throughput screening, can be overcome by employing a custom VC:Nafion ratio (1:0.67), and associated deposition regime, as support.

3.5 References

1. A.L. Dicks. The role of carbon in fuel cells, *J. Power Sources*, 156(2), 128-141 (2006)
2. R.L. Doyle, M.E.G. Lyons, in *Photoelectrochemical Solar Fuel Production*, ed. By S. Giménez and J. Bisquert (Springer 2016), p. 41-104
3. M.J. Lazaro, L. Calvillo, V. Celorrio, J.I. Pardo, S. Perathoner, R. Moliner, in *Carbon Black: Production, Properties and Uses*, ed I.J. Sanders and T.L. Peeten (Nova Science Publishers. 2011), p. 41-68
4. B. Seger, P.V. Kamat, Electrocatalytically active graphene-platinum nanocomposites. role of 2-D carbon support in PEM fuel cells. *J. Phys. Chem. C*, 113(19), 7990-7995 (2009)
5. E. Auer, A. Freund, J. Pietsch, T. Tacke, Carbons as supports for industrial precious metal catalysts. *Appl. Catal. A Gen.*, 173(2), 259-271 (1998)
6. G.L. Puma, A. Bono, D. Krishnaiah, J.G. Collin, Preparation of titanium dioxide photocatalyst loaded onto activated carbon support using chemical vapor deposition: a review paper. *J. Hazard. Mater.*, 157, 209-219 (2008)
7. K. Vytras, I. Svancara, R. Metelka, Carbon paste electrodes in electroanalytical chemistry, *J. Serb. Chem. Soc.*, 70(10), 1021-1033 (2009)
8. X. Li, F. Feng, K. Zhang, S. Ye, D.Y. Kwok, V. Birss, Wettability of Nafion and Nafion/vulcan carbon composite films. *Langmuir*, 28, 6698-6705 (2012)
9. P. Chen, L.K. Wang, G. Wang, M.R. Gao, J. Ge, W.J. Yuan, Y.H. Shen, A.J. Wie, S.H. Yu. Nitrogen-doped nanoporous carbon nanosheets derived from plant biomass: an efficient catalyst for oxygen reduction reaction., *Energy. Environ. Sci.*, 7, 4095-4103 (2014)
10. H. Yu, J.M. Roller, W.E. Mustain, R. Maric. Influence of the ionomer/carbon ratio for low-Pt loading catalyst layer prepared by reactive spray deposition technology., *J. Power Sources*, 283, 84-94 (2015)
11. M. Görlin, J. Ferreira de Arujo, H. Schmies, D. Bernsmeier, S. Dresch, M. Gliech, Z. Jusys, P. Chernev, R. Kraehnert, H. Dau, P. Strasser, Tracking catalyst redox states and reaction dynamics in Ni-Fe oxyhydroxide oxygen evolution reaction electrocatalysts: the role of catalyst support and electrolyte pH. *J. Am. Chem. Soc.*, 139(5), 2070-2082 (2017)

12. J. Lee, B. Jeong, J.D. Ocon, Oxygen electrocatalysis in chemical energy conversion and storage technologies, *Curr. Appl. Phys.*, 13(2), 309-321 (2013)
13. F.M. Sapountzi, J.M. Gracia, C.J. Weststrate, H.O.A. Fredriksson, J.W. Niemantsverdriet, Electrocatalysts for the generation of hydrogen, oxygen and synthesis gas, *Prog. Energy Combust. Sci.*, 58, 1-35 (2016)
14. G. Sasikumara, J.W. Ihma, H. Ryua, Optimum Nafion content in PEM fuel cell electrodes. *Electrochim. Acta*, 50, 601-605 (2004)
15. Z.D. Wei, S.H. Chan. Electrochemical deposition of PtRu on an uncatalyzed carbon electrode for methanol electrooxidation, *J. Electroanal. Chem.*, 569(1), 23-33 (2004)
16. P. Strasser, Q. Fan, M. Devenney, W.H. Weinberg, P. Liu, J.K. Norvskov. High throughput experimental and theoretical predictive screening of materials – a comparative study of search strategies for new fuel cell anode catalysts. *J. Phys. Chem. B.*, 107(40), 11013-11021 (2003)
17. J.J. Hanak, The “multiple-sample concept” in materials research: synthesis, compositional analysis and testing of entire multicomponent systems, *J. Mater. Sci.*, 5, 964-971 (1970)
18. A. Falch, V.A. Lates, H.S. Kotzè, R.J. Kriek, The effect of rapid thermal annealing on sputtered Pt and Pt₃Pd₂ thin film electrocatalysts for aqueous SO₂ electro-oxidation. *Electrocatalysis*, 7, 33-41 (2016)
19. Y. Garsany, I.L.S., K.E. Swider-Lyons, Impact of film dryingprocedures on RDE characterization of Pt/VC electrocatalysts, *J. Electroanal. Chem.*, 662, 396-406 (2011)
20. A. Falch, V.Lates, R.J. Kriek, Combinatorial plasma sputtering of Pt_xPd_y thin film electrocatalysts for aqueous SO₂ electro-oxidation, *Electrocatalysis*, 6(3), 322-330 (2015)
21. A. Falch, V.A.Badets, C. Labrugère, R.J. Kriek, Co-sputtered Pt_xPd_yAl_z thin film electrocatalysts for the production of hydrogen via SO₂(aq) electro-oxidation *Electrocatalysis*, 7(5), 376-390 (2016)
22. G. Li, L. Anderson, Y. Chen, M. Pan, P.Y. Abel Chuang. New insights into evaluating catalyst activity and stability for oxygen evolution reactions in alkaline media, *Sustain. Energy Fuels.*, 2(1), 237-251 (2018)

23. Y. Lee, J.Suntivich, K.J. May, E.E. Perry, Y. Shao-Horn, Synthesis and Activities of Rutile IrO₂ and RuO₂ Nanoparticles for Oxygen Evolution in Acid and Alkaline Solutions, *J. Phys. Chem.*, 3, 399-404 (2012)
24. C.C.L. McCrory, S. Jung, J.C. Peters, T.F. Jaramillo, Benchmarking heterogeneous electrocatalysts for the oxygen evolution reaction *J. Am. Chem. Soc.*, 135, 16977-16987 (2013)
25. C.C.L. McCrory, S. Jung, I.M. Ferrer, S.M. Chatman, J.C. Peters, T.F. Jaramillo, Benchmarking hydrogen evolving reaction and oxygen evolving reaction electrocatalysts for solar water splitting devices *J. Am. Chem. Soc.*, 137, 4347 – 4357 (2015)
26. A. Ganassin, A. Maljusch, V. Colic, L. Spanier, K. Brandl, W. Schuhmann, A. Bandarenka. Benchmarking the performance of thin-film oxide electrocatalysts for gas evolution reactions at high current densities, *ACS Catal.*, 6(5), 3017-3024 (2016)
27. M.G. Walter, E.L. Warren, J.R. McKone, S.W. Boettcher, Q. Mi, E.A. Santori, N.S. Lewis, Solar water splitting cells *Chem. Rev.*, 110(11), 6446-6473 (2010)
28. X. Lu, W.L. Yim, B.H.R. Suryanto, C. Zhao, Electrocatalytic oxygen evolution at surface-oxidized multiwall carbon nanotubes *J. Am. Chem. Soc.*, 137(8), 2901-2907 (2015)
29. B. You, N. Jiang, M. Sheng, S. Gul, J. Yano, Y. Sun, High performance overall water splitting electrocatalysts derived from cobalt-based metal–organic frameworks *Chem. Mater.*, 27(22), 7636-7642 (2015)
30. X. Lu, C. Zhao., Electrodeposition of hierarchically structured three-dimensional nickel-iron electrodes for efficient oxygen evolution at high current densities, *Nat. Commun.*, 6, 1-7 (2015)
31. M.W. Louie, A.T. Bell, An investigation of thin-film Ni–Fe oxide catalysts for the electrochemical evolution of oxygen *J. Am. Chem. Soc.*, 135(33), 12329-12337 (2013)
32. G.F. Chen, T.Y. Ma, Z.Q. Liu, N. Li, Y.Z. Su, K. Davey, S.Z. Qiao, Efficient and stable bifunctional electrocatalysts Ni/Ni_xM_y (M = P, S) for overall water splitting *Adv. Funct. Mater.*, 26(19), 3314-3323 (2016)
33. M.E.G. Lyons, M.P. Brandon, The Oxygen Evolution Reaction on Passive Oxide Covered Transition Metal Electrodes in Aqueous Alkaline Solution, *Int. J. Electrochem. Sci.*, 3, 1386-1424 (2008)

34. R.D. Deegan, Pattern Formation in Drying Drops, *Phys. Rev. E.*, 61, 475-485 (2000)
35. A. Manabe, M.K., T. Hashimoto, T. Hayashida, A. Kato, K. Hirao, I. Shimomura, I. Nagashima, Basic study of alkaline water electrolysis, *Electrochim. Acta*, 100, 249-256 (2013)
36. E. Zoulias, E. Varkaraki., N. Lymberopoulos, C.N. Christodoulou, G.N. Karagiorgis, "A Review on Water Electrolysis", *TCJST*, 4, 41-71 (2004)
37. R. Jervis, N. Mansor, A. J. Sobrido, S. Jones, C. Gibbs, T.P. Neville, J. Millichamp, P.R. Shearing, D.J.L. Brett, The Importance of Using Alkaline Ionomer Binders for Screening Electrocatalysts in Alkaline Electrolyte, *J. Electrochem. Soc.*, 164(14), 1551-1555 (2017)
38. M. Garcia-Mota, A. Vojvodic., H. Metiu, I.C. Man, H.Y. Su, J. Rossmeisl, J.K. Nørskov, *Chem. Cat. Chem.* 3, 1607-1611 (2011)
39. M.Z. Iqbal, R.J. Kriek, Silver/nickel oxide (Ag/NiO) nanocomposites produced via a citrate Sol-Gel route as electrocatalyst for the oxygen evolution reaction (OER) in alkaline medium *Electrocatal.* 9(3), 279-286 (2018)
40. S. Jung, C.C.L. McCrory, I.M. Ferrer, J.C. Peters, T.F. Jaramillo, Benchmarking nanoparticulate metal oxide electrocatalysts for the alkaline water oxidation reaction *J. Mater. Chem. A*, 4(8), 3068-3076 (2016)
41. P. Bronzan, H. Meider-Gorican, Solvent extraction of zirconium and hafnium with some trifunctional phosphine oxides, *Int. Solvent. Extr. Conf. Proc.*, 2235-2247 (1974)
42. S. Guerin, B.E. Hayden, C.E. Lee, C. Mormiche, J.R. Owen, A.E. Russell, B. Theobald, D. Thompson, Combinatorial electrochemical screening of fuel cell electrocatalysts, *J. Comb. Chem.* 6(1), 149-158 (2004)

CHAPTER 4: REACTIVE SPUTTERED $\text{Ir}_x\text{Ni}_y\text{O}_z$ ELECTROCATALYSTS FOR THE OXYGEN EVOLUTION REACTION IN ALKALINE MEDIA

CHAPTER OVERVIEW

Alkaline water electrolysis (AWE), when used with renewable energy sources, is a promising, simple and environmentally friendly technology to produce high purity hydrogen gas for energy conversion and storage. In spite of AWE receiving considerable attention in the past decade, with ongoing research into reducing cost and increasing efficiency, improvement of the electrocatalyst materials used as the anode is still a necessity, as one drawback of AWE is the sluggish oxygen evolution reaction kinetics. In an effort to improve electrocatalytic performance, various $\text{Ir}_x\text{Ni}_y\text{O}_z$ electrocatalyst combinations have been prepared by reactive sputtering onto Vulcan carbon (VC):Nafion supported substrates and subjected to high-throughput screening followed by thorough electrochemical and physical characterisation. Scanning electron microscopy (SEM), Energy-dispersive X-ray spectroscopy (EDX), and X-ray photo-electron spectroscopy (XPS) were used to evaluate morphology and metal/metal oxide composition. Rotating disk electrode (RDE) techniques were employed for electrochemical analysis, which included linear sweep voltammetry (LSV) before and after chronopotentiometry (CP) for a 6-hour period. Overall the $\text{Ir}_x\text{Ni}_y\text{O}_z$ electrocatalyst combinations containing higher amounts of Ir ($\text{Ir}_{92}\text{Ni}_8\text{O}_x$, $\text{Ir}_{68}\text{Ni}_{32}\text{O}_x$ and $\text{Ir}_{62}\text{Ni}_{38}\text{O}_x$) performed the best of the tested mixed metal electrocatalysts. However, evident from this study was the fact that the combination of Ir with Ni did not eminently result in a mixed metal electrocatalyst that can outperform pure Ni.

4.1 Introduction

The development of efficient, environmentally friendly and sustainable energy conversion and storage technologies, as an alternative to traditional fossil fuel energy sources, is crucial. This development is essential to sustain modern society's escalating energy demands and reverse the increased environmental deterioration related to fossil fuel consumption [1, 2]. Hydrogen as an energy vector, in conjunction with renewable energy sources, has the potential to decarbonise energy conservation and storage, which would address the above-mentioned concerns [3, 4]. One fundamental drawback related to hydrogen gas is that it is not naturally available and has to be produced [5]. Two broad categories exist for commercial hydrogen production, i.e. (i) fossil fuel-based, with an inevitable associated carbon footprint, and (ii) renewable hydrogen production technologies. Electrolysis is one of the most promising and environmentally cleanest technologies

for the production of hydrogen gas, especially when driven by electricity generated from renewable sources like wind or solar [1, 6-10].

During water electrolysis, electrical energy is utilised to split water at a cathode and anode, producing H₂ (reaction 2) and O₂ (reaction 3), respectively. The hydrogen evolution reaction (HER) takes place on the cathode while the oxygen evolution reaction (OER) takes place on the anode. In alkaline media, the reactions are [11]:



at standard conditions of 1 atm and 25°C with the overall reaction being:



A current drawback influencing efficient water electrolysis (alkaline- and acid-based) as a whole, is the slow kinetics of the oxygen evolution reaction (OER) at the anode (reaction 2) [8, 9, 12, 13]. To lower the overpotential (energy input to drive the reaction), electrocatalysts with good stability and activity are required. The electrocatalysts currently regarded as the most active anode materials are IrO₂ and RuO₂ and are known to achieve high currents in an acidic medium as the electrolyte [4, 6, 8, 14-17]. A study conducted by Cherevko and co-workers, showed that OER activity increases in the order IrO₂ < RuO₂ ≈ Ir < Ru with dissolution decreasing in the order Ru >> Ir > RuO₂ >> IrO₂, independent of the electrolyte (acid or base) used, with the activity of Ir and IrO₂ in acidic media being greater than in alkaline media [12]. However, these electrocatalysts suffer from poor durability, high cost, scarcity and different degrees of dissolution in both acidic and alkaline media at high potentials [1, 8, 9, 14, 16]. Proton exchange membrane water electrolyzers (PEMWEs) suffer from having to use expensive noble metal electrocatalysts to withstand corrosion, and often require more complex operational designs due to higher temperatures employed [5, 6]. The use of an alkaline medium, on the other hand, has the benefits of utilising cheap(er) materials, while still maintaining reasonable electrocatalyst efficiencies, due to a less corrosive environment, when compared to PEMWEs [9, 18, 19].

AWE is one of the most studied water electrolysis technologies and has been in use since the 1920s for large scale industrial hydrogen production, classifying it as a mature technology [5, 6]. However, AWE still requires an improvement in oxygen evolution kinetics on the anode and considerable effort is poured into the investigation and development of low cost, high current density, low overpotential, stable and sustainable electrocatalysts to serve as the anode in

alkaline media [9, 10, 12-14, 16]. Various metal and metal oxides have been studied with much success in terms of performance and durability for improved AWE [1, 4, 8-10, 12-16, 18-20]. Earth abundant, less expensive and more eco-friendly transition metal oxides exhibit good durability, high thermal and mechanical stability, but requires improvement in terms of current density and overpotential in alkaline media compared to what can be achieved with IrO_2 and RuO_2 in acidic media [1, 8, 15, 16].

Some of the metals studied include Co, Mn, Ni and Fe, with synthesis techniques that vary from catalyst doping, production of nanostructures, thin film sputtering and reactive sputtering for oxide synthesis [4, 8, 9]. Of these metals Co and Mn exhibit lower activity due to the metal-oxide bond being either too weak or too strong, which in turn result in an even more sluggish rate-limiting step compared to the other metals [15]. Trotochaud and co-workers' studies on solution-cast metal oxide thin films indicated that MnO_x had the lowest activity of the studied metals for the OER with a reported overpotential of 541 mV [21]. Studies on CoO_x indicate reasonable activity, but also showed increased activity when combined with other metals, especially when combined with Ni to form NiCoO_x [21, 22]. However, even when combined with Ni to form NiCoO_x , a decrease in activity was observed compared to pure NiO_x [15]. Fe and FeO_x have shown good activity as electrocatalyst for thin film electrolysis studies as well as photo-electrochemical hydrogen generation [21, 23-25]. It has also been proven to be more effective when Fe is combined with other transition metals such as Ni, due to Fe impurities in the crystal structure being responsible for increased activity [21, 23-25]. In general, Ni is one of the most studied and practical electrocatalyst material for the OER in alkaline media, with low cost, acceptable activity and high resistance to corrosion being the main positive characteristics [8, 15, 16]. Nevertheless, Ni and Ni-based oxide electrocatalysts exhibit overpotentials that are still higher than desired, however, they do exhibit greater stability and durability. This together with an ongoing focus to improve their performance, could result in them becoming the electrocatalysts of choice. One attractive route of electrocatalysis research and development is the fine-tuning of metal/metal oxides (mostly Ni-based) by means of compositional content modifications, as an attempt to possibly improve catalytic performance and durability [8, 20]. Therefore, the huge body of literature that is published on Ir and IrO_2 (specifically with regard to acidic media), and the numerous publications on modified Ni-based electrocatalysts (including NiO) for use in alkaline media, would suggest investigating a compositional spread of $\text{Ir}_x\text{Ni}_y\text{O}_z$ electrocatalysts for the OER. This strategy, therefore, could potentially serve to exploit the synergistic effects of Ni and NiO (in alkaline media) together with Ir and IrO_2 (in acidic media), to produce an active and stable electrocatalyst, i.e. $\text{Ir}_x\text{Ni}_y\text{O}_z$. In the event that excellent mass-specific activity (current per mass of noble metal) is achieved, combined with acceptable stability and durability, it can be considered as a competitive electrocatalyst for the OER.

In this study, reactive sputtering is employed to synthesise an array of $\text{Ir}_x\text{Ni}_y\text{O}_z$ electrocatalyst compositions that will be subjected to high-throughput screening as a means of identifying the most active compositions. Upon identification of the most active compositions, in-depth rotating disk electrode (RDE) testing will be conducted. The selected $\text{Ir}_x\text{Ni}_y\text{O}_z$ thin films (will be subjected to physical characterisation employing scanning electron microscopy (SEM), energy-dispersive X-ray spectroscopy (EDX) and X-ray photo-electron spectroscopy (XPS).

4.2 Experimental

4.2.1 Preparation of $\text{Ir}_x\text{Ni}_y\text{O}_z$ electrocatalyst compositions

Supporting structures of electrocatalysts have received a great deal of interest over the last decade as a means of increasing activity due to a higher surface area and increased stability and/or durability, especially during electrocatalyst testing [15, 26]. It is a known phenomenon that glassy carbon (GC) supports corrode in acid as well as alkaline media at high oxidative voltages, which may lead to thin film delamination [27]. Cognisance of this phenomenon is taken throughout electrochemical characterisation and the extent thereof is limited by the use of Vulcan Carbon (VC):Nafion as support on the GC and Au/SiO_2 as substrates. VC has been identified to be a good supporting structure for alkaline water electrolysis due to the increased surface area, stability and the possibility of enhancing the activity of the electrocatalyst [26, 28, 29]. In our previous work, different VC:Nafion ratios were investigated as a support to be used on GC and Au/SiO_2 as substrate and it was found that (i) the electrocatalyst surface area increased, and (ii) electrocatalyst delamination decreased during OER testing in alkaline media [30]. The technique used for preparing the wafer circuit (geometric area of a working electrode pad being 0.09 cm^2) and GC electrode insert surfaces (geometric area of 0.196 cm^2), before depositing the VC:Nafion ink, have been discussed in detail in a previous publication [31]. VC (XC-72R) was dried at 40°C and then used to create a carbon ink with Nafion as the binding agent. 5 wt% Nafion (Sigma Aldrich) was diluted to 1 wt% by using isopropanol (Merck). A 1:0.67 (VC:Nafion) mass ratio was prepared and sonicated for 2h to ensure homogeneous mixing of VC and Nafion. VC:Nafion (10 μl) ink was drop casted onto the GC and dried under a glass beaker to ensure even drying. The VC:Nafion support was loaded onto the Au/SiO_2 substrate subsequent to covering the wafer with a plastic that has pressure sensitive adhesive on one side, so as to adhere to the Au/SiO_2 electrical circuit/wafer. This plastic layer was pre-cut so as to cover everything but the 64 working electrode pads (Figure 4-1).

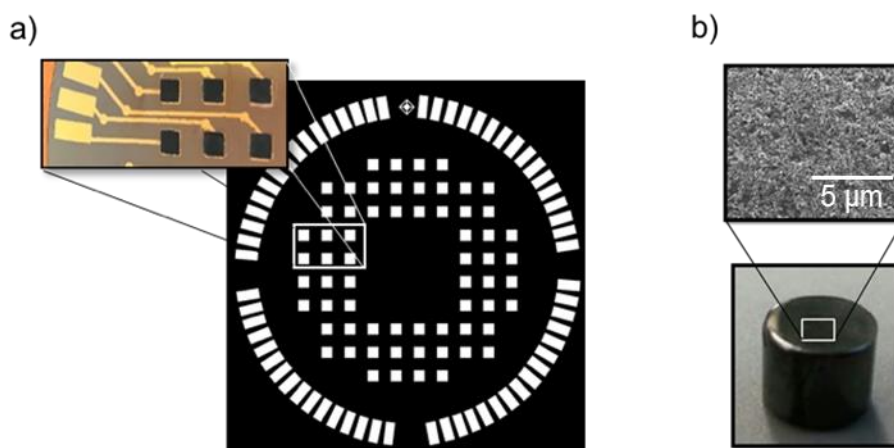


Figure 4-1: a) Illustration of the Au/SiO₂ (working pad geometric area 0.09 cm²) wafer pattern with an inset of the actual working electrodes containing VC:Nafion support, and b) an image of VC:Nafion supported GC (5 mm diameter) used for RDE measurements

Different Ir_xNi_yO_z electrocatalyst compositions (40 nm thick) were deposited by direct current (DC) combinatorial reactive sputtering (PVD Products, USA) from elemental targets (Ir and Ni, 99,995%, ACI alloys; Ni target contained 0.0011% Fe as impurity), while maintaining an O₂ flow rate of 0.005 L/min and an Ar flow rate of 0.025 L/min [32, 33].

4.2.2 Electrochemical characterisation

KOH, rather than NaOH, is used as the electrolyte due to the higher ionic conductivity and mobility of K⁺ ions compared to that of Na⁺ ions [5, 34]. Calibration of the reference electrode was conducted in H₂ saturated 0.1 M KOH employing a polycrystalline Pt working electrode [35]. A scan rate of 5 mV.s⁻¹ and potential range of -0.1 V to -0.9 V vs Hg/HgO was employed [35, 36]. The potential at which hydrogen evolution changed to hydrogen oxidation was measured to be -0.866 V and correlated very well with a reported value of -0.855 V [35]. This value was used to convert all potential values to the Reversible Hydrogen Electrode ($E_{\text{RHE}} = E_{\text{Hg/HgO}} + 0.866 \text{ V}$).

The internal resistance (iR) was determined (13.77 Ω) for an O₂ purged 0.1 M KOH solution with a polycrystalline Pt working electrode and Hg/HgO reference electrode, and the associated iR-drop was compensated for in-situ by employing the EC-lab software (version 11.01).

High-throughput screening was performed with a scan rate of 5 mV.s⁻¹ and a potential range of 0 V – 0.9 V vs Hg/HgO [17, 36-39] under O₂ saturation [40]. No rotation of the working electrodes was possible due to the unique build of the cell and the manner in which the 64 working electrodes were connected to the 64-channel potentiostat (Arbin MSTAT).

Traditional electrochemical characterisation was conducted in a custom manufactured plastic (high density KOH resistant polypropylene) three electrode cell configuration with the GC as working electrode, a Hg/HgO reference electrode (0.1 M KOH) and a Pt spiral counter electrode (both from ALS (Japan), distributed by BAS Inc.), and 0.1 M KOH (CC Immelmann, 0.001% Fe impurity) as electrolyte. A Bio-Logic potentiostat (Bio-Logic, VSP) with EC-Lab software was employed throughout. Linear sweep voltammetry (LSV) measurements were performed with a scan rate of 5 mV.s⁻¹ and a potential range of 0 V – 0.9 V vs Hg/HgO at 1600rpm [17, 36-39] under O₂ saturation [40]. O₂ saturation ensures that the equilibrium potential is not influenced by the O₂ produced during the OER. Chronopotentiometry (CP) measurements were performed to evaluate the loss of activity, also under O₂ saturation, with an applied current of 10 mA.cm⁻²_{geo} for 6 hours.

A benchmarking value of 10 mA.cm⁻²_{geo} for the activity and durability testing of the Ir_xNi_yO_z thin film on VC supported GC was employed [13, 37, 38, 41-44]. This value has been reported as the norm and used specifically for thin film electrocatalyst analysis for the OER [13, 36-39, 41-45].

Overpotential results were obtained by subtracting the equilibrium potential (calculated for 0.1 M KOH as being 1.158 V) from the RHE potential at the benchmarking current density: $\eta = E_{\text{RHE}} - E_{\text{eq}}$.

4.2.3 Physical characterization

The stoichiometry and structural properties of the as-prepared Ir_xNi_yO_z thin films were examined by scanning electron microscopy (SEM) with an integrated energy dispersive X-ray spectroscopy (EDX) system (FEI Quanta FEG 250) [32]. Stoichiometric values were obtained in moving average mode over a time period of 100 s. X-ray photo-electron spectroscopy (XPS, Kratos Axis Supra) was used for surface compositional analysis. All XPS measurements were taken using a monochromatic X-ray source with an aluminium anode, at an emission current of 5 mA and X-ray power of 75 W. Photoelectrons were collected from a sample area of 300 μm x 700 μm, and charge neutralisation was applied throughout. The charge neutraliser uses a filament current of 0.4 A, a filament bias of 1.0 V, and a charge balance of 3.3 V.

4.3 Results and Discussion

Activity (low overpotential, Tafel slope and exchange current density) and stability (minimal loss of current output, sustained overpotential and limited physical deterioration) are two of the most important multifaceted factors that an effective electrocatalyst should possess [36-38, 46]. High-

throughput screening was performed on 64 different $\text{Ir}_x\text{Ni}_y\text{O}_z$ combinations and benchmarked at $10 \text{ mA}\cdot\text{cm}^{-2}_{\text{geo}}$ (0.09 cm^2) to identify the most active electrocatalyst combinations for further RDE evaluation (Figure 4-2).

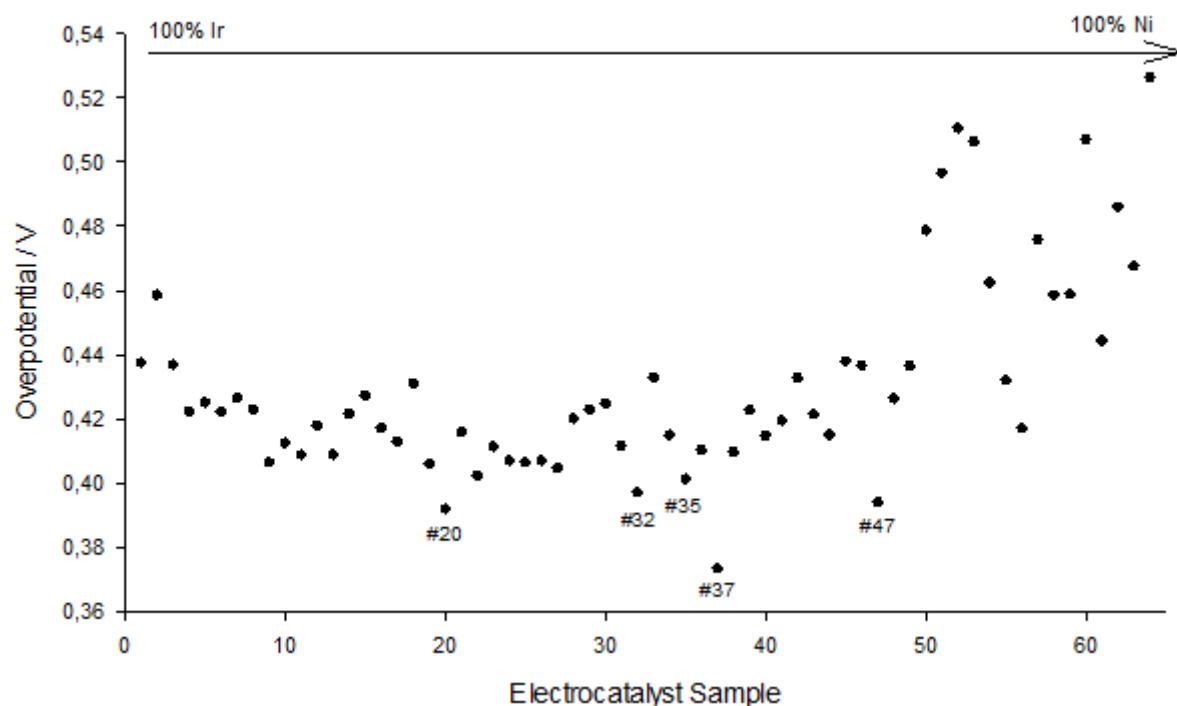


Figure 4-2: Overpotential results from high-throughput screening of 64 different electrocatalysts on a VC:Nafion supported Au/SiO₂ wafer at $10 \text{ mA}\cdot\text{cm}^{-2}_{\text{geo}}$

These 64 $\text{Ir}_x\text{Ni}_y\text{O}_z$ electrocatalyst combinations ranged from 100% Ir content to 100% Ni content. From the LSV measurements of the 64 samples, an overpotential range of 0.37 V – 0.53 V was obtained. Five mixed metal oxide combinations (labelled in Figure 4-2), with the exact elemental compositions determined with EDX analysis, were selected based on the lowest overpotential at $10 \text{ mA}\cdot\text{cm}^{-2}_{\text{geo}}$ (Table 4-1). These overpotential values obtained from high-throughput screening were used to identify potential electrocatalysts for the OER and do not constitute a conclusive evaluation of the produced electrocatalysts. Thus, RDE testing was done to obtain better insight into the electrocatalytic performance of the top five electrocatalyst combinations.

Table 4-1: Electrocatalyst metal compositions confirmed with EDX (atomic %) and overpotential values of the top five electrocatalyst combinations from high-throughput screening

Sample	% Ir	% Ni	Overpotential (mV)
#37	57 ± 4.0	43 ± 4.0	373
#20	92 ± 3.9	8 ± 3.9	392
#47	29 ± 5.9	71 ± 6.1	394
#32	68 ± 5.0	32 ± 5.0	397
#35	62 ± 6.1	38 ± 6.1	401

The selected mixed metal oxide electrocatalyst combinations (including the pure metals and their oxides) were sputtered onto VC:Nafion supported GC (Figure 4-1b) as substrate and subjected to in-depth physical and electrochemical characterisation.

Initial visual impressions of the VC:Nafion supported GC surfaces exhibited a matte greyish coloured metal coverage, with no signs of uncovered VC:Nafion support (black colour). SEM analysis confirmed total coverage of the VC:Nafion support surface with the metal/metal oxide film, hence none of the VC:Nafion support was in direct contact with the alkaline electrolyte [30]. Similar morphologies of the different electrocatalysts supported by VC:Nafion were found with some agglomeration of spherical VC particles (Figure 4-3). This morphology is known to result in an increase in surface area, which allows for increased contact between the electrolyte and the electrocatalyst. The VC:Nafion support also results in better contact between the electrocatalyst film and the smooth GC surface, so as to prevent delamination from occurring during electrochemical characterisation in alkaline media [30]. The use of VC:Nafion support on both the wafer (Figure 4-1a) and GC (Figure 4-1b) substrates not only had the purpose of stabilising the catalyst material and enhancing catalytic activity through increasing the electrocatalyst area, but also served to minimise unavoidable differences between high-throughput screening and RDE measurements. The overpotential values obtained from high-throughput screening (Table 4-1) differ from the RDE measurement values (Table 4-2). This is mainly due to the different cell setups and electrode substrates used (Au/SiO₂ wafer for high-throughput screening and GC for RDE) as well as different control of O₂ formation (rotation at 1600 rpm used during RDE testing and stagnant solution during high-throughput screening).

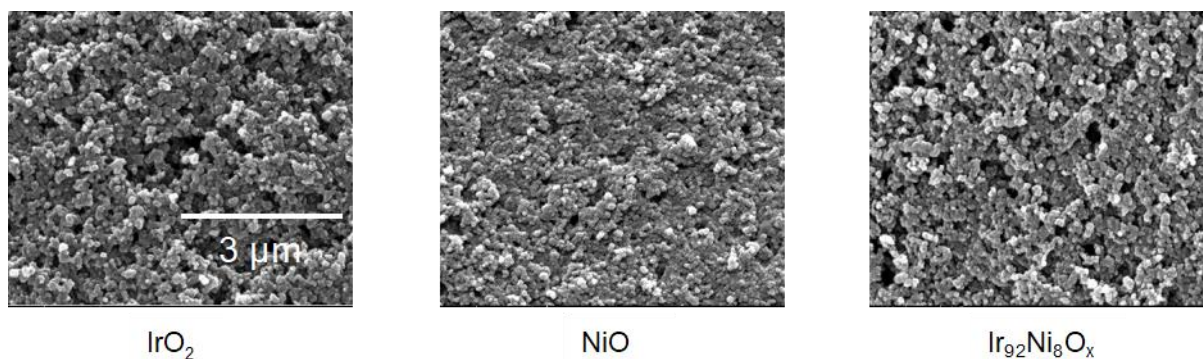


Figure 4-3: Micrographs of the metal/metal oxide films deposited on VC:Nafion GC electrodes. A scale of 3 μm applies to all three micrographs.

Polarisation curves (Figure 4-4) serve as the key performance indicator for the evaluation and comparison of electrocatalysts for the OER. Key performance evaluating parameters that will be discussed, include overpotential, Tafel slope and exchange current density. However, it should be noted that absolute comparisons with literature are to a degree ambiguous, due to differences in experimental testing conditions, for example, no equilibrium corrections done for different temperatures and electrolyte concentrations, unclear iR compensations, and different approaches for normalising data [10, 46, 47].

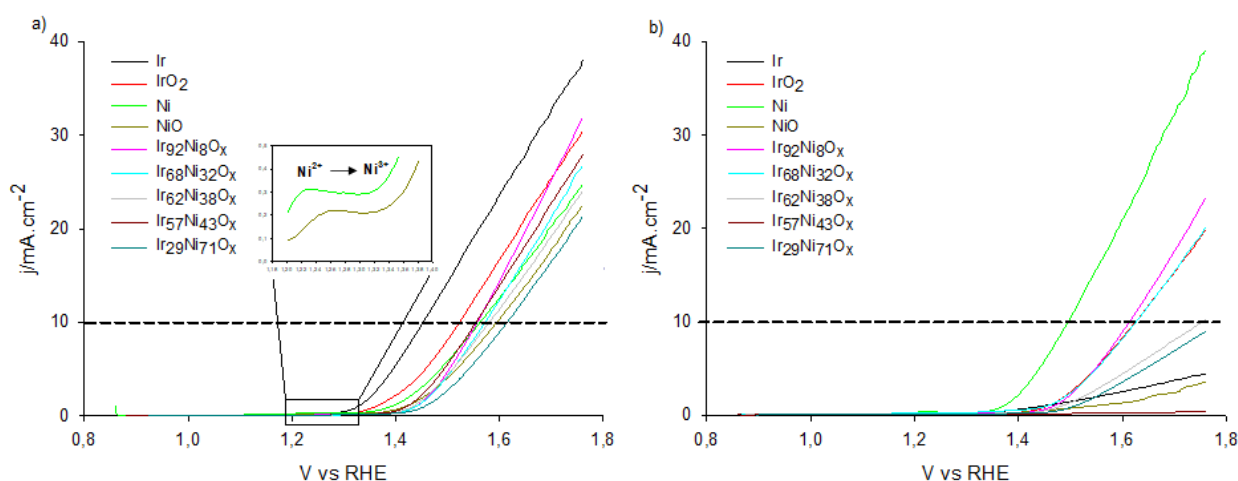


Figure 4-4: Linear sweep voltammetry of Ir, IrO₂, Ni, NiO and selected mixed metal oxide samples a) before, and b) after CP

From Figure 4-4 and Table 4-2, the best performing electrocatalysts in terms of overpotential for fresh as-deposited films, proved to be Ir, IrO₂ for single metal/metal oxide films, and Ir₂₉Ni₇₁O_x of the tested sputtered mixed metal oxide combinations. LSV measurements were also conducted after CP (Figure 4-4b) to compare the increase/decrease of the overpotential relative to the initial LSV measurements. After CP measurements, the electrocatalysts that exhibited the best overpotential initially, together with Ir₅₇Ni₄₃O_x and NiO, had no overpotential values after stability

tests due to the inability to achieve the benchmarking current density (Figure 4-4b). IrO₂, which initially proved to have a low overpotential, together with Ir₆₂Ni₃₈O_x, resulted in the highest overpotential values, achieving the benchmarking current subsequent to the CP run. This is indicative of pure Ir, and the mixed metal combinations (that contain less Ir), not being sufficiently stable in alkaline media [1, 6, 8, 9, 14-16]. NiO, which is considered by many as a good electrocatalyst in alkaline media [8, 15, 16, 20, 48], unexpectedly also lost all activity at the benchmarking current density. Ni, on the other hand, experienced an increase in activity subsequent to stability testing, exhibiting a decrease of 58 mV in overpotential. However, Ni achieved this averaged decrease in overpotential, having a large standard deviation (all data presented are an average of 3 runs per sample), suggesting poor repeatability. It is known that Ni is oxidised at higher current densities to form Ni oxides that are regarded to possess good activity for the OER [8, 20]. In addition to forming active oxides at high current densities, it is evident, though not fully understood, that Ni has a strong affinity towards Fe, which enhances the activity of Ni, with Ni_{0.9}Fe_{0.1}OOH being regarded as a good electrocatalyst for OER [8, 49, 50]. The electrolyte and metal target used for reactive sputtering contained Fe as impurity (0.001% Fe, see section 4.2.1 and 4.2.3), which was most likely absorbed by Ni during stability testing resulting in increased activity of the Ni [49]. Hence, despite the improvement in overpotential exhibited by pure Ni, it cannot be discounted that Fe played a role in achieving this activity. The same phenomenon would be expected for NiO, but this was clearly not the case (in this study) for NiO prepared by reactive sputtering [8, 50]. High oxidation states of Ni, such as Ni³⁺, are active towards the OER and many researchers focus on altering the structure and oxidation state to be beneficial for the OER [51-53]. In Figure 4-4a (inset), a small oxidation phenomenon just above 1.2 V vs RHE was observed for pure Ni and NiO. Studies suggest that this phenomenon corresponds to the oxidation of Ni²⁺ to Ni³⁺ (reaction .4) [73].



This phenomenon is not yet fully understood and requires further research to investigate the generated current as a result of the changing Ni oxidation state and its contribution to the OER. It is thus suggested that the sluggish performance of sputtered NiO towards the OER may be due to the nature of the structure, the oxidation state of Ni and/or the possibility of forming of γ -NiOOH and β -NiOOH (controversy exists in which form of NiOOH is more favourable for the OER, as some literature suggests the γ -state is active for the OER and others suggest the β -state as more active.) [54-57]. Jovic et al. [57] suggests that the formation of NiO₂, however, leads to a substantial reduction in electrical conductivity of the thin film which in turn leads to a reduction in electrocatalytic activity.

Table 4-2: Overpotential of all electrocatalysts before and after CP measurements

Sample (#)	Overpotential before CP (mV)	Overpotential from literature (mV)	Overpotential after CP (mV)	Ref.
Ir	228 ± 2.92	320	-	[58]
IrO ₂	296 ± 66.1	300	401 ± 12.7	[36]
Ni	336 ± 15.8	350	278 ± 36.6	[59]
NiO	370 ± 9.54	260	-	[8]
Ir ₂₉ Ni ₇₁ O _x (#47)	329 ± 12.6		-	
Ir ₉₂ Ni ₈ O _x (#20)	335 ± 24.6		389 ± 6.27	
Ir ₆₈ Ni ₃₂ O _x (#32)	347 ± 14.9		390 ± 19.3	
Ir ₆₂ Ni ₃₈ O _x (#35)	350 ± 17.3		530 ± 15.1	
Ir ₅₇ Ni ₄₃ O _x (#37)	390 ± 15.1		-	

(- Signs of severe deterioration)

Apart from Ni showing an improvement with respect to overpotential after stability testing, the mixed metal oxides achieving the benchmarking current did so with a larger overpotential. A study conducted by Binniger and co-workers concluded that (by using basic thermodynamic considerations) any metal/metal oxide becomes unstable under OER conditions no matter the pH-value [60]. This instability manifests itself through structural changes or dissolution of the electrocatalyst [60]. The authors suggested that this structural change or dissolution is a result of the instability of the oxygen anion in the metal/metal oxide lattice [60]. Ir specifically also undergoes structural changes and dissolution, as concluded by Schalenbach et al [61]. According to their study, Ir forms a stable oxide (IrO₂) between 0.93 V and 1.03 V vs RHE, but forms a soluble species, IrO₄²⁻, when higher voltages are encountered [61]. To investigate if dissolution was a contributing factor to the loss in activity seen for the mixed metal oxide samples, EDX (complete catalyst layer) and XPS (surface of catalyst layer) were used to determine if any change in metal ratios was apparent (Figure 4-5). The EDX values before CP are an average (7 of each sample) of the results, while only one of each sample was used for EDX and XPS after CP.

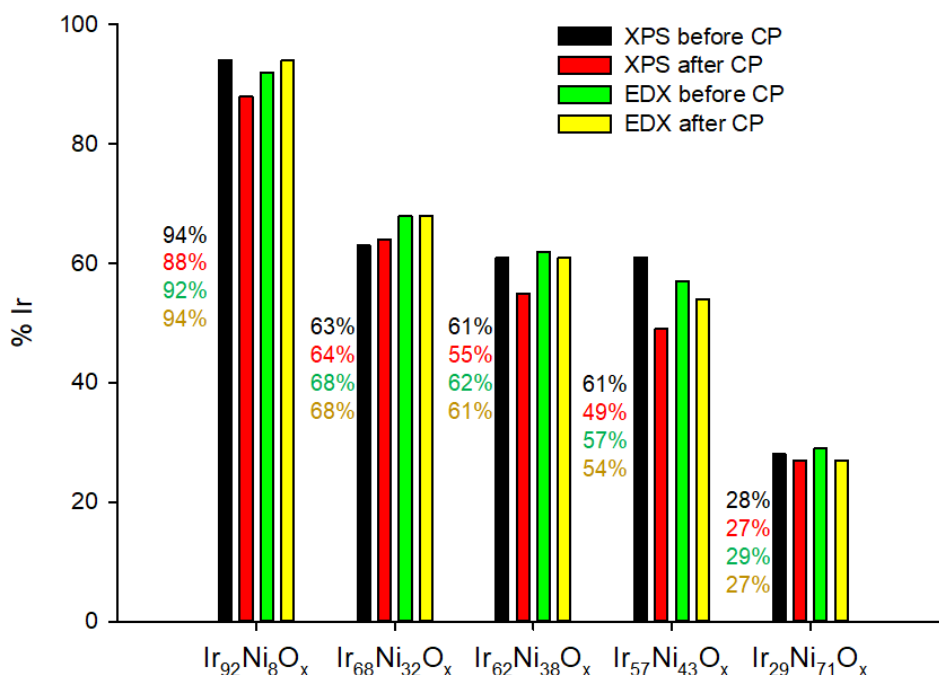


Figure 4-5: EDX and XPS (atomic % Ir) values of the mixed metal oxides before and after CP

EDX and XPS values are in good agreement for metal ratios before CP measurements, proving that the surface ratio and bulk ratio are equivalent, and that co-sputtering is homogeneous. Comparing the values obtained from EDX and XPS after stability, with the respective values before stability, it is clear that Ir is prone to dissolution, with XPS on average showing a greater deviation. This indicates that the loss in Ir is from the surface and to a lesser extent from the bulk. Consequently, this results in an altered metal ratio at the surface being in contact with the active species. The surface becomes more Ni rich, and evident from the overpotential trend of the five sputtered ratios, the higher the Ni content, the poorer the activity (greater overpotential). This loss in Ir, however, did not render the samples' activity as inadequate, as the $\text{Ir}_{92}\text{Ni}_8\text{O}_x$, $\text{Ir}_{68}\text{Ni}_{32}\text{O}_x$ and $\text{Ir}_{62}\text{Ni}_{38}\text{O}_x$ electrocatalyst combinations still reached the benchmarked current after CP measurements (Table 4-2). The $\text{Ir}_{92}\text{Ni}_8\text{O}_x$ and $\text{Ir}_{68}\text{Ni}_{32}\text{O}_x$ samples indicated overall good activity, stability and repeatability in terms of overpotential, however, they did not outperform pure Ni.

Generally, an electrocatalyst is considered to be excellent for the OER if it exhibits an overpotential in the range of 300 - 400 mV [62]. In the case that it falls in this range after ~6h stability testing, the electrocatalyst becomes even more attractive for the OER [11]. If this figure of merit is applied to the tested sputtered electrocatalysts, $\text{Ni} > \text{Ir}_{92}\text{Ni}_8\text{O}_x > \text{Ir}_{68}\text{Ni}_{32}\text{O}_x > \text{IrO}_2$, proves to be the most attractive for the OER. Interestingly, based on the performance of the pure metals (Ni being the best), one would expect the Ir-Ni combinations, containing higher Ni content, to

exhibit improved performance; however, the results clearly prove the opposite. These overpotential performance results require further in-depth analysis as to attain data and information on the overpotential differences seen. It is suggested that alloy formation can occur between Ir and Ni which could alter the intrinsic characteristics of each of the metals.

In addition to characterising the electrocatalysts in terms of overpotential, Tafel plots were constructed from the polarisation graphs (Figure 4-4) and the Tafel slopes and exchange current densities were determined. Tafel slopes are generally used to evaluate rate determining steps in electrochemical reactions but are also used as an activity parameter [9, 36, 63, 64]. The Tafel slopes obtained for the sputtered electrocatalysts are listed in Table 4-3 and depicted in Figure 4-6, keeping in mind that a wide current density range was reported from literature [8, 36, 64]. Low and high overpotential regions exist for determining Tafel slopes for the OER (Figure 4-6a and c), with the change from low to high overpotential being due to four mechanistic possibilities as suggested by Li et al. [36]. These mechanisms include a) the increase in mass transport resistance of OH^- , O_2 and/or electrons (as the OER mechanism is accepted to be a four electron transfer reaction), b) the change in the rate determining step, c) adsorption of reaction intermediates, and d) the change in the concentration/valence state in alkaline media of active sites and electric double layer reconstruction [36, 65]. The blocking effect of the O_2 bubbles formed during the reaction, which affect OH^- adsorption, is, however, minimised by the rotation of the working electrode at 1600 rpm [36]. Ir, IrO_2 and Ni, compare well with literature values with NiO being the exception (Table 4-3). In addition, higher Ir-containing samples exhibit lower Tafel slope values compared to lower Ir-containing samples (Figure 4-6c). Low Tafel slope values are indicative of reduced kinetic overpotential and are attributed to (i) favourable bond strength of OH^- adsorption, which increases electrocatalytic kinetics, and (ii) the increase of active sites, specifically for IrO_2 as discussed by Li et al. [36, 66]. As depicted in Figure 4-6b, all the Ir-containing electrocatalysts produced smaller Tafel slope values for low and high overpotential regions compared to Ni and NiO before CP, clearly indicating better performance. After CP, Ni exhibited an improvement in performance (lower Tafel slope value), while the performance of all the Ir-containing electrocatalysts decreased, showing higher Tafel slope values, when compared to Tafel slope values before stability (CP) testing. Noteworthy is the fact that for the mixed metal oxide combinations, the more Ir-rich $\text{Ir}_{92}\text{Ni}_8\text{O}_x$ exhibited the lowest Tafel slope value after CP for both overpotential regions, very similar to IrO_2 and pure Ni (Table 4-3, values in green), with the more Ni-rich $\text{Ir}_{68}\text{Ni}_{32}\text{O}_x$ and $\text{Ir}_{62}\text{Ni}_{38}\text{O}_x$ values very similar to pure Ni before CP (Table 4-3, values in blue). If Tafel slopes are used to rank the performance of the electrocatalysts, Ni proves to be the best performing after stability testing with $\text{Ir}_{92}\text{Ni}_8\text{O}_x$ being its competitor.

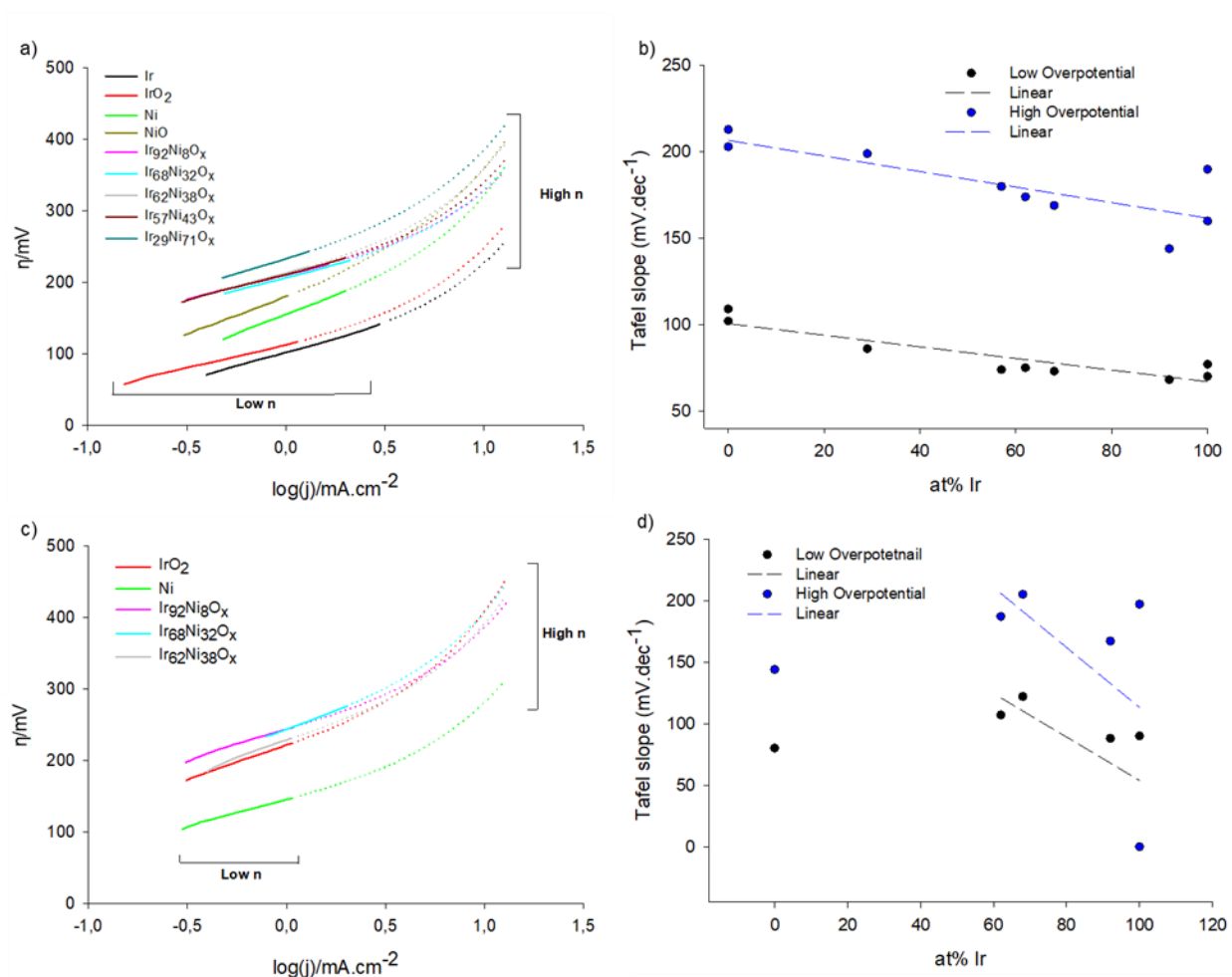


Figure 4-6: a) Tafel plots at low and high overpotential regions of all the tested metal/metal oxides before CP, b) the relationship between the atomic % Ir with the Tafel slope value before CP, c) Tafel plots of tested metal/metal oxides which reached benchmarking current density at low and high overpotential regions after CP and d) the relationship between the atomic % Ir with the Tafel slope value after CP

Table 4-3: Tafel slopes of all electrocatalysts before and after CP measurements

Sample	Tafel slope at low η before CP (mV.dec ⁻¹)	Tafel slope at low η after CP (mV.dec ⁻¹)	Tafel slope from literature (mV.dec ⁻¹)	Tafel slope at high η before CP (mV.dec ⁻¹)	Tafel slope at high η after CP (mV.dec ⁻¹)	Ref
Ir	77 ± 0.5	-	52	190 ± 1.0	-	[58]
IrO ₂	70 ± 0.5	90 ± 9.3	47	160 ± 3.3	197 ± 32.1	[8, 64]
Ni	109 ± 4.4	80 ± 6.5	50	213 ± 14	144 ± 30.2	[8]
NiO	102 ± 9.0	-	50	203 ± 7.6	-	[8, 67]
Ir ₂₉ Ni ₇₁ O _x	86 ± 1.7	-		199 ± 13	-	
Ir ₉₂ Ni ₈ O _x	68 ± 4.1	88 ± 6.6		144 ± 13	167 ± 7.5	
Ir ₆₈ Ni ₃₂ O _x	73 ± 2.7	112 ± 23.1		169 ± 8.8	205 ± 8.4	
Ir ₆₂ Ni ₃₈ O _x	75 ± 7.3	107 ± 20.2		174 ± 4.1	187 ± 22.5	
Ir ₅₇ Ni ₄₃ O _x	74 ± 4.6	-		180 ± 9.9	-	

(- Signs of severe deterioration)

Exchange current density values are dependent on the electrode/electrocatalyst surface (metal composition, roughness of the metal surface due to VC support), electrolyte (concentration of the soluble species, i.e. reactants and products formed, and impurities), and temperature/pressure. The exchange current density provides an indication of the rate of the studied reaction, with a higher value pointing to an accelerated process [66, 68]. Exchange current density values of the various samples were obtained from Tafel plots (Figure 4-6 and Table 4-4). All values obtained indicated that in the higher overpotential region the reaction was accelerated as would be expected due to higher energy input driving the reaction. Even though Ir indicated good exchange current density values before stability testing, exchange current density values could not be obtained after stability testing due to Ir's instability. This was also the case for NiO, Ir₂₉Ni₇₁O_x and Ir₅₇Ni₄₃O_x. It is interesting to note that the exchange current density values of Ni tend to decrease at both the low and high overpotential regions after stability testing, whereas Ir₉₂Ni₈O_x and Ir₆₈Ni₃₂O_x exhibited an increase at both overpotential regions. This suggests that after being run at 10 mA.cm⁻²_{geo} for six hours, the surface changes in the mixed metal oxides were beneficial toward catalysing the OER. Ni proved to perform the best, with Ir₆₈Ni₃₂O_x proving to be the best mixed metal oxide in terms of exchange current density. These exchange current density values are in range with literature values of various electrocatalysts for the OER in alkaline media (nano-NiO_x modified GC = 0.9 x 10⁻⁵ A.cm⁻², Ni 30 at% Cu electrode = 0.003 x 10⁻⁵ A.cm⁻², LiCoO₂ at 323.15 K = 2.78 x 10⁻⁵ A.cm⁻²) and in some cases, the developed sputtered electrocatalysts performed better [63, 68-72].

Table 4-4: Exchange current densities of all electrocatalysts before and after CP measurements

Sample	Exchange current densities before CP (A.cm ⁻²)		Exchange current densities after CP (A.cm ⁻²)	
	Low η /10 ⁻⁵	High η /10 ⁻⁵	Low η / 10 ⁻⁵	High η /10 ⁻⁵
Ir	5.1 ± 0.01	64 ± 0.78	-	-
IrO ₂	0.1 ± 1.3	19 ± 14.6	0.4 ± 0.2	10.3 ± 6.1
Ni	3.1 ± 0.6	28 ± 9.4	1.4 ± 0.2	13.2 ± 4.8
NiO	0.9 ± 0.7	9.9 ± 5.7	-	-
Ir ₂₉ Ni ₇₁ O _x	0.2 ± 0.06	9.8 ± 3.3	-	-
Ir ₉₂ Ni ₈ O _x	0.06 ± 0.04	4.4 ± 1.8	0.2 ± 0.08	5.1 ± 0.8
Ir ₆₈ Ni ₃₂ O _x	0.1 ± 0.03	8.6 ± 2.9	1.3 ± 1.1	12.9 ± 0.5
Ir ₆₂ Ni ₃₈ O _x	0.2 ± 0.1	11.5 ± 8.1	0.7 ± 0.2	8.6 ± 1.9
Ir ₅₇ Ni ₄₃ O _x	0.3 ± 0.1	15.7 ± 4.2	-	-

(- Signs of severe deterioration)

4.4 Conclusion

Various VC:Nafion supported Ir_xNi_yO_z electrocatalyst combinations for the OER in alkaline media were investigated. Reactive physical vapour deposition was employed to produce 40 nm thick metal/metal oxide films on a VC:Nafion supported Au/SiO₂ wafer for high-throughput screening and GCs for RDE measurements. From 64 different Ir_xNi_yO_z electrocatalyst combinations, five electrocatalyst combinations (Ir₉₂Ni₈O_x, Ir₆₈Ni₃₂O_x, Ir₆₂Ni₃₈O_x, Ir₅₇Ni₄₃O_x and Ir₂₉Ni₇₁O_x), exhibiting the lowest overpotential values at a benchmarking current of 10 mA.cm⁻²_{geo}, were selected for RDE studies. Key performance parameters (overpotential, Tafel slope and exchange current density) obtained from LSV analysis indicated in general good activity. Ir proved to initially exhibit the lowest overpotential of all the tested electrocatalysts, with the mixed metal oxides showing overpotentials (329 - 390 mV) in the range considered to be excellent for OER (300 - 400 mV). The mixed metal oxides initially exhibited similar Tafel slopes compared to Ir and IrO₂, suggesting similar mechanistic pathways for catalysing OER. Overall, smaller Tafel slopes were exhibited by all Ir-containing electrocatalyst combinations in comparison with Ni and NiO, which suggests that they are better electrocatalysts than Ni and NiO for the OER. Exchange current density values of the mixed metal oxides proved to be competitive with the single metal oxide (IrO₂ and NiO) electrocatalysts for both low and high overpotential regions, but they still do not outperform the single metal (Ir and Ni) electrocatalysts.

As an electrocatalyst cannot be evaluated based merely on initial performance, the electrocatalysts were subjected to CP for six hours after which LSV was performed again. Ir, NiO, Ir₂₉Ni₇₂O_x and Ir₅₇Ni₄₃O_x were not able to achieve benchmarking current densities after stability testing. IrO₂, Ir₉₂Ni₈O_x, Ir₆₈Ni₃₂O_x and Ir₆₂Ni₃₈O_x achieved benchmarking current densities, but at higher overpotentials that can be attributed to Ir dissolution. Ni interestingly improved after stability testing, however, with a large standard deviation suggesting poor repeatability. Ni also exhibited the best overall Tafel slope values in both regions, with the Ir₉₂Ni₈O_x mixed metal oxide exhibiting similar Tafel slope values compared to Ni and IrO₂ after stability testing, suggesting similar mechanistic pathways for catalysing the OER. In terms of exchange current density, Ni again proved to perform the best, with Ir₆₈Ni₃₂O_x being the best mixed metal oxide.

Taking all the key performance parameters into consideration, it is clear that the combination of Ir with Ni did not result in a mixed metal oxide(s) that outperformed their single metal counterparts. Competitive results were obtained and from the mixed metal oxides, Ir₉₂Ni₈O_x and Ir₆₈Ni₃₂O_x can be labelled as performing on average the best of the tested mixed metal oxide combinations. However, these activities were achieved with rather high Ir metal content. In this respect, the performance of the tested mixed metal oxide combinations does not satisfy the compromise between electrocatalytic performance and cost, as the best performance was achieved with pure Ni. This, however, does not disregard the possibility of employing Ir_xNi_yO_z electrocatalysts in alkaline OER applications. In this study the preparation method was reactive sputtering and the main variable the metal ratio. It may merely be that the mixed metal oxide ratio was not optimally modulated to result in desired synergistic effects arising from the intimate electronic interaction of the components.

4.5 References

1. Y. Chen, K. Rui, J. Zhu, S.X. Dou, W. Sun, Recent progress of nickel-based oxide/(oxy)hydroxide electrocatalysts for oxygen evolution reaction. *Chemistry – A European Journal*, 2018. 25(3): p. 703-713.
2. World Energy Council, *World Energy Resources*. 2013.
3. C.J. Winter, Hydrogen energy - Abundant, efficient, clean: A debate over the energy-system-of-change. 2009. (34) p. 1-52.
4. S.Y. Tee, W.S. Teo, L.D. Koh, S. Liu, C. P. Teng, M.Y. Han, Recent Progress in Energy-Driven Water Splitting. *Advanced Science*, 2017. 4(5): p. 1600337 (1-24)
5. D.D.A. de Fátima Palhares, L.G.M. Vieira, J.J.R. Damasceno, Hydrogen production by a low-cost electrolyzer developed through the combination of alkaline water electrolysis and solar energy use. *International Journal of Hydrogen Energy*, 2018. 43(9): p. 4265-4275.
6. F.M. Sapountzi, J.M. Gracia, C.J. Weststrate, H.O.A. Fredriksson, J.W. Niemantsverdriet, Electrocatalysts for the generation of hydrogen, oxygen and synthesis gas. *Progress in Energy and Combustion Science*, 2016. 58: p. 1-35.
7. G. Cipriani, V. D. Dio, F. Genduso, D. La Cascia, R. Liga, R. Miceli, G.R. Galluzzo, Perspective on hydrogen energy carrier and its automotive applications. *International Journal of Hydrogen Energy*, 2014. 39(16): p. 8482-8494.
8. M.Z. Iqbal, R.J. Kriek, Silver/Nickel Oxide (Ag/NiO) Nanocomposites Produced Via a Citrate Sol-Gel Route as Electrocatalyst for the Oxygen Evolution Reaction (OER) in Alkaline Medium. *Electrocatalysis*, 2018. 9(3): p. 279-286.
9. V. Maruthapandian, T. Pandiarajan, V. Saraswathy, S. Muralidharan, Oxygen evolution catalytic behaviour of Ni doped Mn₃O₄ in alkaline medium. *RSC Advances*, 2016. 6(54): p. 48995-49002.
10. K. Zeng, D. Zhang, Recent progress in alkaline water electrolysis for hydrogen production and applications. *Progress in Energy and Combustion Science*, 2010. 36(3): p. 307-326.
11. Y. Cheng, S.P. Jiang, Advances in electrocatalysts for oxygen evolution reaction of water electrolysis-from metal oxides to carbon nanotubes. *Progress in Natural Science: Materials International*, 2015. 25(6): p. 545-553.

12. S. Cherevko, S. Geiger, O. Kasian, N. Kulyk, J.P. Grote, A. Savan, B.R. Shrestha, S. Merzlikin, B. Beitbach, A. Ludwig, K.J.J. Mayrhofer, Oxygen and hydrogen evolution reactions on Ru, RuO₂, Ir, and IrO₂ thin film electrodes in acidic and alkaline electrolytes: A comparative study on activity and stability. *Catalysis Today*, 2016. 262: p. 170-180.
13. M.W. Louie, A.T. Bell, An Investigation of Thin-Film Ni-Fe Oxide Catalysts for the Electrochemical Evolution of Oxygen. *Journal of the American Chemical Society*, 2013. 135(33): p. 12329-12337.
14. J. Lee, B. Jeong, J.D. Ocon, Oxygen electrocatalysis in chemical energy conversion and storage technologies. *Current Applied Physics*, 2013. 13(2): p. 309-321.
15. R.L. Doyle, M.E.G. Lyons, Chapter 2: The oxygen Evolution Reaction: Mechanistic Concepts and Catalyst Design. 2016: Springer. 559.
16. M.E.G. Lyons, M.P. Brandon, The Oxygen Evolution Reaction on Passive Oxide Covered Transition Metal Electrodes in Aqueous Alkaline Solution Part-1 Nickel. *International Journal of Electrochemical Science*, 2008. 3: p. 1386-1424.
17. Y. Lee, J. Suntivich, K.J. May, E.E. Perry, Y. Shao-Horn, Synthesis and Activities of Rutile IrO₂ and RuO₂ Nanoparticles for Oxygen Evolution in Acid and Alkaline Solutions. *The Journal of Physical Chemistry* 2012. 3: p. 399-404.
18. Z.Y. Li, S.T. Shi, Q.S. Zhong, C.J. Zhang, C.W. Xu, Pt-Mn₃O₄/C as efficient electrocatalyst for oxygen evolution reaction in water electrolysis. *Electrochimica Acta*, 2014. 146: p. 119-124.
19. M.S. El-Deab, M.I. Awad, A.M. Mohammed, T. Ohsaka, Enhanced water electrolysis: Electrocatalytic generation of oxygen gas at manganese oxide nanorods modified electrodes. *Electrochemistry Communications*, 2007. 9(8): p. 2082-2087.
20. T. Reier, Z. Pawolek, S. Cherevko, M. Burns, T. Jones, D. Teschner, S. Selve, A. Bergmann, H.N. Nong, R. Schogl, K.J.J. Mayrhofer, P. Strasser, Molecular Insight in Structure and Activity of Highly Efficient, Low-Ir Ir-Ni Oxide Catalysts for Electrochemical Water Splitting (OER). *Journal of the American Chemical Society*, 2015. 137(40): p. 13031-13040.
21. L. Trotochaud, J.K. Ranney, K.N. Williams, S.W. Boettcher, Solution-Cast Metal Oxide Thin Film Electrocatalysts for Oxygen Evolution. *Journal of the American Chemical Society*, 2012. 134(41): p. 17253-17261.

22. J.S. Sagu, D. Mehta, K.G.U. Wijayantha, Electrocatalytic activity of CoFe_2O_4 thin films prepared by AACVD towards the oxygen evolution reaction in alkaline media. *Electrochemistry Communications*, 2018. 87: p. 1-4.
23. B.M. Hunter, J.R. Winkler, H.B. Gray, Iron Is the Active Site in Nickel/Iron Water Oxidation Electrocatalysts. *Molecules*, 2018. 23(4): p. 903(1-7).
24. D.A. Corrigan, The Catalysis of the Oxygen Evolution Reaction by Iron Impurities in Thin Film Nickel Oxide Electrodes. *Journal of Electrochemical Society*, 1987. 134(2): p. 377-384.
25. A.A. Tahir, K.G.U. Wijayantha, S. Saremi-Yarahmadi, M. Mazhar, V. McKee, Nanostructured $\alpha\text{-Fe}_2\text{O}_3$ Thin Films for Photoelectrochemical Hydrogen Generation. *Chemistry of Materials*, 2009. 21(16): p. 3763-3772.
26. A.L. Dicks, The role of carbon in fuel cells. *Journal of Power Sources*, 2006. 156(2): p. 128-141.
27. Y. Yi, G. Weinberg, M. Prenzel, M. Greiner, S. Heumann, S. Becker, R. Schlögl, Electrochemical corrosion of a glassy carbon electrode. *Catalysis Today*, 2017. 295: p. 32-40.
28. B. Seger, P.V. Kamat, Electrocatalytically Active Graphene-Platinum Nanocomposites. Role of 2-D Carbon Support in PEM Fuel Cells. *The Journal of Physical Chemistry C*, 2009. 113(19): p. 7990-7995.
29. M.J. Lazaro, L. Calvillo, V. Celorrio, J.I. Pardo, S. Perathoner, R. Moliner, Study and application of carbon black vulcan XC-72R in polymeric electrolyte fuel cells. *Carbon Black: Production, Properties and Uses*, ed. T.L.P. I.J. Sanders. Nova Science Publishers, 2011: p. 1-28
30. D. Coertzen, R.J. Kriek, P.B.J. Levecque, A. Falch, Vulcan Carbon as Support for Sputtered Oxygen Evolution Electrocatalysts. *Electrocatalysis*, 2019(10), p. 604-612.
31. A. Falch, V.A. Lates, H.S. Kotzé, R.J. Kriek, The Effect of Rapid Thermal Annealing on Sputtered Pt and Pt_3Pd_2 Thin Film Electrocatalysts for Aqueous SO_2 Electro-Oxidation. *Electrocatalysis*, 2016(7): p. 33-41.
32. A. Falch, V. Lates, R.J. Kriek, Combinatorial Plasma Sputtering of Pt_xPd_y Thin Film Electrocatalysts for Aqueous SO_2 Electro-Oxidation. *Electrocatalysis*, 2015. 6(3): p. 322-330.

33. A. Falch, V.A.Badets, C. Labrugère, R.J. Kriek, Co-sputtered $Pt_xPd_yAl_z$ thin film electrocatalysts for the production of hydrogen via $SO_2(aq)$ electro-oxidation. *Electrocatalysis*, 2016. 7(5): p. 376-390.
34. M.H. Sellami, K. Loudiyi, Electrolytes behavior during hydrogen production by solar energy. *Renewable and Sustainable Energy Reviews*, 2017. 70: p. 1331-1335.
35. P. Chen, L.K. Wang, G. Wang, M.R. Gao, J. Ge, W.J. Yuan, Y.H. Shen, A.J. Wie, S.H. Yu Nitrogen-doped nanoporous carbon nanosheets derived from plant biomass: An efficient catalyst for oxygen reduction reaction. *The Royal Society of Chemistry*, 2014.
36. G. Li, L. Anderson, Y. Chen, M. Pan, P.Y.A. Chuang, New insights into evaluating catalyst activity and stability for oxygen evolution reactions in alkaline media. *Sustainable Energy & Fuels*, 2018. 2(1): p. 237-251.
37. C.C.L. McCrory, S.Jung, J.C. Peters, T.F. Jaramillo, Benchmarking Heterogeneous Electrocatalysts for the Oxygen Evolution Reaction. *Journal of the American Society*, 2013. 135: p. 16977-16987.
38. C.C.L. McCrory, S.Jung, I.M. Ferrer, S.M. Chatman, J.C. Peters, T.F. Jaramillo, Benchmarking Hydrogen Evolving Reaction and Oxygen Evolving Reaction Electrocatalysts for Solar Water Splitting Devices. *Journal of the American Chemical Society*, 2015. 137: p. 4347 - 4357.
39. A. Ganassin, A. Maljusch, V. Colic, L. Spanier, K. Brandl, W. Schuhmann, A. Bandarenka, Benchmarking the Performance of Thin-Film Oxide Electrocatalysts for Gas Evolution Reactions at High Current Densities. *ACS Catalysis*, 2016. 6(5): p. 3017-3024.
40. K.A. Stoerzinger, W.S.Choi, H. Jeon, H.N. Lee, Y. Shao-Horn, Role of Stain and Conductivity in Oxygen Electrocatalysis on $LaCoO_3$ Thin Films. *The Journal of Physical Chemistry*, 2015. 6 p. 487-492.
41. M. Görlin, J.F de Araujo, H. Schmies, D. Bernsmeier, S. Dresp, M. Gliech, Z. Jusys, P. Chernev, R. Kraehnert, H. Dau, P. Strasser, Tracking Catalyst Redox States and Reaction Dynamics in Ni–Fe Oxyhydroxide Oxygen Evolution Reaction Electrocatalysts: The Role of Catalyst Support and Electrolyte pH. *Journal of the American Chemical Society*, 2017. 139(5): p. 2070-2082.

42. X. Lu, W.L. Yim, B.H.R. Suryanto, C. Zhao, Electrocatalytic Oxygen Evolution at Surface-Oxidized Multiwall Carbon Nanotubes. *Journal of the American Chemical Society*, 2015. 137(8): p. 2901-2907.
43. B. You, N. Jiang, M. Sheng, S. Gul, J. Yano, Y. Sun, High-Performance Overall Water Splitting Electrocatalysts Derived from Cobalt-Based Metal–Organic Frameworks. *Chemistry of Materials*, 2015. 27(22): p. 7636-7642.
44. G.F. Chen, T.Y. Ma, Z.Q. Liu, N. Li, Y.Z. Su, K. Davey, S.Z. Qiao, Efficient and Stable Bifunctional Electrocatalysts Ni/Ni_xM_y (M = P, S) for Overall Water Splitting. *Advanced Functional Materials*, 2016. 26(19): p. 3314-3323.
45. X. Lu, C.Zao, Electrodeposition of hierarchically structured three-dimensional nickel-iron electrodes for efficient oxygen evolution at high current densities. *Nature Communications*, 2015.
46. Colli, A.N., H.H. Girault, and A. Battistel, Non-Precious Electrodes for Practical Alkaline Water Electrolysis. *Materials*, 2019. 12(8): p. 1336(1-7).
47. D. Pletcher, X. Li, Prospects for alkaline zero gap water electrolyzers for hydrogen production. *International Journal of Hydrogen Energy*, 2011. 36(23): p. 15089-15104.
48. N. Armaroli, V. Balzani, The Future of Energy Supply: Challenges and Opportunities. *Angewandte Chemie International Edition*, 2007. 46(1-2): p. 52-66.
49. Z. Lu, W. Xu, W. Zhu, Q. Yang, X Lei, J. Liu, Y. Li, X. Sun, X. Duan, Three-dimensional NiFe layered double hydroxide film for high-efficiency oxygen evolution reaction. *Chemical Communications*, 2014. 50(49): p. 6479-6482.
50. L. Trotochaud, S.L. Young, J.K. Ranney, S.W. Boettcher, Nickel–Iron Oxyhydroxide Oxygen-Evolution Electrocatalysts: The Role of Intentional and Incidental Iron Incorporation. *Journal of the American Chemical Society*, 2014. 136(18): p. 6744-6753.
51. M. Tahir, L. Pan, F. Idrees, X Zhang, L. Wang, J.J. Zou, Z.L. Wang, Electrocatalytic oxygen evolution reaction for energy conversion and storage: A comprehensive review. *Nano Energy*, 2017. 37: p. 136-157.
52. H.N. Nong, H.S. Oh, T. Reier, E. Willinger, M.G. Willinger, V. Petkov, D. Teschner, P. Strasser, Oxide-Supported IrNiO_x Core–Shell Particles as Efficient, Cost-Effective, and

- Stable Catalysts for Electrochemical Water Splitting. *Angewandte Chemie International Edition*, 2015. 54(10): p. 2975-2979.
53. Y. Zhao, X. Jia, G. Chen, L. Shang, G.I.N. Waterhouse, L.Z. Wu, C.H. Tung, D. O'Hare, T. Zhang, Ultrafine NiO Nanosheets Stabilized by TiO₂ from Monolayer NiTi-LDH Precursors: An Active Water Oxidation Electrocatalyst. *Journal of the American Chemical Society*, 2016. 138(20): p. 6517-6524.
 54. I.M. Sadiq, A.M. Mohammad, M.E. El-Shakre, M.S. El-Deab, B.E. El-Anadoul, Enhanced electrolytic generation of oxygen gas at binary nickel oxide–cobalt oxide nanoparticle-modified electrodes. *Journal of Solid-State Electrochemistry*, 2013. 17(3): p. 871-879.
 55. A.J. Tkalych, K. Yu, E.A. Carter, Structural and Electronic Features of β -Ni(OH)₂ and β -NiOOH from First Principles. *The Journal of Physical Chemistry C*, 2015. 119(43): p. 24315-24322.
 56. M. Merrill, M. Worsley, A. Wittstock, J. Biener, M. Stadermann, Determination of the “NiOOH” charge and discharge mechanisms at ideal activity. *Journal of Electroanalytical Chemistry*, 2014. 717-718: p. 177-188.
 57. B.M. Jovic, V.D. Jovic, U.C. Lacnjevac, L.J. Gajic-Krstajic, N.V. Krstajic, Electrodeposited Ni-Sn coatings as electrocatalysts for hydrogen and oxygen evolution in alkaline solutions. *Zaštita materijala*, 2016. 57(1): p. 136-147.
 58. S.B. Roy, K. Akbar, J.H. Jean, S.K. Jerng, L. Truong, K. Kim, Y. Yi, S.H. Chun, Iridium on vertical graphene as an all-round catalyst for robust water splitting reactions. *Journal of Materials Chemistry A*, 2019. 7(36): p. 20590-20596.
 59. J. Kubisztal, A. Budniok, Study of the oxygen evolution reaction on nickel-based composite coatings in alkaline media. *International Journal of Hydrogen Energy*, 2008. 33(17): p. 4488-4494.
 60. T. Binninger, R. Mohamed, K. Waltar, E. Fabbri, P. Levecque, R. Kotz, T.J. Schmidt, Thermodynamic explanation of the universal correlation between oxygen evolution activity and corrosion of oxide catalysts. *Scientific Reports*, 2015. 5: p. 12167.
 61. M. Schalenbach, O. Kasian, M. Ledendecker, F.D. Speck, A.M. Mingers, Karl.J.J. Mayrhofer, The Electrochemical Dissolution of Noble Metals in Alkaline Media. *Electrocatalysis*, 2018. 9(2): p. 153-161.

62. A. Manabe, M.Kashiwase, T. Hashimoto, T. Hayashida, A. Kato, K. Hirao, I. Shimomura, I. Nagashima, Basic study of alkaline water electrolysis. *Electrochimica Acta*, 2013. 100: p. 249-256.
63. R.L Doyle, M.E.G. Lyons, An electrochemical impedance study of the oxygen evolution reaction at hydrous iron oxide in base. *Physical Chemistry Chemical Physics*, 2013. 15(14): p. 5224-5237.
64. S. Jung, C.C.L. McCrory, I.M. Ferrer, J.C. Peters, T.F. Jaramillo, Benchmarking nanoparticulate metal oxide electrocatalysts for the alkaline water oxidation reaction. *Journal of Materials Chemistry A*, 2016. 4(8): p. 3068-3076.
65. G. Wu, N. Li, D.R. Zhou, K. Mitsuo, B.Q. Xu, Anodically electrodeposited Co+Ni mixed oxide electrode: preparation and electrocatalytic activity for oxygen evolution in alkaline media. *Journal of Solid-State Chemistry*, 2004. 177(10): p. 3682-3692.
66. S. Gimenez, J. Bisquert, *Photoelectrochemical Solar Fuel Production*, ed. J. Bisquert, S. Gimenez. 2016: Springer.
67. L.A. Stern, X. Hu, Enhanced oxygen evolution activity by NiO_x and Ni(OH)₂ nanoparticles. *Faraday Discussions*, 2014. 176(0): p. 363-379.
68. V.C.B. Pegoretti, P.V.M. Dixini, A.K.S. Rocha, M.F.F. Lelis, M.B.J.G. Freitas, High-temperature (HT) LiCoO₂ recycled from spent lithium ion batteries as catalyst for oxygen evolution reaction. *Materials Research Bulletin*, 2019. 110: p. 97-101.
69. A.K.M. Fazle Kibria, S.A. Tarafdar, Electrochemical studies of a nickel–copper electrode for the oxygen evolution reaction (OER). *International Journal of Hydrogen Energy*, 2002. 27(9): p. 879-884.
70. T. Rauscher, C.I. Bernacker, U. Muhle, B. Kieback, L. Rontzsch, The effect of Fe as constituent in Ni-base alloys on the oxygen evolution reaction in alkaline solutions at high current densities. *International Journal of Hydrogen Energy*, 2019. 44(13): p. 6392-6402.
71. C. Bocca, A. Barbucci, G. Cerisola, The influence of surface finishing on the electrocatalytic properties of nickel for the oxygen evolution reaction (OER) in alkaline solution. *International Journal of Hydrogen Energy*, 1998. 23(4): p. 247-252.
72. I.M Sadiq, A.M. Mohammed, M. E. El-Shakre, M.S. El-Deab, Electrocatalytic activity of nickel oxide nanoparticles-modified electrodes: Optimization of the loading level and

operating pH towards the oxygen evolution reaction. *International Journal of Hydrogen Energy*, 2012. 37(1): p. 68-77.

73. F. Basharat, U.A. Rana, M. Shahib, M. Serwar, Heat treatment of electrodeposited NiO films for improved catalytic water oxidation. *RSC Advances*, 2015. 5(105): p. 86713-86722.

CHAPTER 5: EVALUATION AND CONCLUSION

This chapter is intended to give an overview and evaluation of the dissertation as well as recommendations and areas for improvement from a critical point of view

5.1 Reiteration of the Problem Statement, Aim and Objectives

The use of hydrogen as energy carrier for the generation of clean and renewable electrical energy is very attractive when compared to fossil fuel energy production, especially when combined with renewable energy sources for driving the production of hydrogen [1-5]. For the generation of hydrogen, alkaline water electrolysis (AWE) is one of the most promising and simplest technologies, however this technology suffers from poor oxygen evolution kinetics on the anode which requires the use of efficient electrocatalysts to increase the performance [6-10]. Amongst the electrocatalysts studied to date, various metal and metal oxides supported on different materials as electrode substrates have been studied, i.e. Co, Mn, Ni, Ni-based and Fe (varying in composition and synthesis methods together with different reaction conditions, catalyst analysis techniques and benchmarking used), to compete with mainly Ni as electrocatalysts of choice for alkaline media [5, 8, 9]. Ni and Ni-based oxide electrocatalysts have been proven to exhibit high resistance to corrosion, affordability, and acceptable activity, (however still with higher than desired overpotentials), making it an attractive electrocatalytic material [8, 11, 12]. Even though literature suggest that there are several competitive alternative electrocatalysts, it is still not clear that a definitive alternative electrocatalyst has been chosen to replace the electrocatalyst(s) currently used. Evident from the numerous publications in this field at the moment, the necessity and interest to develop electrocatalysts that are affordable and abundant whilst showing good activity and stability toward the OER, is signified. With the ongoing focus to improve electrocatalysts, the fine-tuning of these Ni and Ni-based electrocatalysts by means of compositional content modifications is important in an attempt to improve their catalytic performance, i.e. exploring synergistic effects [8, 13]. Thus, taking into account the large amount of literature on IrO_2 (known to be very active in acidic media) and the numerous publications on modified Ni-based electrocatalysts (including NiO) used in alkaline media, we suggested an investigation of $\text{Ir}_x\text{Ni}_y\text{O}_z$ electrocatalyst combinations for the OER in alkaline media. The combination of the intrinsic characteristic that Ni-based electrocatalysts exhibit in alkaline media together with the electrocatalytic performance that Ir and IrO_2 possess in acidic media [14], might result in an active and stable electrocatalyst for the OER in alkaline media.

With the above-mentioned criteria in mind, the aim and objectives of this study were formulated (as stated in Chapter 1).

The fundamental aim of this study was to investigate the electrocatalytic activity and stability of various Vulcan carbon (VC) supported $\text{Ir}_x\text{Ni}_y\text{O}_z$ electrocatalysts in alkaline media for the OER, in an attempt to develop improved electrocatalysts in terms of activity and stability.

To achieve this, the main objectives were:

1. Evaluate available literature on the use of VC as support for electrocatalysts.
2. Prepare and investigate different VC:Nafion ratios and identify the VC:Nafion ratio which exhibits the best even coverage of GC substrates, highest activity as well as good stability and durability towards the OER in alkaline media.
3. Scrutinise literature on electrocatalysts progress, characterisation and evaluation applicable to the OER in alkaline water electrolysis.
4. Employ reactive oxide sputtering to prepare 64 different $\text{Ir}_x\text{Ni}_y\text{O}_z$ electrocatalyst combinations, using a VC:Nafion supported Au/ SiO_2 wafer.
5. Subject the 64 different $\text{Ir}_x\text{Ni}_y\text{O}_z$ electrocatalyst combinations to high-throughput screening by employing a specialised electrochemical cell connected to a 64 channel potentiostat and identify the best (top five) $\text{Ir}_x\text{Ni}_y\text{O}_z$ electrocatalyst combinations for the OER.
6. Critically characterise the top five $\text{Ir}_x\text{Ni}_y\text{O}_z$ electrocatalyst combinations, together with their single metal counterparts on GC as substrate, by electrochemical evaluation (rotating disk electrode, RDE) and physical analysis (scanning electron microscope (SEM), Energy-dispersive X-ray spectroscopy (EDX), and X-ray photoelectron spectroscopy (XPS)).
7. Compare and validate where possible, the obtained results with available literature results.
8. Publish results and findings in international accredited scientific journals.

The following sections will demonstrate how the aforementioned objectives were successfully achieved, followed by a discussion of envisaged improvements that can be made and specific topics that can be further investigated.

5.2 Dissertation Overview

The study was divided into five succeeding chapters with Chapters 1 and 2 introducing the theme and focus of this study, and Chapter 3 to 5, illustrating the thought process and approaches in addressing the problem statement (section 1.1) and objectives (section 1.3 and 5.1).

In this study two different substrates were employed (Au/SiO_2 and GC) which served different purposes. Research on thin film electrocatalysts employing these substrates have revealed delamination to be a problem during testing [16, 18]. As a means to eliminate delamination, Ni (one of the known metals to show good activity for the OER in alkaline media) was sputtered onto different ratios of VC:Nafion support, as well as clean smooth GC as electrode for comparison (Chapter 3). The sputtering of the thin film electrocatalysts on top of a VC:Nafion support is a novel approach, which results in the active material not mixing into the bulk of the VC:Nafion support, but being present at the surface with all the active materials being in contact with the reaction of interest. This investigation also served to determine if VC:Nafion can increase the activity of the electrocatalyst as it possesses increased surface area. It was found that the use of VC:Nafion (mass ratio of 1:0.67) as support eliminated delamination of the electrocatalyst during testing completely, even in the case where stability testing was conducted by means of six-hour CP analysis. The Ni on VC:Nafion support also exhibited better overpotential when compared to the unsupported Ni electrocatalysts before stability testing. Increased activity for Ni on clean GC was obtained after stability testing, achieving similar overpotential compared to supported Ni, however with delamination of the Ni on clean GC clearly present. Achieving good activity with no interference from delamination, the VC:Nafion (1:0.67) was used on an Au/SiO_2 wafer containing 64 working electrode pads, as well as on GC's for the characterisation of $\text{Ir}_x\text{Ni}_y\text{O}_z$ electrocatalyst combinations as possible electrocatalysts for the OER in alkaline media.

A PVD combinatorial sputtering technique for reactive sputtering of metal/metal oxides was used to produce 64 different $\text{Ir}_x\text{Ni}_y\text{O}_z$ electrocatalyst combinations on a VC:Nafion supported Au/SiO_2 wafer as substrate (Chapter 4). High-throughput screening was used to evaluate all 64 $\text{Ir}_x\text{Ni}_y\text{O}_z$ electrocatalyst combinations simultaneously. The five $\text{Ir}_x\text{Ni}_y\text{O}_z$ electrocatalyst combinations with the lowest overpotential at 10 mA.cm^{-2} were selected for further characterisation. This included physical characterisation (SEM, EDX and XPS), as well as electrochemical analysis (LSV and CP) in terms of i) activity towards the OER in alkaline media (overpotential, Tafel slope and exchange current density) and ii) the stability of the selected metal/metal oxides, compared to Ir and Ni along with their oxides (Ir and IrO_2 is known to possess excellent activity for the OER in acidic media and Ni and NiO exhibiting good activity and stability in alkaline media). The first RDE technique used to evaluate the electrochemical characteristics of the $\text{Ir}_x\text{Ni}_y\text{O}_z$ electrocatalyst combinations was linear sweep voltammetry (LSV). The LSV data was used to calculate the

overpotential of each electrocatalyst tested, including the pure metals, their oxides and the $\text{Ir}_x\text{Ni}_y\text{O}_z$ electrocatalyst combinations. The overpotential data (at a benchmarking current density of $10\text{mA}\cdot\text{cm}^{-2}$) indicated that the best performing electrocatalysts proved to be Ir and IrO_2 for single metal/metal oxide films, with $\text{Ir}_{29}\text{Ni}_{71}\text{O}_x$ indicating the lowest overpotential of the sputtered mixed metal oxide combinations. Chronopotentiometry (CP, used for stability testing) was performed at a current density of $10\text{mA}\cdot\text{cm}^{-2}$ for six hours, where after a second set of LSV data was obtained. Overpotential calculations obtained from the LSV data after stability tests were used to evaluate the increase/decrease of the overpotential relative to initial LSV measurements. The overpotential data after stability tests indicated that the majority of electrocatalysts that exhibited the lowest overpotential before stability tests together with $\text{Ir}_{57}\text{Ni}_{42}\text{O}_x$ and NiO had no overpotential values due to the inability of achieving the benchmarking current density. Of the metal/metal oxide combinations, $\text{Ir}_{92}\text{Ni}_8\text{O}_x$ exhibited the lowest overpotential after stability tests. Ni on the other hand exhibited a decrease in overpotential (increase in activity) after stability testing. The same phenomena would be expected for NiO, but this was clearly not the case (in this study) for NiO prepared by reactive sputtering.

Tafel plots before and after stability tests were constructed from the LSV measurements. Low and high overpotential regions exist for determining Tafel slopes for the OER with the change from low to high overpotential being due to four mechanistic possibilities [22]. All Ir-containing electrocatalysts showed smaller Tafel slope values compared to Ni and NiO, both for the low and high overpotential regions indicating better performance. After stability testing, Ni indicated improved performance (lower Tafel slope value) with the performance of all Ir-containing electrocatalysts showing an increase in their Tafel slope values. If the Tafel slopes values are used as a performance indicator, the performance of the electrocatalysts can be ranked with Ni proving to be the best performer after stability testing with $\text{Ir}_{92}\text{Ni}_8\text{O}_x$ being its competitor.

Exchange current density as another performance indicator was extracted from Tafel plots constructed from LSV measurements before and after stability tests (higher values indicating an accelerated process/reaction). The exchange current density of Ni and IrO_2 tend to decrease in value for both low and high overpotential regions after stability, whereas $\text{Ir}_{92}\text{Ni}_8\text{O}_x$ and $\text{Ir}_{68}\text{Ni}_{32}\text{O}_x$ exhibited an increase at both overpotential regions. This suggests that after stability tests, these metal/metal oxide combinations' surface changes (Ir dissolution discussed shortly) were beneficial towards catalysing the OER. Again, Ni proved to perform the best, with $\text{Ir}_{68}\text{Ni}_{32}\text{O}_x$ proving to be the best metal/metal oxide combination in terms of exchange current density.

To obtain insight on the physical properties of the prepared electrocatalysts, physical characterisation was conducted. SEM data indicated good VC:Nafion coverage with no exposed GC (Chapter 3), with similar morphologies found for the different electrocatalysts supported on

VC:Nafion (Chapter 4). This morphology showed to increase the activity (however small) of the tested Ni electrocatalysts due to increased surface area, and more importantly, eliminated delamination of electrocatalysts during testing (Chapter 3 and Chapter 4). EDX before stability testing was used to obtain the exact metal content of each electrocatalyst studied to compare with EDX results after stability tests, as it is known that Ir tends to dissolve in alkaline media. As EDX is used to investigate the bulk metal content and not as sensitive to evaluate the surface of the electrocatalysts, XPS was used to evaluate the metal composition on the surface of each of the $\text{Ir}_x\text{Ni}_y\text{O}_z$ electrocatalyst combinations. Comparing the EDX and XPS values after stability tests, it was found that more Ir was lost at the surface of the electrocatalysts compared to the bulk. This leads to the surface of the electrocatalyst that is in contact with the active species to become more Ni rich, which from overpotential data, it is evident that the higher the Ni content, the poorer the activity (greater overpotential) exhibited by the metal/metal oxide combinations.

When considering all the performance parameters (overpotential, Tafel slope and exchange current density) it was found that combining Ir with Ni did not result in a metal/metal oxide combination that could outperform their single metal counterparts. $\text{Ir}_{92}\text{Ni}_8\text{O}_x$ and $\text{Ir}_{68}\text{Ni}_{32}\text{O}_x$ on average showed the best performance of the tested metal/metal oxide combinations while still containing a relatively high amount of Ir. In this respect, the performance of the tested metal/metal oxide combinations do not satisfy the compromise between electrocatalytic performance and cost, as the best performance was achieved with pure Ni. This, however, does not disregard the possibility of employing $\text{Ir}_x\text{Ni}_y\text{O}_z$ electrocatalysts in alkaline OER applications.

5.3 Recommendations and area for improvement

5.3.1 Alternative supports

It is possible that different supporting structures could lead to different (improved) performance outcomes. VC is one of the most basic supporting structures used, with more complex structures like graphite, graphene, nanoparticles and nanotubes being used as supporting structures for electrocatalysis [5, 17, 19]. It is recommended to explore these 'up to date' supports, which could lead to improved performance of the tested $\text{Ir}_x\text{Ni}_y\text{O}_z$ electrocatalyst combinations.

5.3.2 Alternative support binder

Nafion (perfluorosulfonic acid) is generally used as binder in the production of electrocatalyst supports [21, 25]. However, Nafion is not the favoured binder for use in alkaline media due to its

primary role being the facilitating of proton (H^+) transport to and from catalytic sites [26]. However, a more favourable anion binder could prove beneficial for OER studies in alkaline media.

5.3.3 Role of Fe

The intensive literature study conducted in this investigation, specifically on Ni used as electrocatalyst for the anode for the OER in an alkaline media, found that Fe impurities on/in the electrocatalysts could be reasons for improved electrocatalytic performance. These impurities are found in the electrolyte and in the case of combinatorial sputtering (as used in this study) the metal target used in this technique contain trace amounts of Fe. Even though EDX or XPS was not used to determine the possibility and amount of Fe present in the metal/metal oxide electrocatalysts, it is still a possibility that Fe may have been present in the electrocatalysts and affected the electrochemical characteristics of the entire electrocatalyst. It is therefore suggested that further physical characterisation (XPS and x-ray diffraction analysis (XRD)) be conducted on the electrocatalyst to gain better understanding of the observed performance.

5.3.4 Loading of VC:Nafion ink

Loading the VC:Nafion support in Chapter 3 included mixing the VC:Nafion ink by sonication where after 10 μ l of the support was drop casted onto the GC substrate. Subsequent to the publication of Chapter 3, it was realised that lower overpotentials were obtained for Ni (Chapter 4) when compared to the overpotentials obtained for Ni in Chapter 3. Upon closer investigation as to why, it was concluded that sonication is not enough to ensure proper mixing and loading. It was realised that manually shaking the ink (after initial sonication) before each drop casting was the only possible reason for this improvement in overpotential as all the other parameters (i.e. Ni content, sputtering conditions, electrolyte, etc.) were exactly the same. After sonicating for 2h it appears that the VC and Nafion is mixed well (VC is so finely dispersed, the ink appears to be overall black), but after close observation a few minutes after sonication, a degree of separation appears (VC starts settling at the bottom). This will inevitably result in a very small degree of deviation between sample loadings as less conductive VC will be present in each 10 μ l.

The results obtained in Chapter 4 do however not negate the data obtained in Chapter 3 as the sonication mixing method used in Chapter 3 was uniform for the electrocatalysts used in that particular study whereas manual shaking, in addition to sonication, was employed for all electrocatalysts in Chapter 4. Therefore, the study of Chapter 3 and Chapter 4 should be interpreted on their own merit and in line with the specific aim of each chapter. It is therefore strongly recommended (for future studies) to pay close attention to the manner in which the ink is used as a support and that homogenisation just prior to each loading has a positive effect.

5.3.5 General areas for improvement

- The usage of different working temperatures for electrochemical characterisation, as only one temperature (25°C) was used in this study. AWE working temperatures range between 20 - 80°C, which have effects on the performance of the electrocatalyst with one study suggesting working temperature of up to 150°C to increase electrolyte conductivity and increase the rate of the electrochemical reaction kinetics [1, 27].
- Perform more in-depth physical characterisation on the structure of the electrocatalyst (crystallinity, state of the oxide, particle size in the case of the VC:Nafion support) as no information on the type of oxide(s), Fe impurities or crystalline structure of the electrocatalyst was obtained. The physical characterisation in this study was only used to determine metal ratio compositions. This information could lead to a better understanding of the characteristics shown by the studied electrocatalysts (especially if Fe is incorporated into the electrocatalyst).
- Improving the method of casting the VC:Nafion support ink onto the Au/SiO₂ wafer, as precise amounts of VC:Nafion that is present on the surface of each circuit pad deviate slightly. This deviation is due to a degree of overflow when using the “sticker” to load the ink. The use of a thicker “sticker” will prevent overflow from occurring.
- The electrochemical active surface area (ECSA) should also be included in future studies as this electrochemical characterisation technique can add to the comparison of the different electrocatalysts used (especially in terms of current per noble metal content). With this data, improved activity of the electrocatalyst can be investigated in terms of alteration to the support and metal compositions and structure.

5.4 References

1. F.M. Sapountzi, J.M. Gracia, C.J. Weststrate, H.O.A. Fredriksson, J.W. Niemantsverdriet, Electrocatalysts for the generation of hydrogen, oxygen and synthesis gas. *Progress in Energy and Combustion Science*, 2016. 58: p. 1-35.
2. S. Gimenez, J. Bisquert, Photoelectrochemical Solar Fuel Production, ed. J. Bisquert, S. Gimenez. 2016: Springer.
3. C.J. Winter, Hydrogen energy - Abundant, efficient, clean: A debate over the energy-system-of-change. 2009. (34) p. 1-52.
4. C. Angelinetta, S. Trasatti, L.J.D. Atanasoska, Z.S. Minevski, R.T. Atanasoski, Effect of preparation on the surface and electrocatalytic properties of RuO₂ + IrO₂ mixed oxide electrodes. *Materials Chemistry and Physics*, 1989. 22(1): p. 231-247.
5. T. Audichon, E. Mayousse, S. Morisset, C. Morais, C. Comminges, T.W. Napporn, K.B. Kokoh, Electroactivity of RuO₂–IrO₂ mixed nanocatalysts toward the oxygen evolution reaction in a water electrolyzer supplied by a solar profile. *International Journal of Hydrogen Energy*, 2014. 39(30): p. 16785-16796.
6. J.D. Holladay, J. Hu, D.L. King, Y. Wang, An overview of hydrogen production technologies. *Catalysis Today*, 2009. 139(4): p. 244-260.
7. S. Siracusano, N. van Dijk, E. Payne-Johnson, V. Baglio, A.S. Arico, Nanosized IrO_x and IrRuO_x electrocatalysts for the O₂ evolution reaction in PEM water electrolyzers. *Applied Catalysis B: Environmental*, 2015. 164: p. 488-495.
8. E. Fabbri, A. Habereder, K. Waltar, R. Kotz, T.J. Schmidt, Developments and perspectives of oxide-based catalysts for the oxygen evolution reaction. *Catalysis Science & Technology*, 2014. 4(11): p. 3800-3821.
9. X. Lu, C. Zhao, Electrodeposition of hierarchically structured three-dimensional nickel–iron electrodes for efficient oxygen evolution at high current densities. *Nature Communications*, 2015. 6: p. 6616.
10. F. Song, X. Hu, Exfoliation of layered double hydroxides for enhanced oxygen evolution catalysis. *Nature Communications*, 2014. 5: p. 4477.

11. L. Wu, Q. Li, C.H. Wu, H. Zhu, A. Mendoza-Garcia, B. Shen, J. Guo, S. Sun, Stable Cobalt Nanoparticles and Their Monolayer Array as an Efficient Electrocatalyst for Oxygen Evolution Reaction. *Journal of the American Chemical Society*, 2015. 137(22): p. 7071-7074.
12. L. Trotochaud, J.K. Ranney, K.N. Williams, S.W. Boettcher, Solution-Cast Metal Oxide Thin Film Electrocatalysts for Oxygen Evolution. *Journal of the American Chemical Society*, 2012. 134(41): p. 17253-17261.
13. A.N. Colli, H.H. Girault, A. Battistel, Non-Precious Electrodes for Practical Alkaline Water Electrolysis. *Materials*, 2019. 12(8): p. 1336.
14. S. Cherevko, S. Geiger, O. Kasian, N. Kulyk, J.P. Grote, A. Savan, B.R. Shrestha, S. Merzlikin, B. Beitbach, A. Ludwig, K.J.J Mayrhofer, Oxygen and hydrogen evolution reactions on Ru, RuO₂, Ir, and IrO₂ thin film electrodes in acidic and alkaline electrolytes: A comparative study on activity and stability. *Catalysis Today*, 2016. 262: p. 170-180.
15. Y. Yi, G. Weinberg, M. Prenzel, M. Greiner, S. Heumann, S. Becker, R. Schlögl, Electrochemical corrosion of a glassy carbon electrode. *Catalysis Today*, 2017. 295: p. 32-40.
16. D. Coertzen, R.J. Kriek, P.B.J. Levecque, A. Falch, Vulcan Carbon as Support for Sputtered Oxygen Evolution Electrocatalysts. *Electrocatalysis*, 2019(10), p. 604-612.
17. M.J. Lazaro, L. Calvillo, V. Celorrio, J.I. Pardo, S. Perathoner, R. Moliner, Study and application of carbon black vulcan XC-72R in polymeric electrolyte fuel cells. *Carbon Black: Production, Properties and Uses*, ed. T.L.P. I.J. Sanders. Nova Science Publishers, 2011: p. 1-28.
18. A. Falch, V.A. Lates, H.S. Kotzè, R.J. Kriek, The Effect of Rapid Thermal Annealing on Sputtered Pt and Pt₃Pd₂ Thin Film Electrocatalysts for Aqueous SO₂ Electro-Oxidation. *Electrocatalysis*, 2016(7): p. 33-41.
19. A.L. Dicks, The role of carbon in fuel cells. *Journal of Power Sources*, 2006. 156(2): p. 128-141.
20. R.L. Doyle, M.E.G. Lyons, Chapter 2: The oxygen Evolution Reaction: Mechanistic Concepts and Catalyst Design. 2016: Springer. 559.

21. H. Yu, J.M. Roller, W.E. Mustain, R. Maric, Influence of the ionomer/carbon ratio for low-Pt loading catalyst layer prepared by reactive spray deposition technology. *Journal of Power Sources*, 2015. 283: p. 84-94.
22. G. Li, L. Anderson, Y. Chen, M. Pan, P.Y.A. Chuang, New insights into evaluating catalyst activity and stability for oxygen evolution reactions in alkaline media. *Sustainable Energy & Fuels*, 2018. 2(1): p. 237-251.
23. Z. Lu, W. Xu, W. Zhu, Q. Yang, X. Lei, J. Liu, Y. Li, X. Sun, X. Duan, Three-dimensional NiFe layered double hydroxide film for high-efficiency oxygen evolution reaction. *Chemical Communications*, 2014. 50(49): p. 6479-6482.
24. L. Trotochaud, S.L. Young, J.K. Ranney, S.W. Boettcher, Nickel–Iron Oxyhydroxide Oxygen-Evolution Electrocatalysts: The Role of Intentional and Incidental Iron Incorporation. *Journal of the American Chemical Society*, 2014. 136(18): p. 6744-6753.
25. G. Sasikumara, J.W. Ihma, H. Ryua, Optimum Nafion content in PEM fuel cell electrodes. *Electrochimica Acta*, 2004. 50: p. 601-605.
26. X. Li, F. Feng, K. Zhang, S. Ye, D.Y. Kwok, V. Birss, Wettability of Nafion and Nafion/Vulcan Carbon Composite Films. *Langmuir*, 2012. 28: p. 6698-6705.
27. A. Ursua, L.M. Gandia, P. Sanchis, Hydrogen Production from Water Electrolysis: Current Status and Future Trends. *Proceedings of the IEEE*, 2012. 100(2): p. 410-426.

ANNEXURES A: PERMISSION GRANTED BY CO-AUTHORS

Consent by co-authors

All the co-authors, i.e. A. Falch, R.J. Kriek, P.B.J. Levecque, D.R. Jones and C.W. Dunnill, as well as the respective journal(s) (see Appendix for details), were informed that the Masters Dissertation will be submitted in article format for examination and gave their consent.



I, Dr. Anzel Falch, hereby give permission that De Wet Coertzen may submit the article(s)/manuscript(s) for degree purposes



I, Prof. Roelof J. Kriek, hereby give permission that De Wet Coertzen may submit the article(s)/manuscript(s) for degree purposes.



I, Dr. Pieter B. J. Levecque, hereby give permission that De Wet Coertzen may submit the article(s)/manuscript(s) for degree purposes.



I, Dr. Daniel R. Jones, hereby give permission that De Wet Coertzen may submit the article(s)/manuscript(s) for degree purposes.



I, Dr. Charles W. Dunnill, hereby give permission that De Wet Coertzen may submit the article(s)/manuscript(s) for degree purposes.

ANNEXURES B: CONSENT BY JOURNAL(S)

SPRINGER NATURE LICENSE TERMS AND CONDITIONS

Sep 09, 2019

This Agreement between Mr. De Wet Coertzen ("You") and Springer Nature ("Springer Nature") consists of your license details and the terms and conditions provided by Springer Nature and Copyright Clearance Center.

License Number	4664620749483
License date	Sep 09, 2019
Licensed Content Publisher	Springer Nature
Licensed Content Publication	Electrocatalysis
Licensed Content Title	Vulcan Carbon as Support for Sputtered Oxygen Evolution Electrocatalysts
Licensed Content Author	D. Coertzen, R. J. Kriek, P. B. J. Levecque et al
Licensed Content Date	Jan 1, 2019
Type of Use	Thesis/Dissertation
Requestor type	academic/university or research institute
Format	print and electronic
Portion	full article/chapter
Will you be translating?	no
Circulation/distribution	30 - 99
Author of this Springer Nature content	yes
Title	Investigating reactive sputtered Ir(x)Ni(y)O(z) electrocatalysts for the oxygen evolution reaction
Institution name	North-West University
Expected presentation date	Nov 2019
Requestor Location	Mr. De Wet Coertzen Bokamierie Street 4 Mooivallei Park Potchefstroom, North West 2531 South Africa Attn: Mr. De Wet Coertzen
Total	0.00 USD
Terms and Conditions	

Springer Nature Customer Service Centre GmbH Terms and Conditions

This agreement sets out the terms and conditions of the licence (the **Licence**) between you and **Springer Nature Customer Service Centre GmbH** (the **Licensor**). By clicking 'accept'

and completing the transaction for the material (**Licensed Material**), you also confirm your acceptance of these terms and conditions.

1. Grant of License

1. The Licensor grants you a personal, non-exclusive, non-transferable, world-wide licence to reproduce the Licensed Material for the purpose specified in your order only. Licences are granted for the specific use requested in the order and for no other use, subject to the conditions below.
2. The Licensor warrants that it has, to the best of its knowledge, the rights to license reuse of the Licensed Material. However, you should ensure that the material you are requesting is original to the Licensor and does not carry the copyright of another entity (as credited in the published version).
3. If the credit line on any part of the material you have requested indicates that it was reprinted or adapted with permission from another source, then you should also seek permission from that source to reuse the material.

2. Scope of Licence

1. You may only use the Licensed Content in the manner and to the extent permitted by these Ts&Cs and any applicable laws.
2. A separate licence may be required for any additional use of the Licensed Material, e.g. where a licence has been purchased for print only use, separate permission must be obtained for electronic re-use. Similarly, a licence is only valid in the language selected and does not apply for editions in other languages unless additional translation rights have been granted separately in the licence. Any content owned by third parties are expressly excluded from the licence.
3. Similarly, rights for additional components such as custom editions and derivatives require additional permission and may be subject to an additional fee. Please apply to Journalpermissions@springernature.com/bookpermissions@springernature.com for these rights.
4. Where permission has been granted **free of charge** for material in print, permission may also be granted for any electronic version of that work, provided that the material is incidental to your work as a whole and that the electronic version is essentially equivalent to, or substitutes for, the print version.
5. An alternative scope of licence may apply to signatories of the [STM Permissions Guidelines](#), as amended from time to time.

• Duration of Licence

1. A licence for is valid from the date of purchase ('Licence Date') at the end of the relevant period in the below table:

Scope of Licence	Duration of Licence
Post on a website	12 months
Presentations	12 months
Books and journals	Lifetime of the edition in the language purchased

- **Acknowledgement**

1. The Licensor's permission must be acknowledged next to the Licenced Material in print. In electronic form, this acknowledgement must be visible at the same time as the figures/tables/illustrations or abstract, and must be hyperlinked to the journal/book's homepage. Our required acknowledgement format is in the Appendix below.

- **Restrictions on use**

1. Use of the Licensed Material may be permitted for incidental promotional use and minor editing privileges e.g. minor adaptations of single figures, changes of format, colour and/or style where the adaptation is credited as set out in Appendix 1 below. Any other changes including but not limited to, cropping, adapting, omitting material that affect the meaning, intention or moral rights of the author are strictly prohibited.
2. You must not use any Licensed Material as part of any design or trademark.
3. Licensed Material may be used in Open Access Publications (OAP) before publication by Springer Nature, but any Licensed Material must be removed from OAP sites prior to final publication.

- **Ownership of Rights**

1. Licensed Material remains the property of either Licensor or the relevant third party and any rights not explicitly granted herein are expressly reserved.

- **Warranty**

IN NO EVENT SHALL LICENSOR BE LIABLE TO YOU OR ANY OTHER PARTY OR ANY OTHER PERSON OR FOR ANY SPECIAL, CONSEQUENTIAL, INCIDENTAL OR INDIRECT DAMAGES, HOWEVER CAUSED, ARISING OUT OF OR IN CONNECTION WITH THE DOWNLOADING, VIEWING OR USE OF THE MATERIALS REGARDLESS OF THE FORM OF ACTION, WHETHER FOR BREACH OF CONTRACT, BREACH OF WARRANTY, TORT, NEGLIGENCE, INFRINGEMENT OR OTHERWISE (INCLUDING, WITHOUT LIMITATION, DAMAGES BASED ON LOSS OF PROFITS, DATA, FILES, USE, BUSINESS OPPORTUNITY OR CLAIMS OF THIRD PARTIES), AND WHETHER OR NOT THE PARTY HAS BEEN ADVISED OF THE POSSIBILITY OF SUCH DAMAGES. THIS LIMITATION SHALL APPLY NOTWITHSTANDING ANY FAILURE OF ESSENTIAL PURPOSE OF ANY LIMITED REMEDY PROVIDED HEREIN.

- **Limitations**

1. **BOOKS ONLY:** Where '**reuse in a dissertation/thesis**' has been selected the following terms apply: Print rights of the final author's accepted manuscript (for clarity, NOT the published version) for up to 100 copies, electronic rights for use only on a personal website or institutional repository as defined by the Sherpa guideline (www.sherpa.ac.uk/romeo/).

- **Termination and Cancellation**

1. Licences will expire after the period shown in Clause 3 (above).
2. Licensee reserves the right to terminate the Licence in the event that payment is not received in full or if there has been a breach of this agreement by you.

Appendix 1 — Acknowledgements:

For Journal Content:

Reprinted by permission from [the Licensor]: [Journal Publisher (e.g. Nature/Springer/Palgrave)] [JOURNAL NAME] [REFERENCE CITATION (Article name, Author(s) Name), [COPYRIGHT] (year of publication)]

For Advance Online Publication papers:

Reprinted by permission from [the Licensor]: [Journal Publisher (e.g. Nature/Springer/Palgrave)] [JOURNAL NAME] [REFERENCE CITATION (Article name, Author(s) Name), [COPYRIGHT] (year of publication), advance online publication, day month year (doi: 10.1038/sj.[JOURNAL ACRONYM].)]

For Adaptations/Translations:

Adapted/Translated by permission from [the Licensor]: [Journal Publisher (e.g. Nature/Springer/Palgrave)] [JOURNAL NAME] [REFERENCE CITATION (Article name, Author(s) Name), [COPYRIGHT] (year of publication)]

Note: For any republication from the British Journal of Cancer, the following credit line style applies:

Reprinted/adapted/translated by permission from [the Licensor]: on behalf of Cancer Research UK: : [Journal Publisher (e.g. Nature/Springer/Palgrave)] [JOURNAL NAME] [REFERENCE CITATION (Article name, Author(s) Name), [COPYRIGHT] (year of publication)]

For Advance Online Publication papers:

Reprinted by permission from The [the Licensor]: on behalf of Cancer Research UK: [Journal Publisher (e.g. Nature/Springer/Palgrave)] [JOURNAL NAME] [REFERENCE CITATION (Article name, Author(s) Name), [COPYRIGHT] (year of publication), advance online publication, day month year (doi: 10.1038/sj.[JOURNAL ACRONYM].)]

For Book content:

Reprinted/adapted by permission from [the Licensor]: [Book Publisher (e.g. Palgrave Macmillan, Springer etc)] [Book Title] by [Book author(s)] [COPYRIGHT] (year of publication)

Other Conditions:

Version 1.2

Questions? customercare@copyright.com or +1-855-239-3415 (toll free in the US) or +1-978-646-2777.